OPTIMIZATION OF HETEROLOGOUS PROTEIN SECRETION IN YEAST

by

Thomas M. Malott

A dissertation submitted in partial fulfillment of the requirements for the degree of

Doctor of Philosophy

(Chemical and Biological Engineering)

at the

UNIVERSITY OF WISCONSIN-MADISON

2015

Date of final oral examination: 3/9/2015

The dissertation is approved by the following members of the Final Oral Committee:

Eric V. Shusta, Professor, Chemical and Biological Engineering
Sean P. Palecek, Professor, Chemical and Biological Engineering
Regina M. Murphy, Professor, Chemical and Biological Engineering
Brian F. Pfleger, Associate Professor, Chemical and Biological Engineering
Audrey P. Gasch, Associate Professor, Genetics

OPTIMIZATION OF HETEROLOGOUS PROTEIN SECRETION IN YEAST

Thomas M. Malott

Under the supervision of Professor Eric V. Shusta

at the University of Wisconsin-Madison

Abstract

Currently there are over 5,400 biopharmaceuticals in clinical development with 833 in phase III clinical trials. It takes ten to fifteen years to bring a drug to market and costs over 1.2 billion dollars per drug when adjusted for failure rate. Pharmaceutical companies need to be able to recoup this cost. Thus, there is a substantial need for safe and robust approaches for large scale production of therapeutic proteins. The yeast, *Saccharomyces cerevisiae,* has been proven to be an economic host for the production of several FDA approved protein therapeutics due to its rapid, high cell density growth in simple media. However, after years of effort, many proteins remain difficult to produce in yeast and in other recombinant hosts.

For the studies reported here, a neurotrophin known as Brain Derived Neurotropic Factor (BDNF) was chosen as the target protein. This important growth factor signals the survival of nerve cells and has considerable therapeutic potential for Alzheimer's, Parkinson's, and stroke patients. Past efforts to

express BDNF in bacteria have largely yielded inactive aggregates owing to its complex cysteine knot structure and large undefined hydrophobic regions. While properly folded BDNF has been produced in mammalian cell hosts, the yields remain low for this difficult to fold protein. Thus, in this thesis, several parallel research paths were initiated to improve folding and production of BDNF in yeast. These included engineering the BDNF protein itself, employing an engineered pro-region to assist BDNF folding, and engineering the unfolded protein response pathway of yeast.

First, using a directed evolution approach in partnership with Dr. Michael Burns, BDNF was mutated and using yeast display technology screened for improved expression and binding to its native TrkB and p75 receptors. BDNF mutants were identified that had 4 to 5-fold improvements in expression and 2 to 5-fold improvements in per molecule binding activity as yeast displayed proteins. These improvements translated to BDNF proteins secreted from yeast as well. In addition to being secreted largely as soluble homodimers, BDNF mutants were capable of stimulating TrkB receptor phosphorylation.

While these results were exciting, there would be potential for unwanted immunogenic effects due to the introduction of BDNF mutation. Taking advantage of the fact that BDNF is naturally produced as a pro-protein which is cleaved during secretory processing to yield mature BDNF, the native neurotropic proregion was placed in front of unmutated BDNF. This led to a substantial increase in binding activity on the yeast surface, but expression levels

remained low, leaving room for improvement. In collaboration with Dr. Michael Burns, the pro-region was selectively mutated and evolved in an analogous way to that described above for the BDNF protein itself. In this way, evolved pro-regions capable of improving TrkB binding 1.6 to 1.9-fold and expression 2.5 to 2.9-fold were obtained. When an evolved pro-region was combined with an evolved BDNF mutant, there was over a 200-fold synergistic improvement in binding activity over wild-type BDNF. As before, these improvements translated well to secretion, and secretion was improved up to 170-fold over wild-type BDNF.

Although effective, both of these methods were neurotrophin isoform specific, and even when combined, production levels remained two orders of magnitude under yeasts full potential of g/L titers. Thus, we investigated a new approach targeted to engineering the yeast host itself. One of the most relevant pathways related to heterologous protein secretion is the Unfolded Protein Response (UPR) pathway. Upon activation initiated by protein misfolding, its central transcription factor, hac1p, directly promotes the expression of over 380 genes leading to a cascade that ultimately affects the regulation of over 1,500 genes. This response can modulate every part of the secretory pathway to help restore cellular function and reduce cellular stress.

Thus, we employed transcription factor engineering approaches where the spliced *HAC1* gene was mutated and this library of *HAC1* mutants was coexpressed with yeast surface-displayed BDNF. After screening as before for

improved BDNF folding and expression as a result of differential *HAC1* regulation, clones with 2 to 3-fold improvements in surface expression and 1 to 2-fold improvements in binding activity where obtained. Upon secretion, these mutant *HAC1*s expression cassettes improved wild-type BDNF expression 2.3-fold and activity up to 5.5-fold. The improvements were found to be the result of serendipitous promoter region mutations that could tune the UPR response level, rather than mutations in the *HAC1* gene itself. To further explore this finding, *HAC1* expression resultant UPR activity was rationally tuned. Low UPR activation resulted in improved folding up to 2.5-fold and improved expression up to 2-fold, while high UPR activation yielded 4-fold improved expression at the expense of folding. Thus, for BDNF it appears that there exists an optimal UPR activation level for combined improvements in folding and expression. Moving forward, these findings suggest that the secretion of any protein of interest could be improved by simply tuning UPR activation.

Acknowledgements

First and foremost, I would like to thank my advisor, Professor Eric Shusta, for all his years of patient mentoring and for taking the time to train me well. By rights he should be listed as coauthor on this document, since every step of the way, his wise counsel carried this research and was instrumental to its writing.

In addition, I owe gratitude to the group members in the Shusta and Palecek labs who were always willing to listen and offer insightful suggestions, especially in regards to crafting my oral defense. Their encouragement and optimistic outlook brightened the walls of Engineering Hall. Furthermore, I would like to thank my undergrads (Kevin Metcalf, Arthya Puguh, Daniel Caron, Huicheng Shi, David Paul, and Claudia Roen) for working with me on these projects and the staff at the University of Wisconsin Flow Cytometry Facility and Biotechnology Center for their excellent advice and services in sorting all my libraries.

Lastly, I am extremely grateful for my family and friends for their invaluable support and care. They all patiently listened to my complaints, helped celebrate my successes and were sympathetic in my trials. While there are too many to name, I would like to especially thank my parents, Mike and Nancy Malott, and my sisters, Christine and Elaine, for providing me the best possible home, education, and up-bringing. Without them, I would never have made it this far.

In addition, I want to thank the people at international club (Terrell Smith, Rick and Jill Feldkamp, Deb Meyer, Kiyoko Foster, and Mary Malischke) for all their prayers and support; Tim and Mag for letting me be a part of their family and for providing countless hours of relaxation and enjoyment; Lon and Andrea Matz for letting me live with them during my final transition from grad school; and most importantly, I am extremely thankful to Sarah Boswell for being by my side every step of the way these last eight years. Her self-sacrificing thoughtfulness and encouragement did the most to uplift my spirits and keep me going these last couple years.

Table of Contents

Abstract i
Acknowledgements v
Table of Contents vii
List of Figures ix
List of Tables x
Chapter 1: Introduction 1
1.1.1 Pharmaceutical Need for Better Heterologous Expression System 1
1.1.2 Protein and Cellular Engineering Approaches Tried 2
1.1.3 Transcription Factor Engineering 3
1.1.4 Secretory Pathway and Unfolded Protein Response 4
1.1.5 Transcription Factor Engineering of Hac1p 7
1.1.6 Targeting BDNF for optimization 9
1.1.7 Yeast Surface Display 10
1.1.8 Research Goals: 11
Chapter 2: Directed Evolution of Brain-Derived Neurotrophic Factor for Improved Folding and Expression in *Saccharomyces cerevisiae* 14
2.1 Abstract 14
2.2 Introduction 16
2.3 Materials and Methods 18
2.3.1 Strains, plasmids, materials, and media 18
2.3.2 Surface display binding and affinity measurements 19
2.3.3 BDNF library construction and screening 21
2.3.4 Protein secretion and purification 23
2.3.5 Western Blotting 24
2.3.6 TrkB and p75 ELISA 25
2.3.7 Size exclusion chromatography 26
2.3.8 PC12 phosphorylation 26
2.4 Results 28
2.4.1 Creation of a BDNF scaffold capable of binding its natural receptors 28
2.4.2 Mutation effects on surface displayed and secreted BDNF binding activity and expression 35
2.4.3 Fidelity and biological activity of secreted BDNF mutants 43
2.5 Discussion 47
Chapter 3: Pro-Leader Engineering for Improved Yeast Display and Secretion of Brain Derived Neurotrophic Factor 53
3.1 Abstract 53
3.2 Introduction 55
3.3 Materials and Methods 58

3.3.1 Cells, Media, and Plasmids 58
3.3.2 Flow Cytometry 59
3.3.3 Library Construction and Screening 60
3.3.4 Protein Secretion and Purification 62
3.3.5 Western Blotting 63
3.3.6 ELISA Assays 64
3.3.7 PC12 TrkB Phosphorylation Assays 64
3.4 Results 66
3.4.1 Effects of wild-type pro-region on BDNF display and production 66
3.4.2 Directed evolution of BDNF pro-region 70
3.4.3 Effects of evolved pro-regions on properties of surface-displayed BDNF 72
3.4.4 Effects of evolved pro-regions on properties of secreted BDNF 75
3.4.5 Effects of engineered pro-regions on proteolytic pro processing for displayed and secreted BDNF 78
3.5 Discussion 81
Chapter 4: Improving Heterologous Protein Production in *Saccharomyces cerevisiae* by Tuning the Unfolded Protein Response 87
4.1 Abstract 87
4.2 Introduction 89
4.3 Materials and Methods 91
4.3.1 Cells, Media, and Plasmids 91
4.3.2 Flow Cytometry 93
4.3.3 Library Creation and Sorting 93
4.3.4 Protein Secretion and Purification 96
4.3.5 Western Blotting 96
4.3.6 ELISA Assay 97
4.3.7 qPCR 98
4.4 Results 99
4.4.1 Effects of wild-type HAC1 on BDNF display and production 99
4.4.2 HAC1 Libraries effect on BDNF production 101
4.4.3 Direct evolution of HAC1 101
4.4.4 Deletions in promoter region 103
4.4.5 Tuning HAC1 expression 109
4.5 Discussion 110
Bibliography 113

List of Figures

Figure 1.1. Schematic of the secretory pathway in yeast....6
Figure 1.2. UPR activation in yeast....8
Figure 1:3: Schematic of yeast surface display technologies....12
Figure 2.1 Production of BDNF using yeast....29
Figure 2.2. Directed evolution of BDNF....30
Supplemental Figure 2.S1. Apparent TrkB binding affinity....34
Figure 2.3. Comparison of BDNF binding and expression properties....36
Figure 2.4. Structural locations of identified mutations....38
Figure 2.5. Evaluation of cysteine mutations....39
Figure 2.6. Surface capture of secreted BDNF mutants....42
Figure 2.7. Size-exclusion chromatography analysis....44
Figure 2.8. TrkB phosphorylation....45
Figure 3.1: Effects of wild-type pro-region....68
Figure 3.2: Directed evolution of the BDNF pro-region....71
Figure 3.3: Analysis of improved pro-regions on BDNF secretion....76
Figure 3.4: ClustalW alignment of human BDNF, NGF, and NT3 pro-regions....84
Figure 4.1: BDNF production and screening....100
Figure 4.2: Assessing libraries fitness....102
Figure 4.3: Gal promoter deletions....105
Figure 4.4: Results of Directed Evolution on....106
Figure 4.5: Hac1p clone's effect on BDNF secretion....107
Figure 4.6: Cellular response to promoter mutations....108

List of Tables

Table 2.1. Properties of BDNF mutants. 32
Table 3.1: Mutations and properties of evolved BDNF pro-regions. 74

Chapter 1: Introduction

1.1.1 Pharmaceutical Need for Better Heterologous Expression System

Protein drugs are quickly becoming the major focus of pharmacology research, because they can affect the body in ways not possible through small molecules (1). They are known to treat over 200 diseases (2). While there is much excitement about these drugs, they are very expensive, costing hundreds of thousands of dollars per patient per year (3). There is great need for a robust host capable of safely producing large quantities of protein (4, 5). While bacteria such as *E. coli* may seem an obvious choice, it lacks the appropriate machinery to properly perform the posttranslational modifications crucial for pharmaceuticals, and has high downstream purification cost (4). Thus, most current biotech companies depend on mammalian cells for their host systems (5). These hosts tend to be more expensive to cultivate and have safety concerns regarding the potential for viral transmission. Furthermore, even though companies have been able to achieve high titers of antibodies in mammalian cells through trial and error, most non-antibody proteins, like T – cell receptors, are still secreted in low volumes (6). Yeast holds promise for being a safe (GRAS) and economical production host (4, 7) They possess many of the eukaryotic folding and posttranslational modification machinery necessary to

make more complex proteins, while their rapid growth to high cell densities in simple media keeps production cost low. However, even though they have the ability to achieved gram per liter secretion rates (4, 7), titers for most proteins are far from optimum.

1.1.2 Protein and Cellular Engineering Approaches Tried

In the past, researchers have tried to increase protein expression in yeast by rationally designing mutations in the protein. This has been met with only limited success since many beneficial mutations are currently impossible to predict *a priori* with our incomplete understanding of protein structure and function. Some success has been achieved through evolution of the protein's sequence (8). This is a relatively quick way to find beneficial mutations. However, the results are very protein specific and may be undesirable for use as drugs due to the possibility of an immunogenic response to the unnatural protein.

One alternative to engineering the protein is to engineer the host organism. This can be accomplished by random mutagenesis of the host's genome. This technique often results in higher protein production as in the case of bioinsecticide production in Bacillus thuringiensis (9),. However, it is often very difficult to determine which mutations lead to the improved phenotype; and thus is not generalizable. Another method is to overexpress or knockout genes thought to be important in the secretory pathway (10, 11). However, these too

tend to be protein specific (12, 13) and require preliminary knowledge of gene functions and pathways. Knowledge of the secretory pathway in yeast is limited, and these pathways involve hundreds of genes in complicate networks. To overcome this, former lab member, Dr. Alane Wentz, explored the effects of single gene overexpression on a global scale [6]. Each of the 6,000 known yeast genes were singly overexpressed and screened for their ability to improve the folding and expression of four heterologous proteins. Even then, only 3 to 7-fold improvements were gained. The intricacies of the system often require multiple genes to be altered simultaneously. As a result, very little of sequence space has actually been investigated (6).

1.1.3 Transcription Factor Engineering

A new approach to cellular engineering is to take a more global focus by engineering transcription factors (14). This mimics natural evolution, and previous studies have shown this to be a promising area for exploration. In one such study, substantial gains in glucose and ethanol tolerance were obtained by engineering a TATA binding protein, SPT15. This affected the expression level of hundreds of genes. Upon closer inspection, this phenotype was found to be the result of many genes working together and could not have been achieved by simultaneously overexpressing any two genes (15).

Later that same group showed that multiple phenotypes, ethanol tolerance and metabolite overproduction, could be achieved in E. coli by engineering the sigma factor to affect RNA polymerase's promoter preferences on a global level. They were able to quickly achieve significant improvements in areas were only limited gains had been made through traditional means (16, 17). Other groups have followed and have engineered the cyclic AMP receptor transcription factor in E. coli for improvement in 1-butanol tolerance and osmotolerance.(18, 19)

1.1.4 Secretory Pathway and Unfolded Protein Response

The secretory pathway in yeast starts when a ribosome/mRNA complex is targeted to the Endoplasmic Reticulum (ER). Once bound to an ER pore, the protein is translated across the ER membrane into the interior. Here, the nascent protein binds chaperones like Protein Disulfide Isomerase (PDI) and Binding Immunoglobulin Protein (BiP) which assist its folding. After the protein is properly folded and glycosylated, it is targeted to transport vesicles and shuttled to the Golgi apparatus. Then, any final posttranslational modifications are performed, and the protein is sorted to an exocytotic vesicle. The exocytotic vesicle is released and fuses with the plasma membrane to release its contents. As protein flux increases, the chaperones become overwhelmed and unfolded protein begins to accumulate inside the ER. Chronically misfolded proteins can be degraded through the ER Associated Degradation (ERAD) pathway. If some

misfolded proteins slip by the ER checkpoint and proceeds to the Golgi, they can be returned to the ER through retrograde transport or targeted to a vacuole for destruction (20, 21) (Figure 1.1).

When foreign proteins are expressed in high volumes inside the yeast, they saturate these quality control pathways. This buildup leads to cellular stress and starts a chain of events known as the unfolded protein response (UPR) (23) (Figure 1.2). Every part of the secretory pathway is affected by this response. Examples of secretory proteins or functions upregulated include chaperones, foldases, protein degradation, vesicle trafficking, and vacuolar targeting (22) (Figure 1.1). As unfold protein builds up in the ER, all the free BiP, an important ER chaperone, binds to the unfolded proteins to assist their folding. This causes bound BiP to dissociate from the transmembrane protein, Ire1p, allowing Ire1p to sense unfolded proteins in the ER and oligomerize. While all the events that initiate the UPR are still unknown, it is known that, though not critical, dissociation of BiP plays an important regulatory role (24, 25). The oligomerization of Ire1p allows it to transautophosphorylate, activating their endoribonuclease domains (26). Active endoribonuclease domains now catalyze the splicing of *HAC1u* mRNA by removing the 252-bp intron and allowing tRNA ligase to create the active 717 bp gene (27, 28).

Once translated, hac1p protein homodimerizes through its leucine zipper region. Then hac1p's basic region hydrogen bonds to the major groove of at least three DNA promoters called Unfolded Protein Response Elements (UPRE)

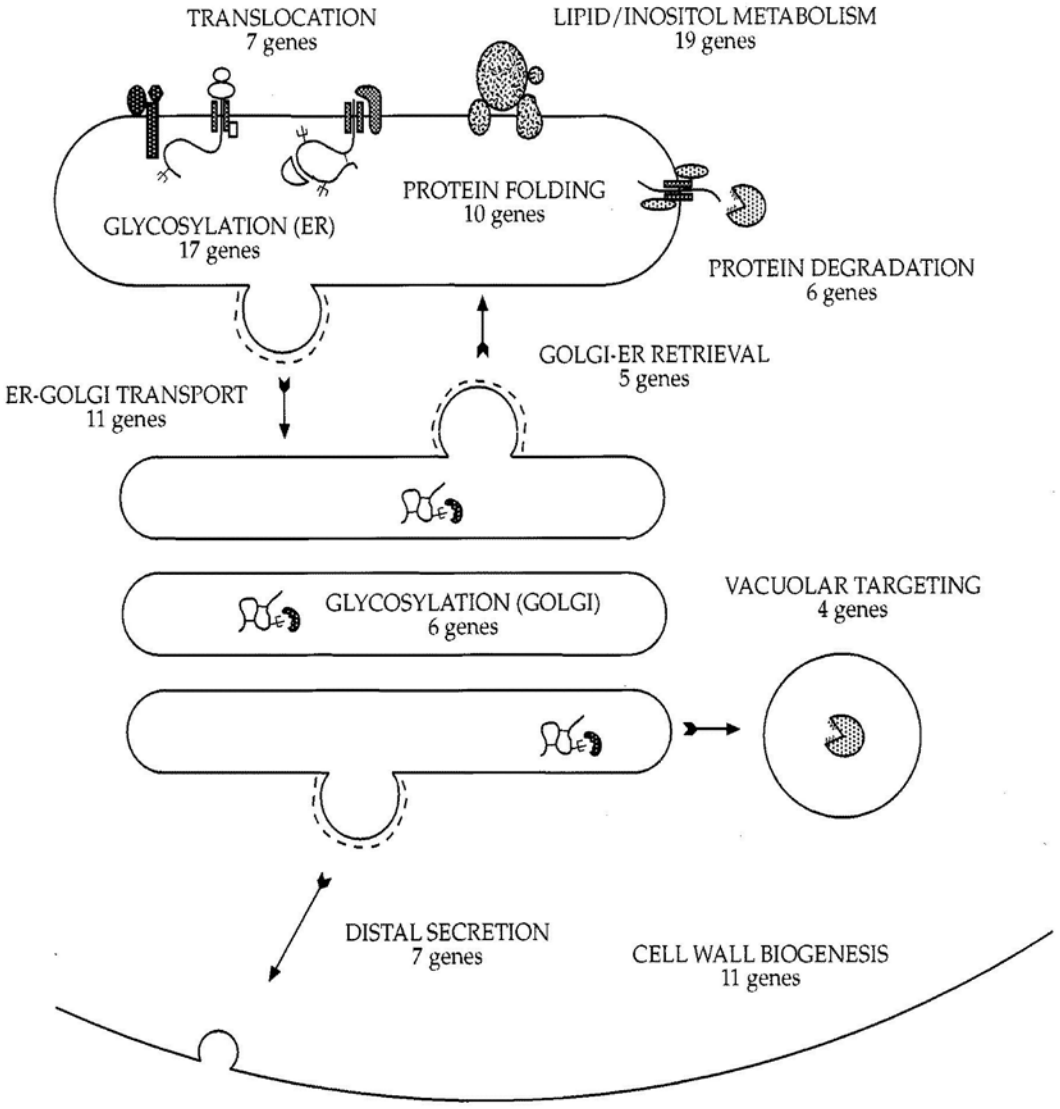

Figure 1.1. **Schematic of the secretory pathway in yeast**. After the nascent protein is translated into the ER and properly folded, it is transported to the Golgi where it is sorted and sent outside the cell. The number of genes directly upregulated by the UPR for this process are shown for each step. Taken from (22)

(28-30). In addition, hac1p interacts closely with another transcription factor, Gcn4p, to effectively promote many hac1p dependent genes. Furthermore, hac1p must also interact with other coactivators such as Gcn5p and Ada5p to connect with TATA binding proteins and recruit RNA polymerase to the gene (Figure 1.2) (30-32). This directly regulates over 380 genes or about 7% of the genome. Some of these genes affected are transcription factors central to other pathways. Some of these pathways include ERAD to degrade unfolded proteins (22, 33), phospholipid biosynthesis to expand the ER to create room for the incoming flux of chaperons (22), and COPII vesicle formation to increase transport from the ER to the Golgi (34), which has been found to be a limiting step in the secretory pathway (21). This ultimately leads to differential regulation in over 1,500 genes during heterologous protein secretion (35). The net effect of this response is to relieve cellular stress through either facilitating the foreign protein's folding and secretion or by degrading it. Completely turning off this response leads to high levels of cellular stress and low secretion rates, while completely turning on the UPR may lead to downregulation and degradation of the protein (36, 37).

1.1.5 Transcription Factor Engineering of Hac1p

One of the most relevant pathways for heterologous secretion in yeast is the UPR. By utilizing the power of transcription factor engineering, the whole

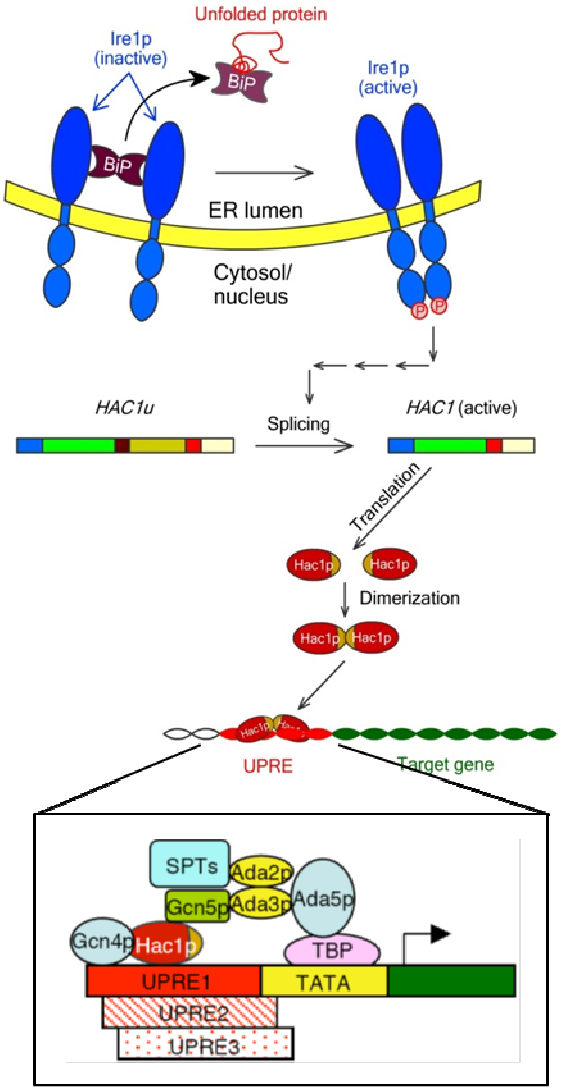

Figure 1.2. UPR activation in yeast. As unfold protein builds up in the ER, BiP disassociates from Ire1p, allowing Ire1p to activate by oligomerization and splice *HAC1u*. Once translated, hac1p dimer binds to the UPR elements to upregulate target genes. Adapted from (23)

UPR can be simultaneously controlled. Through engineering hac1p's binding affinity, turnover frequency, promoter activation strength, and protein-protein interactions, varying levels and styles of UPR can be achieved (23). For example, hac1p mutants that decrease hac1p's turnover rate have been shown to improve cell viability under ER stress conditions 50-fold (38). Furthermore, by mutating hac1p, it is possible to change more than just UPR activation level or turnover frequency. Hac1p has been shown to bind to UPRE 1 and UPRE 2 in unique ways, and it is likely that the resulting protein conformational shifts affect its interactions with other protein. In addition, hac1ps capable of selectively binding to either UPRE 1 or UPRE 2 have been engineered (39), opening up the possibility for differential activations of separate parts of the UPR pathway, giving rise to unique and unexpected results.

1.1.6 Targeting BDNF for optimization

We chose to optimize the clinically relevant Brain-Derived Neurotropic Factor (BDNF). This important growth factor is prevalent throughout the central nervous system and is essential for neuronal plasticity and neuron survival. Aberrant levels of BDNF have been implicated in many neurological diseases and psychiatric conditions. A few examples include Alzheimer's, Parkinson's, Schizophrenia, and addictions. (40, 41). Although currently BDNF has not been successful in clinical trials due to inefficient delivery across the blood brain barrier

(42, 43), promising technologies to overcome this are being developed. When BDNF was conjugated to an anti-transferrin molecular Trojan horse, it was able to target the brain and undergo receptor-mediated transport across the blood brain barrier. This was tested as a therapy in rats and found to reduce stroke volume 70% (44).

Although a small 14 kDa protein, BDNF has a complex structure. Its three disulfide bonds, cysteine knot structure, and lack of a well-defined hydrophobic core make this protein difficult to produce. In bacteria it is produced as insoluble aggregates which must be refolded, often yielding a low fidelity product with poor biological activity(45). Even though yeast contain chaperones and foldases to assist with disulfide bond formation, they do not have any naturally occurring cysteine knot proteins, and as a consequence, secrete BDNF as unfold aggregates (46, 47)

1.1.7 Yeast Surface Display

Yeast surface display was developed by Wittrup *et al* to facilitate the screening of large genetic libraries used during directed evolution (48, 49). This important technology allows for the rapid assessment of the amount and fidelity of BDNF produced on a cellular basis. BDNF is secreted as a fusion protein to Aga2p. Coexpression of the Aga1p anchor protein allows Aga2p to be covalently linked to the cell wall via disulfide bonding to Aga1p. This attachment to the

yeast surface links the improved phenotype to the genotype of the clone, enabling its selection. The total amount of BDNF produced on the cell surface can be assayed using antibodies against the c-*myc* epitope tag. In an analogous way, BDNF activity could be monitored by binding to either of its natural receptors, Tropomyosin receptor kinase B (TrkB) or Low-affinity nerve growth factor receptor (p75). These can then be labeled with fluorescent secondary antibodies and analyzed on a flow cytometer (Figure 1.3). This has been extensively used in the past for sorting libraries for improved protein production (6, 50, 51), and they have found good correlations between yeast surface-displayed levels and secretion levels (47, 50)

1.1.8 Research Goals:

The goal for this thesis was to identify effective methods for improving heterologous protein secretion in *Saccharomyces cerevisiae* in terms of both folding and secretion levels, specifically for the target therapeutic, BDNF. This goal was achieved using three different approaches: 1) Directly modifying the protein to aid its folding. 2) Directly modifying BDNF's native leader region to impart chaperon-like abilities to aid BDNF's folding. 3) Directly modifying the hac1p transcription factor to optimally activate the UPR for BDNF production.

Chapter 1 details the first approach of directly mutating the human BDNF protein, and screening for improvements in BDNF production. Positive clones

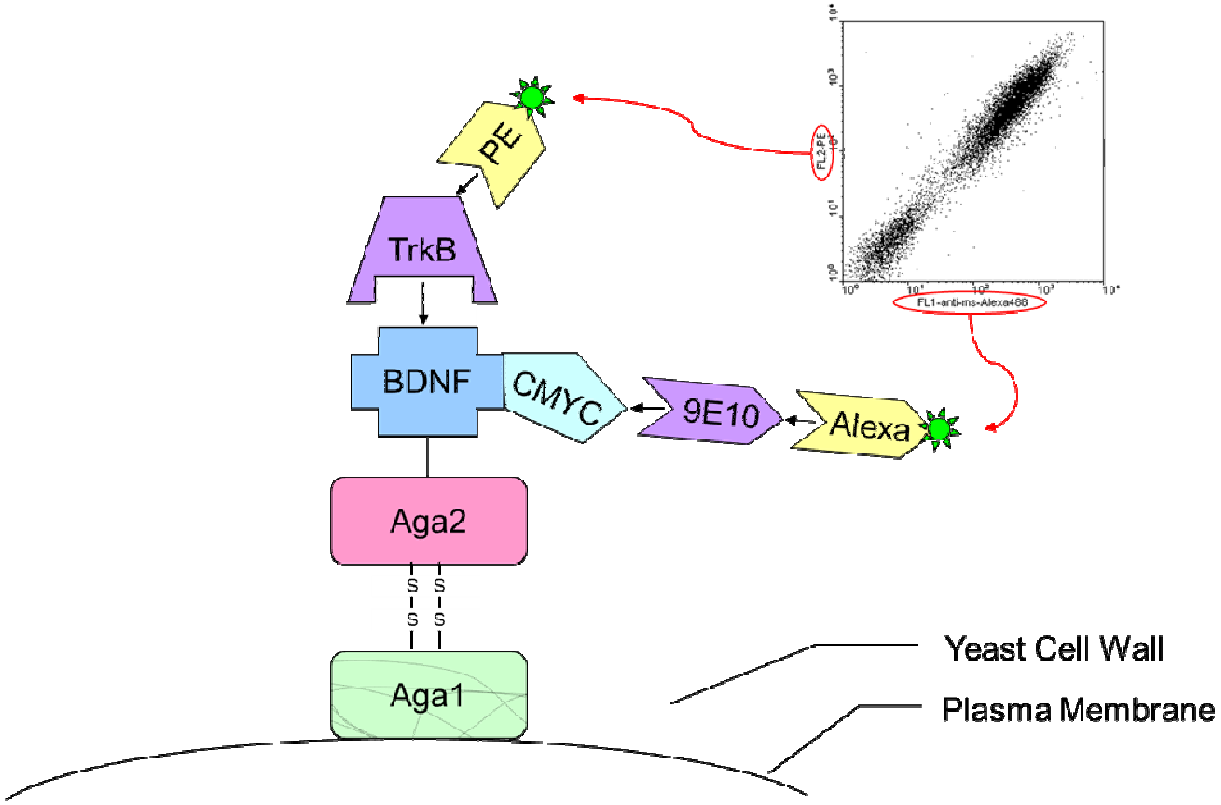

Figure 1:3: Schematic of yeast surface display technologies. The protein of interest, in this case BDNF, is secreted as a fusion to the Aga2p and covalently tethered to the yeast surface via disulfide bonds to the Aga1 anchor protein. This allows for easy labeling with fluorescent antibodies and analysis on a flow cytometer. The sample dot plot in the upper right, contains the individual fluorescence values for 10,000 cells.

were isolated that improved both the folding and expression level of BDNF, and their beneficial mutations characterized

Chapter 2 details the second approach where unmutated BDNF secretion was improve both in terms of fidelity and secretion level by the addition of the human BDNF pro-region. Further improvements were obtained by mutating this leader sequence and screening for BDNF expression and folding. Positive clones were characterized and mutations analysed. Cleave site engineering was performed to allow for better pro- processing

Chapter 3 details the final approach of tuning the unfold protein response by mutating the hac1p transcription factor and screening for improved production of BDNF. Isolated clones where characterized and found to be tuning overall UPR activation level. BDNF folding and expression was tracked as a function of UPR activation.

Chapter 2: Directed Evolution of Brain-Derived Neurotrophic Factor for Improved Folding and Expression in *Saccharomyces cerevisiae*

(This chapter was adapted from Burns, M.L.; Malott, T.M.; Metcalf, K.J.; Hackel, B.J.; Chan, J.R.; Shusta, E.V., (2014) *Appl Environ Microbiol (47))*

2.1 Abstract

Brain-derived neurotrophic factor (BDNF) plays an important role in nervous system function and has therapeutic potential. Microbial production of BDNF has resulted in low fidelity protein product, often in the form of large insoluble aggregates incapable of binding to cognate TrkB or p75 receptors. In this study, employing yeast display and secretion systems, it was found that BDNF was poorly expressed and partially inactive on the yeast surface, and BDNF was secreted at low levels in the form of disulfide-bonded aggregates. Thus, in order to improve the compatibility of yeast as an expression host for BDNF, directed evolution approaches were employed to improve BDNF folding and expression levels. Yeast surface display was combined with two rounds of directed evolution employing random mutagenesis and shuffling to identify BDNF mutants having 5-fold improvements in expression, 4-fold increases in specific TrkB binding activity and restored p75 binding activity, both as displayed and

secreted proteins. Secreted BDNF mutants were found largely in the form of soluble homodimers that could stimulate TrkB phosphorylation in transfected PC12 cells. Site directed mutagenesis studies indicated that a particularly important mutational class involved the introduction of cysteines proximal to the native cysteines that participate in the BDNF cysteine knot architecture. Taken together, yeast is now a viable alternative for the production and engineering of BDNF.

2.2 Introduction

Brain-derived neurotrophic factor (BDNF) is a member of the neurotrophin family that substantially influences mammalian neuronal function from development through adulthood(52). BDNF has also been posited to play a role in brain trauma and several neurodegenerative disorders including Alzheimer's and Parkinson's diseases(53). As demonstrations of its potential as a therapeutic, BDNF has been shown to be neuroprotective in stroke(44), Alzheimer's Disease(54), Parkinson's Disease(55), Huntington's Disease(56), and peripheral nerve injury(57). BDNF elicits its biological functions through specific interactions with the tropomyosin receptor kinase B (TrkB) and p75 neurotrophin receptors(58, 59), and it is biologically active as a homodimeric protein formed through hydrophobic interactions between each monomer's core(60-62). Moreover, each 122 amino acid monomer of BDNF possesses three intramolecular disulfide bonds in a cysteine knot configuration. These complex folding and assembly requirements governing the production of BDNF and other highly homologous neurotrophin family members, like nerve growth factor (NGF), have resulted in low heterologous productivity(63), likely as a byproduct of the aggregation-prone nature of these proteins(64).

Platforms for neurotrophin production include immortalized mammalian cell lines(63), bacteria(45), insect cell lines(65), and yeast(66). In particular, microbial hosts like bacteria and yeast have the advantages of facile genetic

modification, robust scaling, and comparatively low cost. However, previous attempts to produce BDNF in *E. coli* have yielded mainly insoluble proteins having mismatched disulfide bonds that required isolation and refolding; and even after refolding, the biological activity was attenuated(45, 67). As a partial resolution, bacterial host engineering in the form of co-overexpression of Dsb disulfide bonding machinery in bacteria could raise soluble BDNF production to 35%(45). Similarly, despite the eukaryotic protein folding and processing machinery of yeast, production of NGF in yeast resulted in low fidelity product(66). Here we report that yeast also primarily produces BDNF in an inactive and misfolded form. Yeast surface display has been used to identify better folded and secreted variants of single-chain T-cell receptors(68), FCAbs(69), epidermal growth factor receptor(70), among others(71). Thus, yeast surface display approaches were employed to improve the protein folding and processing properties of BDNF. Two rounds of directed evolution were used to identify mutations that resulted in BDNF having better specific binding activity towards both TrkB and p75, along with higher expression levels on the yeast surface. Subsequently, compared with wild-type BDNF, the mutants led to much improved secretion titers and specific activity in receptor binding ELISAs, and the top performing BDNF mutants were demonstrated to be capable of triggering TrkB receptor phosphorylation.

2.3 Materials and Methods

2.3.1 Strains, plasmids, materials, and media

An open reading frame encoding residues 1-119 of mature human BDNF were subcloned into the pCT-ESO yeast display vector(72) to drive yeast display of BDNF as a fusion to the yeast mating protein agglutinin, Aga2p. The resultant pCT-ESO-BDNF construct encoded Aga2p-HA-BDNF-c-*myc* (Figure 2.1 A). Similarly, the mature human BDNF open reading frame was subcloned into the pRS316-GFP(73) for yeast secretion yielding pRS316-BDNF, and encoding BDNF-c-*myc*-His_6. Anti-fluorescein single-chain antibody 4-4-20 was used as a control for some experiments(74). Control strains were created using empty plasmids containing nutritional markers alone (pRS-314, pRS-316). Vectors were transformed into the yeast secretion BJ5464 strain (Yeast Genetic Stock Center, Berkeley, CA), the yeast display strain EBY100(75), and the yeast display strain AWY100(74), as appropriate. All transformations were performed using the lithium acetate method(76) and yeast grown in minimal medium (2% dextrose, 0.67% yeast nitrogen base) buffered at pH 6.0 with 50 mM sodium phosphate and containing either 1% Casamino Acids (SD-CAA; lacking tryptophan and uracil) or 2x SCAA amino acid supplement (SD-SCAA, 190 mg/liter Arg, 108 mg/liter Met, 52 mg/liter Tyr, 290 mg/liter Ile, 440 mg/liter Lys, 200 mg/liter Phe, 1260 mg/liter Glu, 400 mg/liter Asp, 480 mg/liter Val, 220 mg/liter Thr, 130 mg/liter Gly, lacking leucine, tryptophan, and uracil). Leucine

(200 mg/liter), tryptophan (20 mg/liter), and uracil (20 mg/liter) were supplemented when necessary for proper auxotrophic selection. Induction of protein display and secretion was performed in the same medium, with the dextrose substituted for by 2% galactose. Fresh transformants were used in all experiments.

2.3.2 Surface display binding and affinity measurements

For surface display, yeast clones were grown in SD-CAA at 30^{o}C to an OD_{600nm} of 1.0, and then induced for display in an equal volume of SG-CAA for 18 hours at 20^{o}C. Ice cold phosphate-buffered saline (PBS) with 1 mg/ml bovine serum albumin (BSA) at pH 7.4 (PBS-BSA) was used in all washes, and included in primary and secondary antibody labeling solutions. Yeast ($2x10^{6}$) were collected washed in PBS-BSA and immunolabeled for flow cytometric analysis. Immunolabeling was conducted for 30 minutes at 4^{o}C using the following primary labels: anti-c-*myc* epitope antibody 9e10 (30-50 µg/ml, Covance, CA, USA), anti-HA epitope antibody 12Ca5 (25 µg/ml, Roche, IN, USA), anti-His_4 antibody (2 µg/ml, Qiagen, CA, USA), recombinant human TrkB/Fc chimera (TrkB) (5 µg/ml, R&D Systems, MN, USA), and recombinant human NGF receptor/TNFRSF16/Fc chimera (p75) (5 µg/ml, R&D Systems). After washing three times with PBS-BSA, secondary labels were applied for 30 minutes at 4^{o}C: anti-human immunoglobulin (Ig) G conjugated to phycoerythrin (PE) (1:45, Sigma, MO, USA), and anti-mouse

IgG conjugated to Alexa Fluor 488 (Alexa488) (1:500, Invitrogen, CA, USA). Following three washes with PBS-BSA, cells were analyzed on a Becton Dickinson FACSCalibur benchtop flow cytometer. Geometric means for the positive populations were corrected by subtracting the geometric means for the nondisplaying yeast population. When there was peak overlap between the displaying and nondisplaying populations, peak deconvolution methods were employed as described previously(77). In many cases, the TrkB and p75 binding signals were subsequently divided by the anti-c-*myc* signal to represent the data as binding per molecule.

Dimer determination using flow cytometry was performed using co-transformation of selected pRS316-BDNF (secreted BDNF with a His_6 tag) and pCT-ESO-BDNF (display without a His_6 tag) plasmids into the AWY100 yeast surface display strain. His_6 labeling, and hence surface capture by dimerization, was determined using the anti-His_4 antibody (2 µg/ml, Qiagen).

Apparent affinity measurements were determined in surface display format using serially diluted TrkB receptor diluted in PBS-BSA. Flow cytometric geometric mean fluorescent signals were adjusted for background fluorescence. Apparent affinity (K_D) calculations were then made using a non-linear least squares estimation for single receptor single ligand binding using Athena Visual as previously described(78). All statistical comparisons throughout the manuscript were performed using an unpaired, two-tailed students *t*-test.

2.3.3 BDNF library construction and screening

Mutagenic libraries were constructed as described previously(70, 79, 80). Briefly, in both directed evolution (DE) Rd1 and RD2 a BDNF mutant library was generated by error-prone PCR using the triphosphate derivatives of nucleotide analogues: 2'-deoxy-p-nucleoside-5'-triphosphate and 8-oxo-2'-deoxyguanosine-5'-triphosphate (TriLink Biotech, CA, USA)(81). Mutated BDNF open-reading frames were introduced into a digested pCT-ESO acceptor vector by homologous recombination. In this way, a library of $4x10^6$ transformants was created for DE Rd1. Sequence analysis prior to sorting indicated a total mutation rate of approximately 0.2-3.8% or between 1 and 14 base pair changes per BDNF mutant. For DE Rd2, a mixture of individual clones isolated from DE Rd1 were shuffled(82) in a 1:1 ratio with wild-type BDNF and subjected to a low rate of additional mutagenesis. This second round library comprised $1.1x10^7$ transformants.

Libraries were grown in selective media at 30°C to an OD_{600nm} of 1.0 and induced for 18 hours at 20°C. Surface display labeling was conducted as described above using a number of induced cells that were 10x the library size. The overall directed evolution screening strategy is depicted in Figure 2.2 A. For DE Rd1, the library was screened using both folding/activity (with the TrkB receptor) and expression (sorting rounds 1 and 3 used anti-c-*myc* antibody and sorting round 2 used anti-HA antibody). Saturating concentrations of TrkB

receptor were employed to bias screen towards folding fidelity rather than affinity improvements. TrkB concentrations of 5 μg/mL (35 nM) were validated as saturating by using wild-type BDNF displaying yeast. Cells were sorted using a Becton Dickinson FACSVantage SE flow cytometric sorter at the University of Wisconsin Comprehensive Cancer Center. Sort gates were set to collect dual positive high fluorescence events, and stringency was increased between sorting rounds (from 2.0-0.5% of the total population). Sorted yeast cells were maintained for one passage in SD-CAA with 50mM citrate replacing phosphate and supplemented with 25mg/L Kanamycin (Sigma). The recovered pools were subsequently passaged into standard SD-CAA media and induced for the next round of sorting as described above for the initial library. Individual clones were isolated and analyzed from a population by plating on nutritionally selective plates, and designated “T” or “B” simply because they came from different stringency sort gates in the final round of sorting. Plasmid DNA was recovered from yeast colonies using the Zymoprep II yeast plasmid miniprep kit (Zymo Research, CA, USA), amplified in DH5α cells (Invitrogen), and sequenced at the University of Wisconsin Biotechnology Center to determine mutagenic alterations. Retransformation into the parental EBY100 display strain confirmed the improvements in folding, activity and expression were due to the harbored mutated BDNF genes.

DE RD2 consisted of four sorting rounds, again using increasing stringency (2.0-0.5%). In the first sort of DE Rd2, the library was labeled with

TrkB in combination with anti-c-*myc* antibody. After this sort, the pool was further sorted along parallel paths either continuing with TrkB plus anti-c-*myc* antibody or employing p75 labeling alone for three additional rounds. The individual clones isolated from sorting for all four rounds using TrkB and anti-c-*myc* were labeled as “K” mutants, while those recovered from sorting the last three rounds using p75 were labeled as “P” mutants.

2.3.4 Protein secretion and purification

Yeast harboring the pRS-316-BDNF plasmids were grown 1-2 days in minimal media at 30^{o}C and diluted to a uniform OD_{600nm} of 0.1 and grown for 2 additional days at 30^{o}C. Protein expression was induced by switching to SG-CAA (with 1 mg/ml BSA as a nonspecific carrier) at 20^{o}C for 3 days. Cell-free supernatants were then collected for Western blot analysis, ELISA analysis or purification.

For protein purification, 50 mL yeast cultures were grown and induced for protein secretion. The K8, P10, or pRS-316 mock-transfected supernatants were dialyzed twice overnight at 4^{o}C against 2 L PBS, pH 8.0. The dialyzed His_6-tagged protein material was then batch purified using 250 µl superflow Ni-NTA beads (Qiagen). The BDNF-loaded beads were washed three times in 750 µl wash buffer containing 20 mM imidazole (6.9 g/L NaH_2PO_4-H_2O, 17.5 g/L NaCl, 1.36 g/L imidazole, pH 8.0) and BDNF recovered using elution buffer containing

250 mM imidazole (6.9 g/L NaH_2PO_4-H_2O, 17.5 g/L NaCl, 17 g/L imidazole, pH 8.0). Purified material was stored for up to two weeks at 4°C prior to use in activity experiments without noticeable loss of activity in TrkB binding ELISA.

2.3.5 Western Blotting

Western blotting was performed as described previously(83). Briefly, secreted BDNF in the form of supernatants and purified proteins were resolved by reducing SDS-polyacrylamide gel electrophoresis using either 12.5% or 10-20% Tris-glycine mini gradient gels (Invitrogen). Non-reducing Western blots were performed as described above, but in the absence of DTT. Resolved proteins were transferred to nitrocellulose, and membranes were probed with primary antibody 9e10 (1:1500 dilution, Covance, CA, USA), and a horseradish peroxidase (HRP)-conjugated anti-mouse secondary antibody (1:2,000; Sigma, MO, USA), followed by enhanced chemiluminescence detection with the Amersham ECL system and exposure to Amersham Hyperfilm ECL. Films at various exposure times were analyzed with ImageJ software to determine band intensities and the slope of the intensity versus exposure time curve in the unsaturated, linear region was then utilized to determine relative protein concentrations and, hence, relative secretion levels. Absolute protein concentrations for secreted BDNF mutants K8 and P10 were determined to be 1 mg/L as measured by Western blotting with anti-BDNF antibody (1:750,

Promega) primary labeling and secondary anti-chicken HRP (1:4,000, Promega) labeling with comparison to BDNF standard (50 ng/ml, Peprotech).

2.3.6 TrkB and p75 ELISA

Enzyme-linked immunosorbent assays (ELISA) were used to determine binding activity of secreted BDNF protein. Nunc-Immuno 96-well Maxisorp plates (Nunc, NY, USA) were coated with the TrkB-Fc or the p75-Fc receptor (10 µg/ml, R&D Systems) overnight at 4°C and blocked for 2 h with 250 µl PBS-BT (PBS at pH 7.4 with 1 mg/ml BSA and 0.1% Tween 20). One hundred microliters of BDNF supernatant dilution series were added at 4°C for 1 hour. BDNF protein standard (Peprotech, NJ, USA) was used as a positive control. Wells were washed four times with 250 µl PBS-BT between all labeling steps. Captured BDNF was detected by primary anti-c-*myc* 9e10 labeling (10 µg/ml, Covance) for 30 min at 4°C, and subsequent secondary anti-mouse-HRP labeling (1:2,000, Sigma) for 30 min at 4°C. Samples were incubated with 100 µl of the tetramethylbenzidine two-component microwell peroxidase substrate kit (Kirkegaard and Perry Laboratories, MD, USA). The reaction was stopped with 100 µl of 2M H_3PO_4 and absorbance at 450 nm was measured. Data in the linear range of supernatant dilution were used to determine the slope of the absorbance versus concentration curve. The slope was then normalized by the amount of total BDNF protein in the ELISA sample as determined by quantitative

Western blotting with the c-*myc* epitope to yield and specific activity to the TrkB and p75 receptors (i.e. TrkB ELISA activity/c-*myc* and p75 ELISA activity/c-*myc*).

2.3.7 Size exclusion chromatography

A Superdex 75 10/300 GL (GE Healthcare, Sweden) size exclusion column and a BioCAD 700E chromatography workstation (PerSeptive Biosystems, MN, USA) were used for size exclusion chromatography. Samples were run at 0.5 ml/min using either 250 µl Gel Filtration Standard (BioRad, CA, USA) or 300 µl purified K8. Samples were collected off the column at one minute intervals and a fraction of each elution subjected to chemical-crosslinking by the addition of 0.1% gluteraldehyde (Fisher Scientific, GA, USA) for one hour at room temperature. Cross-linking was quenched using a 2M Tris, 0.1M NaOH solution. Elution fractions with and without crosslinking were then evaluated by Western blotting under reducing conditions with anti-c-*myc* detection as described above.

2.3.8 PC12 phosphorylation

BDNF-dependent tyrosine phosphorylation of TrkB receptors was performed as previously described(63, 84, 85). Briefly, PC12 cells stably transfected with rat TrkB(86) were grown to confluence in poly-L-lysine coated (0.1 mg/ml, Sigma MO, USA) T75 flasks in culture medium (DMEM (Sigma, MO, USA) supplemented with 10% horse serum (Sigma MO, USA), 5% fetal bovine

serum (Sigma MO, USA), 100 units/ml penicillin, 100 µg/ml streptomycin, 2 mM L-glutamine (Sigma MO, USA), and 200µg/ml G418 (Sigma MO, USA)) at 37ºC. Two confluent T75 flasks per sample were prepared by starvation in serum-free medium for 30 minutes. BDNF standard (100 ng/ml, Peprotech, NJ, USA) or purified K8 and P10 were added at 450 ng/ml. To each T75 flask, 2 ml of BDNF-containing samples were added and incubated for 5 minutes at 37ºC. Flasks were then washed with ice cold PBS, pH 7.4 and lysed at 4ºC in 1 ml radioimmunoprecipitation buffer (50 mM Tris, pH 7.4, 150 mM NaCl, 1% Triton-X 100, 0.5% sodium deoxycholate, 0.1% SDS, 2mM EDTA, 2.5mM NaF) containing 1mM PMSF (Roche), 1mM sodium orthovanadate (Sigma), and complete protease inhibitors (Calbiochem Novabiochem Corp, CA, USA). Lysates were subsequently immunoprecipitated with 1 µg rabbit anti-pan-Trk IgG (C-14, Santa Cruz, CA, USA) at 4ºC for 2 hours. To this mixture, 25 µl of cross-linked 6% Protein A beaded agarose supplied as a 50% slurry (Pierce, IL, USA) were added and incubated at 4ºC for 1-2 hours. Samples were washed 3x with 1 ml ice cold Lysis buffer and 1x with 1 ml ice cold sterile ddH_2O. Immunoprecipitated complexes were eluted using 1x Laemmli loading buffer and boiling for 5 minutes, separated on 8% SDS/PAGE (Invitrogen, CA, USA), and transferred to nitrocellulose with overnight blocking in 5% milk. Blots were probed either overnight with anti-phosphoTrk (1:1,000, Cell Signaling Technology, MA, USA) or 1.5 hours with anti-pan-Trk IgG (C-14, Santa Cruz) and an anti-rabbit HRP (1:10,000, Sigma) secondary antibody.

2.4 Results

2.4.1 Creation of a BDNF scaffold capable of binding its natural receptors

BDNF was displayed on the yeast cell surface by standard fusion to the C-terminus of the a-agglutinin subunit Aga2p (Figure 2.1 Ai), and full-length BDNF was detected on the yeast surface via the c-*myc* tag, albeit at relatively low levels (Figure 2.1 B). Binding of the surface-displayed protein to its natural receptors, TrkB and p75, was assessed as a measure of proper folding and homodimer assembly. While TrkB binding was detected, binding to p75 was not detected (Figure 2.1 B). Moreover, BDNF secreted to the culture medium was in the form of disulfide-bonded aggregates as evidenced by its inability to enter a nonreducing SDS-PAGE gel and by lack of substantial activity in a TrkB ELISA (Figure 2.1 C). Combined, these data suggested that secreted BDNF, and to some extent displayed BDNF, was produced in a largely inactive, misfolded form that was in some way capable of evading the yeast quality control machinery.

Therefore, to facilitate BDNF folding and processing in yeast, we engineered BDNF through two successive rounds of directed evolution (Figure 2.2 A). For directed evolution round 1 (DE Rd1), a randomly mutagenized $4x10^6$ member BDNF library was screened using the dual criteria of increased TrkB binding activity and increased cell surface expression (Figure 2.2 A, and see Materials and Methods for details). After three rounds of FACS-based sorting, the enriched pools indicated substantial improvements in TrkB binding and full-

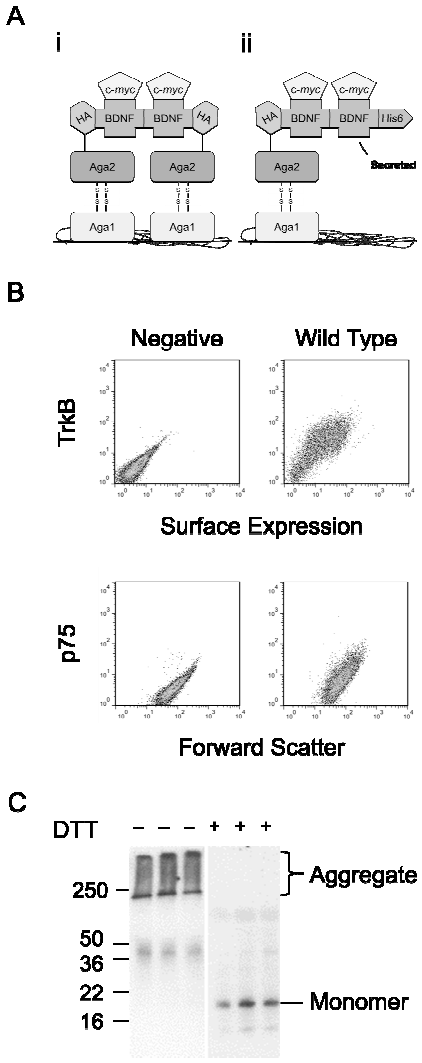

Figure 2.1 Production of BDNF using yeast. (A) Schematic of surface displayed BDNF constructs displayed (i) as a dimer of two surface-display proteins, and (ii) as a dimer of one surface-display protein and one secreted and captured protein. (B) Expression and receptor binding properties of wild-type BDNF displayed on yeast surface using scheme (i). Sample flow cytometric dot plots of surface-displayed wild-type BDNF co-labeled with its natural receptor TrkB and an anti-c-*myc* antibody to monitor full-length expression or alternatively, p75 labeling alone. Negative sample is unlabeled BDNF-displaying yeast. Quantified data is reported in Table 2.1. (C) Western blots of secreted wild-type BDNF with or without reduction by DTT. Supernatants from triplicate independent transformants were analyzed. Molecular weights are indicated in kDa.

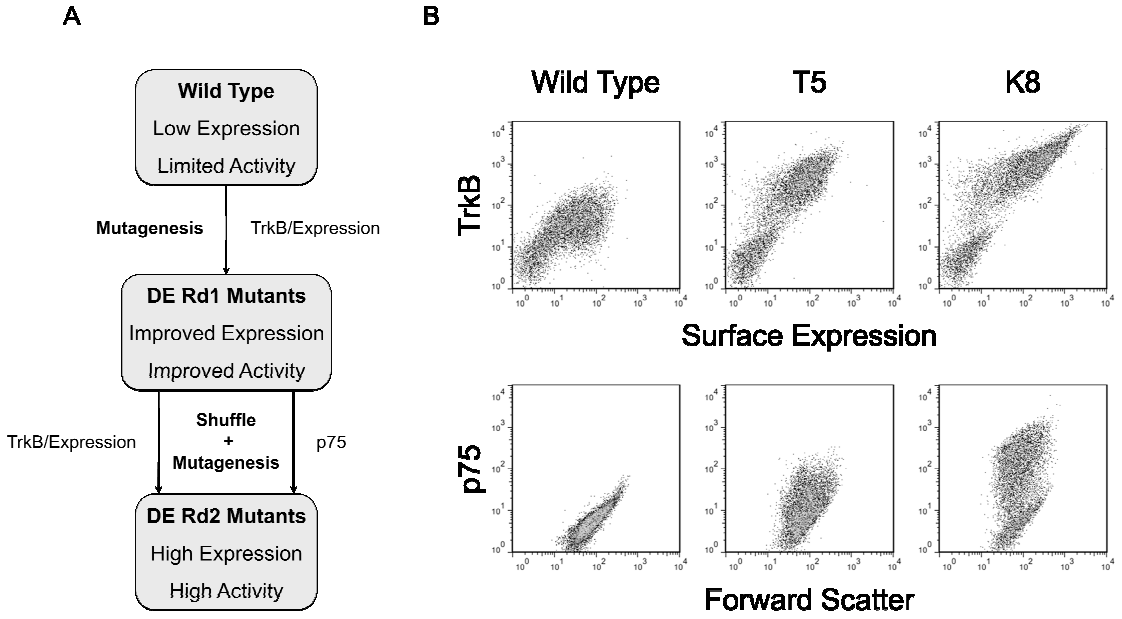

Figure 2.2. Directed evolution of BDNF. (A) Flow chart of the directed evolution process illustrating outcomes and screening criterion. (B) Flow cytometric data illustrating the directed evolution improvement in BDNF activity (TrkB and p75) and full-length expression (anti-c-*myc* antibody) as a surface displayed protein. Mutant T5 is shown as an example of DE Rd1 mutants and K8 as an example of DE Rd2 mutants. Quantified data are displayed in Table 2.1 for all DE Rd1 and Rd2 mutants assessed.

length expression. Individual BDNF mutants were isolated and evaluated for their receptor binding and expression properties (Table 2.1). On average, the DE Rd1 mutants showed a 4-fold increase in TrkB labeling and a 1.6-fold average increase in full-length expression of over wild-type BDNF indicating an average 2.5-fold increase in receptor binding per molecule (Figure 2.2 B). Since the screen and clonal evaluation was performed at saturating TrkB concentration, these binding per molecule values represent a “specific activity” for surface displayed BDNF. Interestingly, while p75 binding was not detected for displayed wild-type BDNF, it became evident in many of the mutants in the DE Rd1 enriched pool. Accordingly, individual DE Rd1 mutants exhibited clear binding to p75 (Figure 2.2 B, Table 2.1). Given that p75 was not included in the DE round 1 screening process, and since p75 and Trk receptors have distinct binding epitopes on neurotrophins(60, 87), these results suggest that the improvements in specific activity are resulting from a general improvement in folding fidelity of the BDNF mutants, rather than from an isolated improvement in the vicinity of the TrkB binding site.

Since sequencing revealed non-overlapping mutations in the unique clones derived from DE Rd 1 (Table 2.1), it was hypothesized that additional improvement could be achieved by combination of these alterations through molecular shuffling. Thus, a second round of directed evolution (DE Rd2) was conducted in which the unique clones isolated from DE Rd1 were shuffled and subjected to a low level of additional mutagenesis. Since folding fidelity

Table 2.1. Properties of BDNF mutants.

Amino Acid Position	Wild Type	DE Rd1				DE Rd2						
		T4	T5	B2	B5	P1	P3	P5	P10	K3	K6	K8
11	Ser	-	-	-	Cys	Cys	Cys	Cys	Cys	Cys	Cys	-
34	Gly	-	Glu	-	-	Glu	Glu	-	-	Glu	-	Glu
40	Glu	-	-	Asp	-	-	-	-	Asp	-	-	Asp
41	Lys	-	-	Glu	-	-	-	Glu	Glu	-	Glu	Glu
48	Gln	-	-	Arg	-	-	-	Arg	Arg	-	Arg	Arg
50	Lys	-	-	-	-	-	-	-	-	Ala	-	-
61	Met	-	-	-	Thr	-	-	-	-	-	-	-
66	Glu	Gly	-	-	-	Gly	-	Gly	Gly	Gly	-	-
67	Gly	-	Cys	-	-	-	-	-	-	-	-	Cys
73	Lys	-	-	Glu	-	-	-	-	-	-	-	-
83	Thr	-	-	-	-	-	-	-	-	Ala	-	-
95	Lys	-	-	Glu	-	-	-	-	-	-	-	-
108	Ser	Ala	-	-	-	Ala	Ala	Ala	Ala	-	Ala	Ala
115	Ile	-	-	-	-	-	-	Ser	Ser	-	-	-
c-*myc* [a]	1.0 ± 0.1	1.4 ± 0.1	1.4 ± 0.1	1.4 ± 0.1	2.4 ± 0.1	5.0 ± 0.7	4.2 ± 0.4	4.1 ± 0.2	5.2 ± 0.4	5.1 ± 0.1	3.1 ± 0.3	3.4 ± 0.1
TrkB/c-*myc* [b]	1.0 ± 0.1	3.1 ± 0.1	3.9 ± 0.3	2.0 ± 0.3	1.5 ± 0.1	2.7 ± 0.3	2.6 ± 0.3	2.7 ± 0.1	2.4 ± 0.1	3.0 ± 0.1	2.9 ± 0.2	4.0 ± 0.3
p75/c-*myc* [c]	none	1.6 ± 0.1	1.0 ± 0.1	none	0.6 ± 0.1	5.0 ± 0.9	3.4 ± 0.3	5.9 ± 0.2	4.7 ± 0.5	2.9 ± 0.1	3.4 ± 0.3	3.4 ± 0.3

All values listed in table are expressed as mean ± S.D. of triplicate independent transformants

a. Full-length expression on yeast surface as determined by c-*myc* epitope labeling and flow cytometry and normalized to wild-type BDNF.
b. Specific binding activity towards TrkB as determined by flow cytometry and normalized to wild-type BDNF.
c. Specific binding activity towards p75 as determined by flow cytometry and normalized to mutant T5.

$p<0.05$ for all values of TrkB and c-*myc* with respect to wild-type BDNF and $p<0.05$ for all values of p75 with respect to T5.

appeared to be linked to p75 binding for mutants isolated in DE Rd1, we introduced p75 as a further conformational screening criterion for DE Rd2 in parallel to employing solely TrkB during the sorting process (Figure 2.2 A and see Materials and Methods for details). Enriched DE Rd2 pools exhibited an additional increase in TrkB binding and full-length expression along with a notable increase in p75 binding. On a clonal mutant BDNF basis, TrkB binding and full-length expression increased together such that the specific activity towards TrkB was not further increased over DE Rd1 (Table 2.1 and Figure 2.2 B). However, regardless of whether p75 was included as a screening criterion in DE Rd2 (e.g. “P” p75 or “K” TrkB mutants), specific activity towards p75 was found to increase an average of 4.1-fold over the DE Rd1 clone, T5. Sequence analysis revealed that the BDNF mutants selected in DE Rd2 were primarily a result of shuffled combination of the mutations from DE Rd1 (Table 2.1). As mentioned above, screens in both DE Rd1 and DE Rd2 were biased towards improvements in folding fidelity rather than improvements in affinity by screening using saturating TrkB and p75 concentrations. To confirm, apparent TrkB binding affinities for several DE Rd1 and Rd2 BDNF mutants were measured and as expected, apparent TrkB binding affinities were not improved. Instead, while the apparent affinities of BDNF mutants remained in the low nanomolar range, they were marginally decreased compared with wild-type BDNF (Supplemental Figure 2.S1). In summary, each BDNF clone isolated after DE Rd2 demonstrates

A

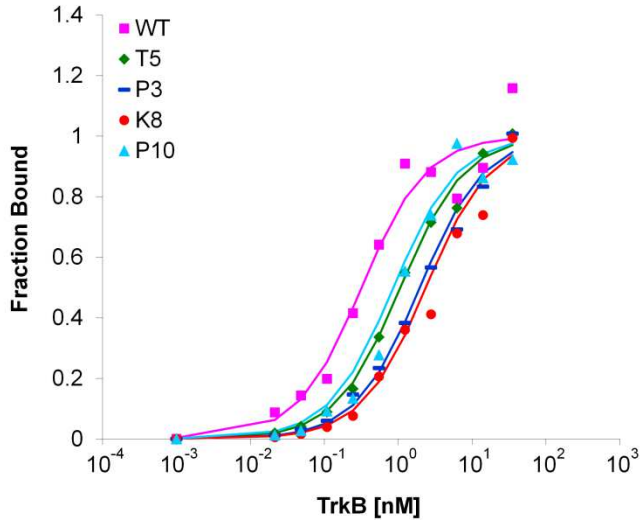

B

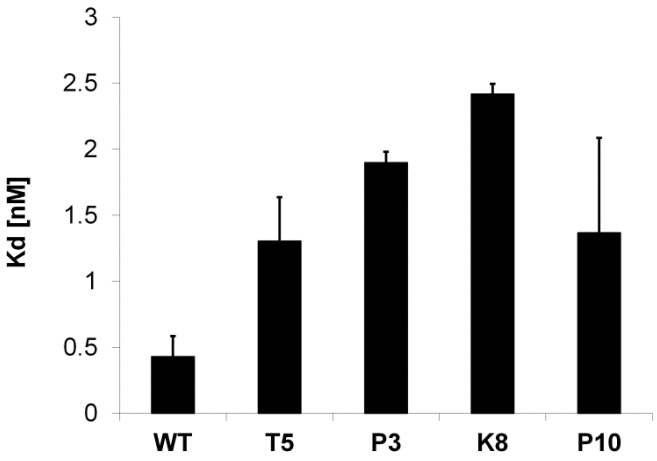

Supplemental Figure 2.S1. Apparent TrkB binding affinity for selected mutant BDNF constructs. (A) Using yeast surface display, the apparent binding affinity to TrkB was determined. Single titration curves are shown. (B) Quantified apparent TrkB binding affinity (K_D) derived from duplicate titrations originating from two independent yeast transformants for each mutant, mean ± S.D..

improved specific activity to both natural receptors, TrkB and p75, likely as a result of improved folding and processing in yeast.

2.4.2 Mutation effects on surface displayed and secreted BDNF binding activity and expression

To further explore the individual mutants and the effects of certain mutations on expression and specific activity, we compared BDNF mutants as surface displayed and secreted proteins. Mutagenesis in DE Rd1 served to improve the folding fidelity of BDNF displayed on the yeast surface as evidenced by improved specific activity towards TrkB and p75, combined with small improvements in the display of full-length protein (Table 2.1). Using receptor binding ELISAs, secreted DE Rd1 mutant T5 exhibited improved TrkB binding activity compared to wild-type BDNF, and unlike wild-type BDNF, secreted T5 exhibited p75 binding activity as was observed on the yeast surface (Table 2.1 and Figs. 3A and 3B). The secreted and surface display protein expression levels correlated quite well for the individual BDNF mutants studied with 5-fold improvements in secretion yield for many Rd2 mutants (Figs. 3C and 3D). However, the specific TrkB binding activity of most Rd2 mutants was not further increased over Rd1 levels either on the surface or as soluble protein suggesting that these mutants could be generally classified as “expression” mutants (Figure 2.3 A, e.g. Rd2 mutants K6, P5, P3). However, when Glu40Asp was present in

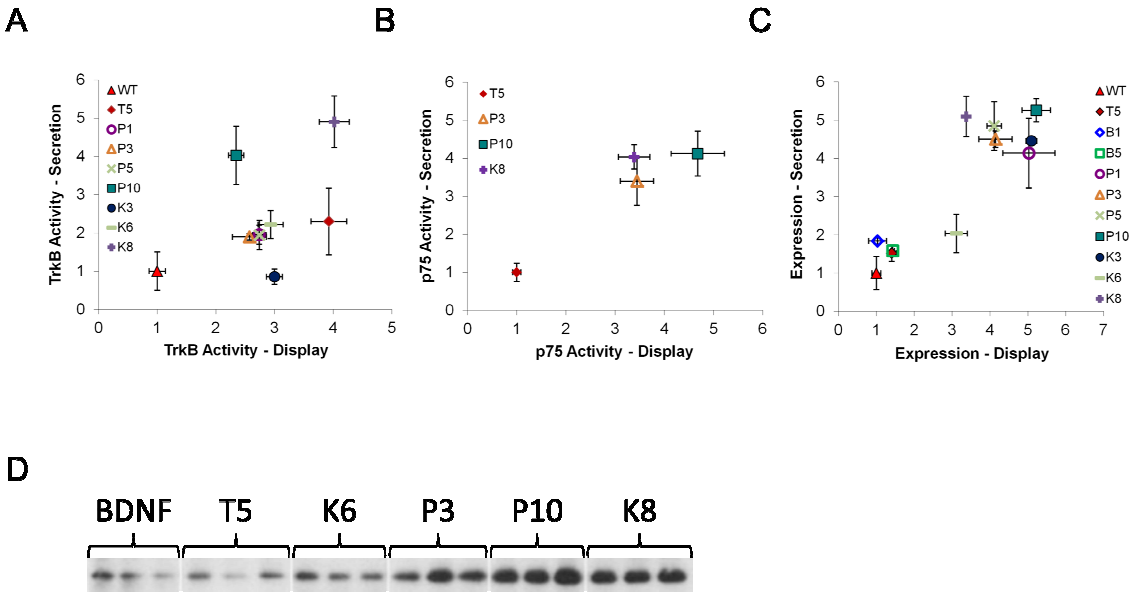

Figure 2.3. Comparison of BDNF binding and expression properties as displayed and secreted proteins. (A) Specific binding activity towards the TrkB receptor as measured on the yeast surface by flow cytometry (Display) or for secreted protein by ELISA (Secretion). TrkB binding activity is expressed per full-length molecule as assessed by the c-*myc* epitope and normalized to wild-type BDNF activity. (B) Specific binding activity towards the p75 receptor determined as in (A), and normalized to the T5 BDNF mutant. (C) Relative expression levels determined by flow cytometry (Display) or Western blot (Secretion), and normalized to wild-type BDNF. For panels A-C, data are expressed as mean ± S.D. of triplicate independent transformants. (D) Sample Western blot data used to generate relative secretion values reported in Figure 2.3 C.

addition to the “expression” mutations, the specific TrkB binding activity of secreted BDNF protein was improved substantially (compare P10 to P5 and K8 to K6 and T5, $p<0.05$). In addition, improved specific p75 binding activity on the yeast surface correlated well with improved binding activity as secreted protein for those mutants tested (Figure 2.3 B). Taken together, P10 and K8 had the best combination of expression and binding properties as secreted proteins.

An interesting set of mutations involved cysteine residues that reside proximal to the native cysteines forming the intramolecular cysteine knot disulfide bond architecture (Figure 2.4 B). The predominant cysteine mutation in DE Rd2 was the Ser11Cys mutation which is two amino acids removed from the native Cys13 residue. The other DE Rd2 cysteine mutation, found only in the K8 mutant, was Gly67Cys which is directly adjacent to the native Cys68 residue. Cysteines 13 and 68 participate in two different disulfide bonds within the cysteine knot structure (Figure 2.4 B). To determine the extent of involvement the cysteine modifications had on the observed improvements in cell surface BDNF expression and binding activity, we created several additional BDNF mutant constructs with alterations at positions 11, 13, 67, and 68 and analyzed them using yeast surface display (Figure 2.5). Beginning with mutant P3 having the fewest mutations in DE Rd2, the Cys11 mutation was reverted to the wild-type Ser residue (P3 Cys11Ser); and while the specific binding activity towards TrkB was not affected ($p>0.05$), the expression level and specific binding activity towards p75 were substantially decreased ($p<0.05$). When the Cys67 mutation

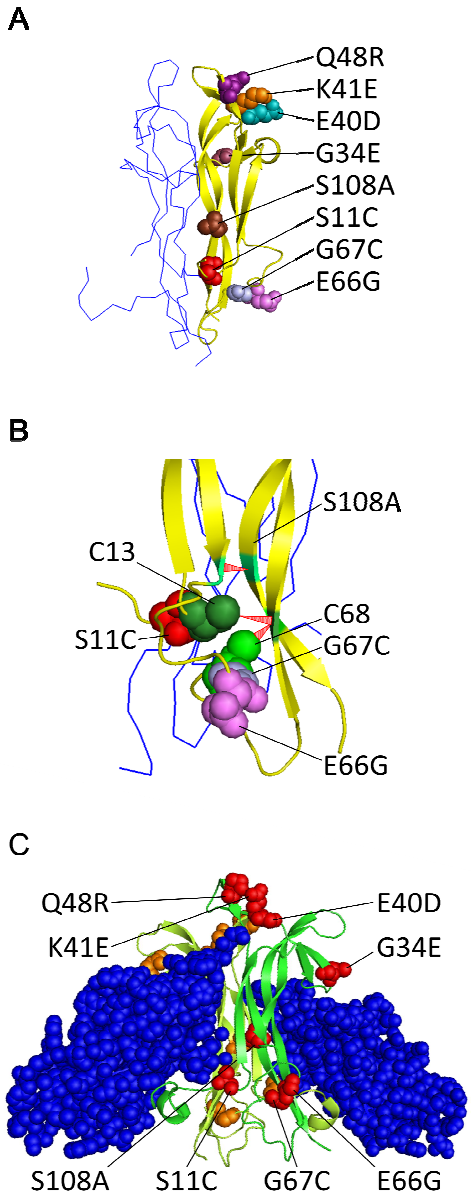

Figure 2.4. Structural locations of identified mutations. (A) BDNF (yellow) and Neurotrophin 4 (blue) heterodimer structure (1HCF.pdb, (44)) with residues subject to mutation in P10 and K8 highlighted. (B) Enlarged view of cysteine knot protein core highlighting the native Cys13 and Cys68 residues as well as the Ser11Cys and Gly67Cys mutations along with the three intramolecular disulfide bonds (red lines). (C) Structure of Neurotrophin 4 homodimer (dark/light green) binding to the TrkB receptor (blue) (1B8M.pdb, (10)). The homologous NT4 residues corresponding to the P10 and K8 mutations are highlighted (red/orange).

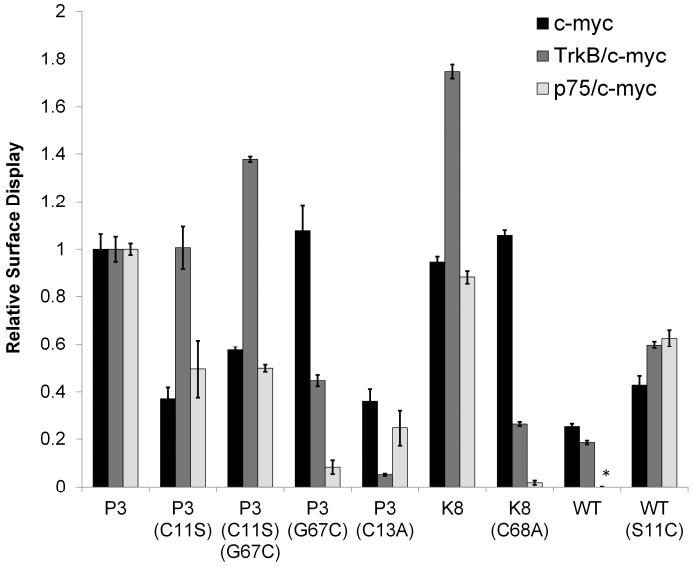

Figure 2.5. Evaluation of cysteine mutations by site directed mutagenesis and yeast surface display. Cysteine mutations and reversions were incorporated into the P3, K8, and wild-type BDNF (WT) constructs. Specific binding activity towards p75 and TrkB along with full-length expression level (c-*myc*) were measured by flow cytometry. Data represent mean ± S.D. of triplicate independent transformants. * Labeling not detected for this construct.

found in the K8 mutant was added in replacement of the Cys11 in the P3 mutant (P3 Gly67Cys, Cys11Ser), protein expression level and p75 binding activity remained reduced compared with the P3 parent ($p<0.05$). There was a small increase in specific binding activity towards TrkB similar to the increase observed when comparing K8 and the rest of the DE Rd2 mutants including P3 (Figure 2.3 A, $p<0.05$). Since Gly67Cys could not complement the effects of Cys11Ser reversion, the Ser11Cys and Gly67Cys mutations appeared to play different roles, at least in the P3 background. Thus, to check for a possible synergy of the two Cys mutations, the Gly67Cys mutation was added to the P3 mutant (P3 Gly67Cys), but specific binding activity towards both TrkB and p75 were reduced ($p<0.05$). Moreover, knocking out the natural cysteine in either P3 (Cys13Ala) or K8 (Cys68Ala) had substantial detrimental effects on the binding activity for both receptors ($p<0.05$) suggesting that neither of the cysteine mutations was simply replacing the natural cysteine in the disulfide-bonding network. Finally, when the predominant DE Rd2 Ser11Cys mutation was added as the sole mutation to wild-type BDNF, surface expression along with both TrkB and p75 specific binding activity were increased compared to wild-type BDNF ($p<0.05$), though not to the levels observed for P3. These data indicated that while important, other mutations in addition to Ser11Cys are required for proper BDNF folding and processing to the yeast surface. In addition to the cysteine modifications, the Gly34Glu and the Ser108Ala mutations were found in the majority of isolated mutant BDNF constructs often in coordination with Ser11Cys. Mutant P3

combines these three alterations and expression, TrkB binding, and P75 binding were all improved indicating these constitute a “minimal mutant” that has reasonable expression and binding function both on the surface and as soluble protein (Table 2.1 and Figure 2.3).

Biologically active BDNF exists as a homodimer held together by hydrophobic interactions, and TrkB and p75 receptors engage both monomers in a homodimeric pair(60, 87, 88). Thus, we next assessed preservation of the dimerization interface amongst the most favorable K8 and P10 mutants on the yeast surface. First, BDNF dimerization was demonstrated by co-expressing a secreted BDNF construct with a traceable epitope (His6) simultaneously with the Aga2p-fused surface tethered construct bearing the c-*myc* epitope tag (Figure 2.1 Aii). Thus, association between a tethered BDNF monomer and a secreted BDNF monomer could be detected simply by measuring the amount of His6 epitope (secreted BDNF) captured on the yeast surface, along with maintenance of TrkB binding activity. In this way, it was demonstrated that the K8 and P10 mutants associate via putative dimerization since the secreted forms could be specifically captured on the yeast surface by tethered K8 or P10 (Figure 2.6). In contrast, K8 showed no capture of an irrelevant single-chain antibody (4-4-20), nor did display of a highly expressed c-*myc* epitope lead to any K8 capture, indicating that the capture is specific to the pairing of BDNF monomers (Figure 2.6). Furthermore, tethered K8 could capture secreted P10 and bind TrkB,

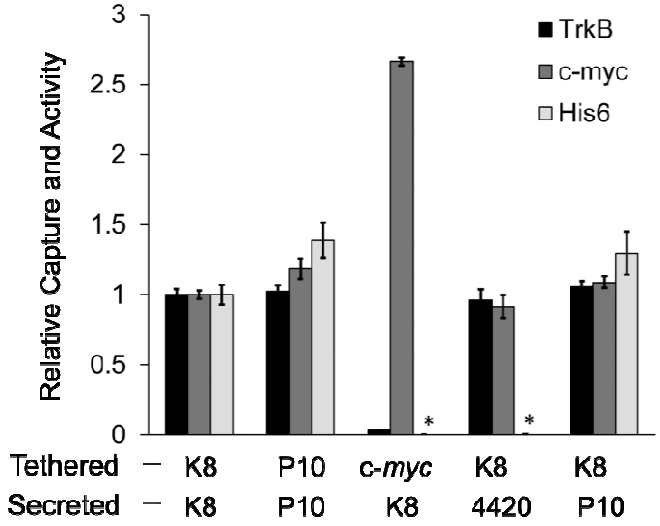

Figure 2.6. Surface capture of secreted BDNF mutants. Co-expression of surface display and secretion constructs was performed as indicated in Figure 2.1 Aii prior to evaluation of TrkB binding, c-*myc* (tethered display) and His6 (secreted and captured display) epitope tags by flow cytometry. All labeling is normalized to that for the K8 mutant. Tethered c-*myc* sample is an Aga2p fusion with the c-*myc* epitope (i.e. Figure 2.1 Aii without the BDNF insertion). The secretion sample 4420 represents an anti-fluorescein single-chain antibody. * His6 labeling not detected for these constructs. Reported are mean ± S.D. of triplicate independent transformants.

indicating that dimerization interactions occur between two distinct mutants and suggesting a conservation of the dimerization interface (Figure 2.6).

2.4.3 Fidelity and biological activity of secreted BDNF mutants

To further validate that the BDNF mutants maintained their homodimeric structures, we next purified K8 via the six histidine tag (purified yield ~1 mg/L) and investigated molecular isoforms using size exclusion chromatography (SEC) combined with chemical crosslinking. SEC elution fractions were subjected to gluteraldehyde crosslinking to investigate monomer, dimer, or higher order multimer formation. As Figure 2.7 indicates, the majority of the secreted K8 protein is in the form of BDNF homodimers, as confirmed by chemical crosslinking prior to Western blot analysis (~70%, 21-24 minutes). A small amount of K8 BDNF is secreted in the form of large molecular weight aggregates at early elution times (~15%, 17-19 minutes), and very little in the form of monomer (~2%, 26 minutes). Finally, an examination of the secretion product by Western blot in the presence or absence of reducing agent and crosslinking indicates the presence of homodimers (Figure 2.7 B, +G.A. –DTT) that can be disrupted by SDS treatment (Figure 2.7 B, -G.A. –DTT), indicating hydrophobic homodimerization as opposed to any newly introduced disulfide-based dimerization via the Gly67Cys mutation. Taken together, these experiments indicate that the secreted mutant BDNF exists largely as noncovalent

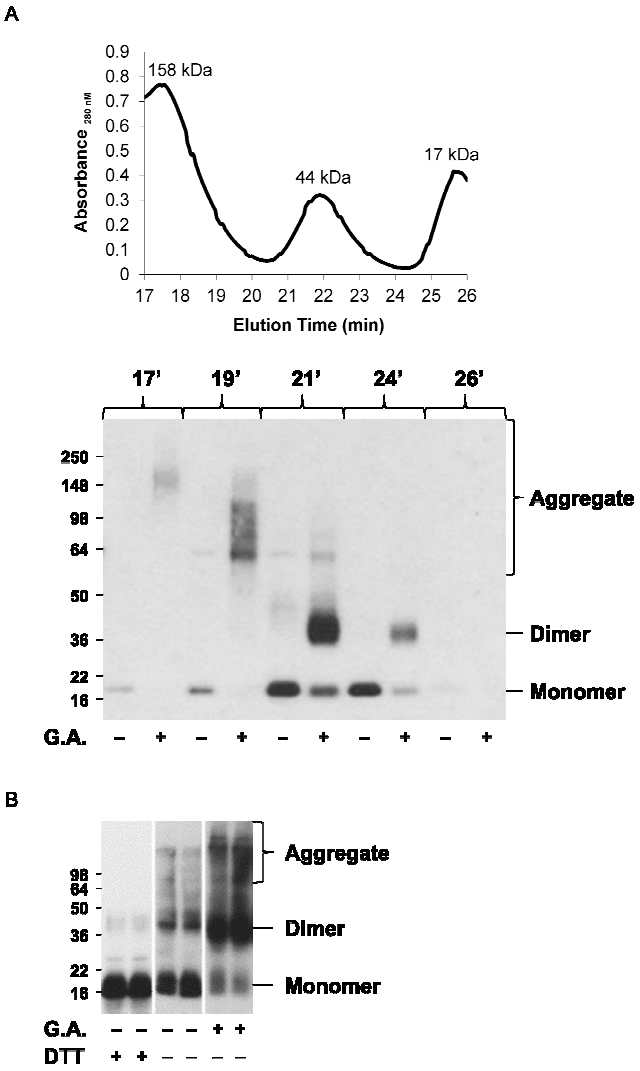

Figure 2.7. Size-exclusion chromatography analysis of secreted and purified K8 BDNF mutant. (A) Top panel is elution chromatogram of molecular weight standards. Bottom panel is Western blot of K8 sample eluates aligned by elution time with the molecular weight standards. Samples were run under reducing conditions with (+) and without (-) gluteraldehyde (G.A.) crosslinking. (B) Western blot of secreted and purified K8 under both reducing and nonreducing SDS-PAGE conditions (+/- DTT) and with and without crosslinking (+/- G.A.). A slightly overexposed blot is presented to allow viewing of all BDNF species.

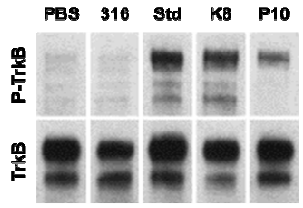

Figure 2.8. TrkB phosphorylation by K8 and P10 BDNF mutants. TrkB-transfected PC12 cells were exposed to commercial wild-type BDNF (Std), BDNF mutant K8 (K8), BDNF mutant P10 (P10), and two negative controls: yeast supernatant from cells containing an empty secretion vector (316), and a saline treated sample (PBS). Western blotting of pan-TrkB immunoprecipitated product is shown with detection of either phosphorylated Trk receptor (P-Trk) or total Trk receptor.

homodimers, contrasting significantly with the large disulfide-bonded aggregates observed for secreted wild-type BDNF (Figure 2.1 C).

Finally, in addition to the ELISA-based binding activity demonstrated for secreted BDNF mutants, K8 and P10 BDNF mutants were tested for their capability to elicit biological activity in the form of intracellular phosphorylation of TrkB receptors. The K8 and P10 proteins were purified and added to pre-starved TrkB-transfected rat adrenal pheochromocytoma cells (PC12)(89). Specific phosphorylation of the TrkB receptor was demonstrated for both K8 and P10 (Figure 2.8).

2.5 Discussion

In this report, the yeast display and secretion properties of BDNF were improved substantially through directed evolution. Wild-type BDNF was secreted in small quantity as a misfolded aggregate capable in some way of evading the normally stringent yeast quality control mechanisms(90). Similarly, wild-type BDNF was expressed at relatively low levels on the yeast cell surface, and while it was capable of binding TrkB, binding to p75 was not detected. The capability for misfolded heterologous proteins to overcome yeast quality control is not unique to BDNF, and has been observed for display of epidermal growth factor receptor extracellular domain, and binding loop inserted green fluorescent proteins, which were expressed on the yeast cell surface in a partially misfolded state(70, 72). During DE Rd1, it was discovered that the BDNF mutants were better displayed on the yeast surface, and possessed better specific binding activity towards TrkB and unlike wild-type BDNF, could bind the p75 receptor. During DE Rd2, several mutants were identified whose effects of increased specific binding activity to TrkB and p75 translated well from the yeast surface to secreted protein. In particular, the improved properties of mutants K8 and P10 as secreted proteins appeared to be driven at least in part by the Glu40Asp mutation (Figure 2.4 A). This fairly conservative mutation is localized to the solvent exposed BDNF surface outside of the putative TrkB and p75 binding sites(60, 87), suggesting that the improvements in specific TrkB and p75 binding

activity may be a result of the Glu40Asp mutation playing an important role in locking in the folded conformation of the secreted BDNF. Mutant K8 was secreted at 1 mg/L, and the formation of large molecular weight aggregates in secreted product was substantially decreased (compare Figure 2.7 B, –DTT lane with Figure 2.1 C wild-type BDNF) with the majority of the material being produced in dimeric form as evidence by chemical crosslinking experiments. Additionally, secreted K8 and P10 mutants both were capable of triggering receptor phosphorylation in a cellular context. Taken together, these evolved BDNF mutants are capable of overcoming deficits in yeast secretory processing to exhibit much better expression, folding fidelity, and activity than wild-type BDNF.

In addition to the key Glu40Asp mutant, all DE Rd2 mutants possessed a cysteine mutation at either amino acid position 11 (Ser11Cys) or 67 (Gly67Cys) that are proximal to the native cysteine residues at positions 13 and 68, respectively (Figure 2.4 B). The native Cys13 and Cys68 residues are involved in two of the three intramolecular disulfide bonds that comprise the cysteine-knot configuration of each BDNF monomer(91). Analysis of the receptor binding properties of P3 having the native Cys13 changed to alanine or K8 having the native Cys68 changed to alanine yielded substantial deficits in folding and expression indicated that these native cysteine residues remain crucial for mutant BDNF processing. Moreover, reversion of the Ser11Cys mutation was detrimental to expression and overall fold for P3 BDNF, indicating the specific

impact of this mutation. The Ser11Cys mutation is a conservative change in terms of physiochemical properties, other than the capability to participate in disulfide bonds. Moreover, the aforementioned processing deficits upon mutation of the native cysteines also suggested that the native cysteines are not likely replaced in the disulfide-bond network by the proximal Ser11Cys or Gly67Cys mutations in P3 or K8, respectively. An additional possibility is for the new proximal cysteine residues to drive homodimer assembly by intermolecular disulfide bonding. However, nonreducing Western blotting indicated that the homodimeric interactions of the BDNF mutants were hydrophobic in nature, and the mutations instead substantially reduced the aberrant disulfide bonded aggregates observed with wild-type BDNF. Thus, it may be plausible that the new proximal cysteine residues provided by Ser11Cys or Gly67Cys enable transient non-native disulfide formation in productive folding intermediates that yield more efficient native disulfide pairing, although further detailed study would be required to test this hypothesis. In addition, the Glu66Gly mutation just two residues removed from the native Cys68 was present in many DE Rd2 mutants such as P10. However, the Glu66Gly mutation did not appear in concert with the Gly67Cys mutation, perhaps indicating that this region of the protein offered structural challenges to folding that could be addressed by either mutation. As a comparative example, yeast display and directed evolution of tumor necrosis factor receptor identified expression-enhancing proline mutations that helped lock adjacent cysteine residues into correct orientations for disulfide bonding(92).

Finally, when Ser11Cys was introduced as the only mutation into wild-type BDNF, the protein was more well expressed and could bind both TrkB and p75, but not to the level of P3, indicating that other mutations arising from the DE process are playing important roles.

An examination of the mutations present in K8 and P10 indicates that they are all located in BDNF regions that are not predicted to make contact with TrkB, based on BDNF and NT4/5 structural homology in combination with the solved NT4/5-TrkB structure (Figure 2.4 C)(60, 93). (60)(60)(60)(60)(60)Given that the screening pressures were for improved expression and folding as measured by receptor binding at saturating concentrations, identification of mutations that all lie outside of the putative BDNF-TrkB interface(60) indicated the screening pressure effectively focused towards better folded mutants rather than higher affinity mutants. Indeed, while BDNF mutation improved the specific activity towards TrkB (binding/molecule), affinity measurements indicated some decrease in the apparent TrkB binding affinities (Kd) for the mutant BDNF constructs, although they still remained in the low nanomolar range as previously reported(94, 95). If critical, the BDNF binding affinity to its receptors could always be improved as desired in further protein engineering efforts(79, 96).

Residues Glu40, Lys41, and Gln48 were previously shown to be part of a BDNF loop region that when swapped into a BDNF-NGF chimera could help improve TrkB binding and activity of the chimeric molecule indicating a capacity to affect the folded conformation(97, 98). Moreover, during loop swapping

experiments, expression levels were also diminished, suggesting that this loop region can affect expression as well(97). Mapping onto these observations, we found that mutations in this same loop region were capable of improving protein expression and specific activity of BDNF towards the TrkB receptor, likely through improved folding fidelity. Each of the Glu40Asp, Lys41Glu, and Gln48Arg mutations incorporates an amino acid with sidechain properties that lead to addition or change of charge in these solvent exposed residues. Mutational change to charged residues at solvent exposed protein interfaces has been show previously to elicit improvements in expression, stability, activity and solubility of engineered proteins(68, 99).

Finally, Ser108 is located within the highly conserved hydrophobic interface that leads to neurotrophin homodimer formation(100), and most of the DE Rd2 mutants, including K8 and P10 contain the Ser108Ala mutation (Figure 2.4 A). The addition of another nonpolar hydrophobic residue could possibly help promote proper neurotrophin assembly by influencing the hydrophobic dimerization interface. Interestingly, while BDNF and NT3 have a serine at position 108, NGF and NT4 possess an alanine at this position, and it is known that BDNF can heterodimerize with both NT3 and NT4(93, 100) indicating that the Ser108Ala change is tolerated at the interface. Indeed, the homodimeric (K8:K8 and P10:P10) and heterodimeric (K8:P10) pairing of the BDNF mutants by surface capture indicated maintenance of the hydrophobic dimerization interface in the presence of the Ser108Ala mutation as well as the other

mutations present in the K8 and P10 versions of BDNF. In conclusion, this work demonstrates that yeast surface display combined with directed evolution approaches can be used to improve the expression and folding properties of BDNF. Moreover, the successful surface display of well-folded BDNF will enable use of the yeast display protein engineering toolkit for applications such as neurotrophin affinity maturation, stability engineering and epitope mapping.

Chapter 3: Pro-Leader Engineering for Improved Yeast Display and Secretion of Brain Derived Neurotrophic Factor

(This chapter was produced by Michael L. Burns[1], Thomas M. Malott[1], Kevin J. Metcalf, Arthya Puguh, Jonah R. Chan, Eric V. Shusta and was submitted to Biotechnology Journal for publication)
[1] These authors contributed equally

3.1 Abstract

Brain derived neurotrophic factor (BDNF) is a promising therapeutic candidate for a variety of neurological diseases. However, it is difficult to produce as a recombinant protein. In its native mammalian context, BDNF is first produced as a pro-protein with subsequent proteolytic removal of the pro-region to yield mature BDNF protein. Therefore, in an attempt to improve yeast as a host for heterologous BDNF production, the BDNF pro-region was first evaluated for its effects on BDNF surface display and secretion. Addition of the wild-type pro-region to yeast BDNF production constructs improved BDNF folding both as a surface-displayed and secreted protein in terms of binding its natural receptors TrkB and p75, but titers remained low. Looking to further enhance the chaperone-like functions provided by the pro-region, two rounds of directed evolution were performed, yielding mutated pro-regions that further improved the display and secretion properties of BDNF. Subsequent optimization of the

protease recognition site was used to control whether the produced protein was in pro- or mature BDNF forms. Taken together, we have demonstrated an effective strategy for improving BDNF compatibility with yeast protein engineering and secretion platforms.

3.2 Introduction

Brain-derived neurotrophic factor (BDNF) is a member of the neurotrophin family which also includes nerve growth factor (NGF), neurotrophin-3 (NT-3), and neurotrophin-4 (NT-4). The neurotrophins elicit biological function through interactions with the p75 neurotrophin receptor (p75) and members of the tropomyosin receptor kinase (Trk) receptor family. Neurotrophins are paramount to the development and function of the mammalian peripheral and central nervous systems, playing roles in neuronal survival, differentiation, and synaptic plasticity (53, 101-105). As a result, neurotrophins have often been considered as potential therapeutics (106).

Neurotrophins function as noncovalent dimers with each monomer possessing the cysteine-knot motif comprising a network of three intramolecular disulfide bonds. There have been many efforts to produce recombinant neurotrophins in microbial hosts, albeit with limited success (45, 66, 67, 107, 108). Attempts to use bacterial systems to produce BDNF result in largely insoluble protein with mismatched disulfide bonds that requires refolding (67, 107, 109). Moreover, after refolding, the proteins possess low biological activity (67). Although yeast possess a eukaryotic folding and quality control apparatus that includes chaperones and foldases to assist secretory folding of disulfide-bonded proteins, attempts to produce NGF resulted in recombinant protein having very low specific activity (66). In previous work, we observed a similar

result when attempting to produce BDNF using yeast, but found that the BDNF expression level and folding fidelity could be improved by directed evolution of the BDNF protein itself (47). However, many therapeutic and scientific applications might be better served by approaches that could improve BDNF production in the absence of mutation.

All neurotrophins are naturally produced as pro-proteins with the pro-region aiding in both the expression and folding of mature neurotrophin (110, 111). Mature neurotrophins are produced by cleavage of the pro-region by pro-protein convertases including furin (112, 113). In addition, several domains of the pro-region were found to be important for the biosynthesis of NGF during normal processing (110), and the pro-region has been suggested to function as a chaperone by aiding in the proper folding of mature neurotrophins (111, 114, 115). While the exact nature of chaperone activity imparted by the pro-region is still being resolved, the chaperone interaction is suggested to occur by direct intramolecular association between the neurotrophin and its conjugated pro-region (112, 116). Importantly, in terms of heterologous neurotrophin production, conjugation to the pro-region was shown to significantly improve oxidative refolding yields and kinetics of NGF from *E.coli* inclusion bodies (111, 114, 115). Taken together, these data indicate that the pro-region may assist neurotrophin processing within the cell, suggesting that a heterologous production system could benefit from employing the native neurotrophin pro-region. In this report, we have therefore investigated the capacity for the pro-region to improve yeast

BDNF production. Inclusion of the wild-type BDNF pro-region in the expression constructs led to improved surface display and secretion of active BDNF. Directed evolution of the pro-region further increased titers and specific activity of yeast-produced BDNF, and modification of the protease recognition site could regulate the balance of pro- or mature BDNF.

3.3 Materials and Methods

3.3.1 Cells, Media, and Plasmids

Saccharomyces cerevisiae strains EBY100 (*MAT*a *AGA1*::*GAL*1-*AGA*1::*URA*3 *ura*3-52 *trp1 le*u2Δ1 *his*3Δ200 *pep*4::*HIS*3 *prb*1Δ1.6R *can*1 *GAL*) (75) was used for BDNF surface display experiments. Secretion experiments were conducted using the *S. cerevisiae* strain BJ5464 (*MAT*α *ura*3-52 *trp1 le*u2Δ1 *his*3Δ200 *pep*4::*HIS*3 *prb*1Δ1.6R *can*1 *GAL)(Yeast Genetic Stock Center, Berkeley, CA).* Human pro-BDNF, consisting of amino acids -110 to -1 of the human BDNF pro-region and amino acids 1-120 of mature human BDNF, were constructed through primer assembly and subcloned into the pCT4RE backbone (117). Secretion construct, pRS-316-ProBDNF was created by subcloning BDNF and pro-BDNF open reading frames from pCT4RE vectors into pRS-316GAL-OX26 (10) (Figure 3.1A). Yeast transformations were performed using the lithium acetate method (118), and fresh transformants were used for each experiment. SD-CAA medium (20.0 g/L dextrose, 10.19 g/L $Na_2HPO_4 \cdot 7H_2O$, 8.56 g/L $NaH_2PO_4 \cdot H_2O$, 6.7 g/L yeast nitrogen base, 5.0 g/L casamino acids (Becton Dickinson, Franklin Lakes, NJ)) was used for yeast growth. SG-CAA medium (dextrose replaced by galactose in SD-CAA) was used for induction of both yeast display and secretion.

3.3.2 Flow Cytometry

Flow cytometry was used for mutagenic library sorting and quantification of BDNF expression and folding on the yeast surface. For surface display, yeast cells were grown in 3 ml SD-CAA medium at 30 °C to reach an OD_{600nm} of approximately 1.0 and induced in the same volume of SG medium for 18 h at 20 °C. After induction, $2x10^6$ surface-displaying yeast cells (0.2 OD_{600nm}) were collected per sample and analyzed by flow cytometry. Yeast cells were washed using PBS-BSA (8 g/L NaCl, 0.2 g/L KCl, 1.44 g/L Na2HPO4, 0.24 g/L KH2PO4, 1 g/L BSA, pH 7.4) prior to labeling. Surface-displayed BDNF was detected by antibody labeling of epitopes using mouse anti-c-*myc* antibody, 9e10, (30-50 µg/ml, Covance, Berkeley, CA) or rabbit anti-FLAG antibody (0.8 µg/ml, Sigma, St. Louis, MO). Receptor binding was determined using recombinant human TrkB/Fc chimera (TrkB) (5 µg/ml, R&D Systems, Minneapolis, MN) and recombinant human NGF receptor/TNFRSF16/Fc chimera (p75) (5 µg/ml, R&D Systems, Minneapolis, MN). These concentrations are sufficient to saturate all BDNF constructs and mutants examined in this study, and hence TrkB and p75 binding when normalized to total protein expressed on the surface (c-*myc* signal) serve as comparative metrics of proper BDNF folding. All samples were incubated with their respective primary labels for 30 minutes at 4°C, washed with PBS-BSA, and subsequently labeled with goat anti-human IgG conjugated to phycoerythrin (PE) (1:45, Sigma, St. Louis, MO), goat anti-human IgG

conjugated to Alexa Fluor 488 (Alexa488) (1:200, Life Technologies, Grand Island, NY), goat anti-mouse IgG conjugated to phycoerythrin (PE) (1:45, Sigma, St. Louis, MO), goat anti-mouse IgG conjugated to Alexa Fluor 488 (Alexa488) (1:500, Life Technologies, Grand Island, NY), or goat anti-rabbit IgG conjugated to Alexa Fluor 488 (Alexa488) (1:500, Life Technologies, Grand Island, NY). After washing in PBS-BSA, samples were resuspended in PBS-BSA and analyzed on a Becton Dickinson FACSCalibur bench top flow cytometer.

3.3.3 Library Construction and Screening

Mutagenic BDNF pro-region libraries were created using error-prone PCR and homologous recombination. Pro-regions were randomly mutated using varying concentrations of triphosphate analogues 2'-deoxy-p-nucleoside-5'-triphosphate and 8-oxo-2'-deoxyguanosine-5'-triphosphate (TriLink Biotech, San Diego, CA), and by altering the number of PCR cycles. The library was then created in yeast via homologous recombination by combining mutagenic PCR product with NheI to BamHI digested pCT4RE acceptor vector and transforming as previously described (80, 119). A library of $2.6x10^7$ individual transformants was created for Round 1 of directed evolution. After improved clones were identified as described below, a second mutagenic library was created by shuffling DNA from the entire isolated Round 1 pool and the wild-type pro-region (82), along with an additional low rate of mutagenesis. Briefly, pooled Round 1

clones were isolated using whole-cell PCR, mixed with wild-type pro-region in a 1:1 ratio, and amplified using the mutagenesis protocol described above. The resulting mutagenic pro-regions were digested with DNase I (0.056 µg/µl, Boehringer Mannheim, Indianapolis, IN) for 15 minutes at room temperature. The DNased fragments were PCR-assembled, amplified, purified, and inserted into the pCT4RE acceptor vector using homologous recombination to create a library of $1.5x10^7$ transformants for Round 2 of directed evolution.

Sorting of the pro-region libraries was done in the following way. Libraries were grown in selective media at 30°C to an OD_{600nm} of 1.0 and induced for 18 hours at 20°C. Surface display labeling was performed on 10x the library size of induced cells as described in the flow cytometry section of the methods. Directed evolution Round 1 sorting was conducted using a double-label of TrkB and 9e10 for 4 successive sorts. For directed evolution Round 2, the library was sorted for TrkB/9e10 labeling in sort 1 and then divided into two libraries that were subsequently sorted exclusively on either TrkB/9e10 or p75. Sorting gates were set to collect improved double-positive (TrkB/9e10) or single-positive (p75) populations with increasing stringency as sorting progressed (from an initial 2.0% to a final 0.5% of the total population). Cells were sorted using a Becton Dickinson FACSVantage SE flow cytometric sorter at the University of Wisconsin Comprehensive Cancer Center. Once sorting was completed, individual yeast colonies were isolated after plating on nutritionally selective media. Plasmid DNA was recovered from yeast colonies using the Zymoprep II yeast plasmid

miniprep kit (Zymo Research, Irvine, CA), amplified in DH5α cells (Life Technologies, Grand Island, NY), and sequenced at the University of Wisconsin Biotechnology Center to determine mutagenic alterations. Retransformation into the parent display strain confirmed the improvements were due to the mutated BDNF genes. All statistical evaluation was performed using an unpaired, two-tailed Student t-test.

3.3.4 Protein Secretion and Purification

Yeast harboring BDNF clones were inoculated in volumes of 3 ml SD-CAA medium, grown overnight at 30 °C, and diluted to a uniform OD_{600nm} of 0.1. Cultures were then expanded for 3 days to an OD_{600nm} between 8 and 10. Protein secretion was induced in the same volume of SG-CAA medium for 3 days at 20 °C. Cell free supernatants were analyzed by Western blotting or ELISA as described below. For batch purification, 50 ml cultures were grown and induced. The supernatant was recovered from the induced sample and dialyzed twice against 10 L of PBS, and adjusted to 10 mM imidazole content. Next, 250 µl superflow Ni-NTA beads (Qiagen, Valencia, CA) were then added to the dialyzed supernatant to bind the His6-tagged neurotrophin at 4^{o}C for 30 min. The beads were then washed with 750 µl 20 mM imidazole buffer (6.9 g/L NaH_2PO_4-H_2O, 17.5 g/L NaCl, 1.36 g/L imidazole, pH 8.0). BDNF protein was

recovered using 1 ml 250 mM imidazole buffer (6.9 g/L NaH_2PO_4-H_2O, 17.5 g/L NaCl, 17 g/L imidazole, pH 8.0).

3.3.5 Western Blotting

Polyacrylamide gel electrophoresis and Western blotting methods were consistent with those described previously (120). Prior to electrophoretic separation, samples were deglycosylated using the endoglycosidase $EndoH_f$ to remove pro-region glycans (NEB, Ipswich, MA). Bis-Tris gradient protein gels 4-12% (Life Technologies, Grand Island, NY) were used for electrophoretic separation and proteins were transferred to nitrocellulose membranes. 9e10 (1:1500, Covance, Berkeley, CA) was used for primary labeling of the nitrocellulose membranes, and anti-ms IR Dye® 800CW (1:15,000, LI-COR, Lincoln, NE) was used for detection. Membranes were imagined using the Odyssey® Classic Imaging System (LI-COR) and quantified using Image Studio 4.0. All samples were assayed in triplicate and normalized to final yeast cell density by OD_{600nm}. Relative pro-BDNF and mature BDNF expression levels were determined for each clone and expressed either as total protein (pro-BDNF + BDNF) or mature protein (BDNF only).

3.3.6 ELISA Assays

Enzyme-linked immunosorbent assays (ELISA) were used to evaluate receptor binding for secreted BDNF. The wells of a 96-well MaxiSorp^{TM} plate were loaded with 100 µl TrkB-Fc (10 µg/ml, R&D Systems, Minneapolis, MN) overnight at 4 °C then blocked for 2 h in 250 µl PBS-BT (PBS, pH 7.4 with 1 mg/ml BSA, 1 ml/L Tween 20). Wells were washed four times in 250 µl PBS-BT. A dilution series of supernatant samples (diluted into control yeast supernatants to total volume of 100 µl) were added and incubated at 4 °C for 1 hour. Wells were washed four times with 250 µl PBS-BT followed by incubation with 100 µl 9e10 (10µg/ml, Covance, Berkeley, CA) at 4 °C for 30 min. Following four more PBS-BT washes, 100 µl anti-mouse horseradish peroxidase (1:2000, Sigma, St. Louis, MO) was added for 30 min at 4 °C. After an additional four washes with PBS-BT, the wells were developed with peroxidase substrate (Kirkegaard and Perry Laboratories, Gaithersburg, MD) and the optical density at 450 nm was determined. Signal intensities in the linear range were used for all comparisons. Values were normalized to protein concentration as determined by Western blotting to yield specific TrkB binding activities.

3.3.7 PC12 TrkB Phosphorylation Assays

TrkB phosphorylation assays were performed as described previously (47). Briefly, TrkB-transfected PC12 cells were assayed for BDNF-dependent

tyrosine phosphorylation of TrkB (Colangelo 2005; Jaboin 2002; Kaplan 1991). PC12 cells were grown in DMEM media (Sigma, St. Louis, MO) containing 5% fetal bovine serum (Sigma, St. Louis, MO), 10% horse serum (Sigma, St. Louis, MO), 100 units/ml penicillin, 100 µg/ml streptomycin, 2 mM L-glutamine (Sigma, St. Louis, MO), and 200µg/ml G418 (Sigma, St. Louis, MO). Cells were allowed to reach confluence in T75 (Fisher Scientific, Waltham, MA) poly-L-lysine (0.1 mg/ml, Sigma, St. Louis, MO) coated flasks. Cells were washed in ice-cold PBS and starved in serum-free media for 30 minutes at 37ºC. Purified BDNF samples diluted in PBS+BSA (150-300 ng/ml) were then added to the starved PC12 cells and incubated for 5 minutes at 37ºC. Cells were then washed with cold PBS and lysed. The lysates were subsequently immunoprecipitated with rabbit antipan-Trk IgG (C-14; Santa Cruz Biotechnology, CA, USA) at 4°C for 2 h and recovered using protein A agarose beads (Pierce, IL, USA). Eluted samples were separated on 8% SDS-PAGE gels (Invitrogen), transferred to nitrocellulose membranes, and blocked overnight in 5% milk. Blots were probed either overnight with anti-phospho-Trk (1:1,000; Cell Signaling Technology, MA, USA) or for 1.5 h with anti-pan-Trk IgG (C-14; Santa Cruz) and then an HRP-conjugated anti-rabbit secondary antibody (1:10,000; Sigma).

3.4 Results

3.4.1 Effects of wild-type pro-region on BDNF display and production

BDNF was displayed on the yeast cell surface as a fusion to the N-terminus of the Aga2p subunit, rather than the standard yeast display format of fusion to the C-terminus of Aga2p (Figure 3.1A). In this orientation, it is possible to both tether BDNF to the yeast surface and preserve the native pro-region-BDNF connectivity. First, employing a construct lacking the pro-region (Figure 3.1A, pCT4RE-BDNF), mature BDNF could be displayed as a full-length protein as indicated by the presence of both the FLAG and c-*myc* epitopes on the yeast cell surface (Figure 3.1B). However, binding of the natural ligands, TrkB and p75, is minimal, indicating defective BDNF folding and processing (Figure 3.1C). It should be noted that the Trk and p75 receptors have distinct binding epitopes on neurotrophins (60, 88); and accordingly, we have employed binding of BDNF by saturating levels of TrkB and p75 as a proxy for improved folding fidelity throughout this study. If instead, the wild-type BDNF pro-region was included in the display construct (Figure 3.1A, pCT4RE-proBDNF, and Figure 3.1B), surface expression was lowered 2.8-fold (Figure 3.1C, $p<0.05$). However, BDNF folding was improved 18-fold in terms of TrkB binding activity per molecule (TrkB/c-*myc*), and 2-fold in terms of p75 binding activity per molecule (p75/c-*myc*), indicating a chaperone-like effect of the pro-region (Figure 3.1C, $p<0.05$).

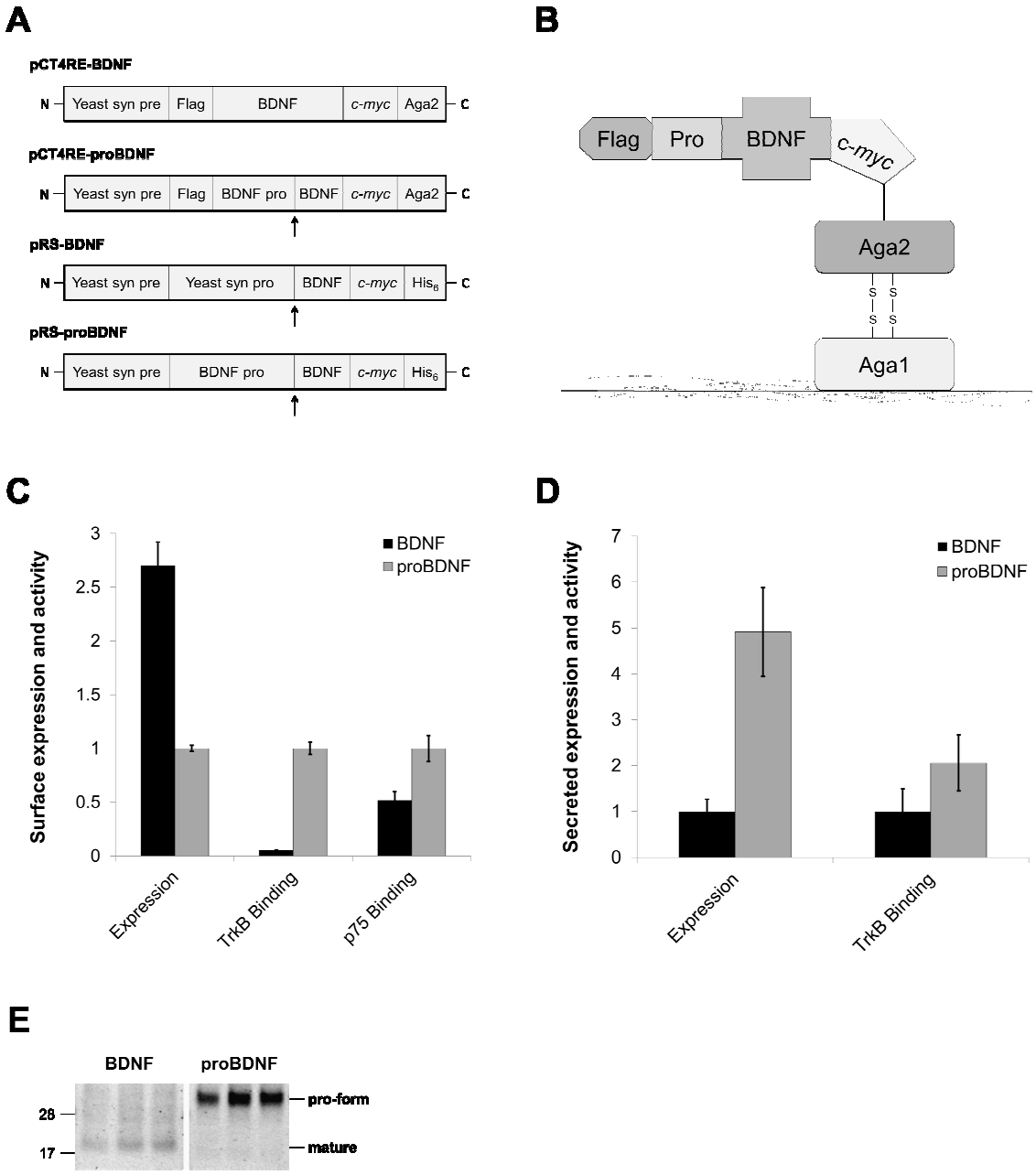
A
pCT4RE-BDNF
N
Yeast syn pre
Flag
BDNF
c-myc
Aga2
C
pCT4RE-proBDNF
N
Yeast syn pre
Flag
BDNF pro
BDNF
c-myc
Aga2
C
pRS-BDNF
N
Yeast syn pre
Yeast syn pro
BDNF
c-myc
His6
C
pRS-proBDNF
N
Yeast syn pre
BDNF pro
BDNF
c-myc
His6
C
B
Flag
Pro
BDNF
c-myc
Aga2
S
S
S
S
Aga1
C
Surface expression and activity
BDNF
proBDNF
3
2.5
2
1.5
1
0.5
0
Expression
TrkB Binding
p75 Binding
D
Secreted expression and activity
BDNF
proBDNF
7
6
5
4
3
2
1
0
Expression
TrkB Binding
E
BDNF
proBDNF
28
17
pro-form
mature

Figure 3.1: Effects of wild-type pro-region. A) The pCT4RE display constructs and the pRS secretion constructs are shown schematically with their pro-region cleavage site marked (arrow). B) The pCT4RE-proBDNF construct is shown tethered to the yeast cell surface. With proper processing, the pro-region is proteolytically cleaved, yielding mature BDNF expressed as a fusion to the Aga2p mating protein on the yeast cell surface. C-*myc* and FLAG epitope tags are present to quantify expression and cleavage, respectively, by flow cytometry. C) Expression (c-*myc*) and binding to receptors (TrkB and p75) of surface-displayed wild-type pro (pCT4RE-proBDNF) versus BDNF (pCT4RE-BDNF). Samples were analyzed by flow cytometry and normalized to pro-BDNF and expressed as means ± S.D., from three independent yeast transformants. D) Expression level and activity of secreted proBDNF (pRS-proBDNF) and BDNF (pRS-BDNF). Expression level was assessed by Western blotting with total amounts (pro-form and mature BDNF) being summed for the proBDNF construct. Activity was assessed by TrkB ELISA with binding signals given on a per molecule basis. Both activity and expression were normalized to BDNF samples and expressed as means ± S.D. from secretion samples derived from three independent transformants. E) Sample Western blot data used to quantify comparative expression levels of BDNF and pro-BDNF in panel D). Secretion samples from triplicate independent transformants are depicted. Molecular mass markers (kDa) are shown on the left and sizes corresponding to pro-form and mature BDNF are denoted on the right.

If instead, BDNF was secreted, the wild-type pro-region (Figure 3.1A, pRS-proBDNF) increased total BDNF production 4.9-fold, compared with BDNF secreted with a standard yeast-derived pro leader (Figure 3.1A, pRS-BDNF) (Figure 3.1D, $p<0.05$). Secreted protein derived from the wild-type pro-region containing construct comprised both mature and uncleaved pro-form BDNF, with the majority of the protein being in the pro-form (Figure 3.1E). A TrkB ELISA assay was used to compare the folding fidelity of the secreted BDNF products since BDNF can bind its receptors both in its pro- and mature forms (121). These ELISA data indicated that secreted pro-BDNF possessed 2.1-fold more TrkB binding activity per molecule compared with BDNF secreted with a standard yeast-derived pro leader (Figure 3.1D, $p<0.1$). Taken together, these results suggested that the BDNF pro-region aided in the production of properly folded surface displayed or secreted BDNF, and could also improve secretion yields. However, absolute surface display levels were low and per molecule receptor binding activities (TrkB/c-*myc* and p75/c-*myc*) were substantially reduced compared to those that could be achieved with the evolved BDNF variants known as K8 and P3 that lack a pro-region (47), indicating remaining room for improvement in the folding and processing of pro-BDNF.

3.4.2 Directed evolution of BDNF pro-region

In an effort to further improve BDNF expression and activity, the wild-type BDNF pro-region was mutated while leaving the mature BDNF coding region unchanged. A library created by random mutagenesis and having 2.6 $x10^7$ clones was subsequently screened for pro-regions that mediated both increased expression (c-*myc*) and improved folding (TrkB) (Figure 3.2A). After four rounds of flow cytometric sorting, the c-*myc* expression level for the entire sorted library pool improved 2-fold (Figure 3.2B, clone 44 example), while TrkB labeling increased 3-fold compared to wild-type pro-BDNF, translating to a 1.5-fold overall increase in TrkB binding activity per molecule (TrkB/c-*myc*). Although it was not used as a screening criterion in the first round of directed evolution, p75 binding activity per molecule for this pool also increased 1.5-fold over wild-type pro-BDNF (Figure 3.2B, clone 44 example), suggesting an overall improvement in the folding and processing fidelity of the displayed BDNF protein.

To drive additional improvement, plasmid DNA was harvested from the entire pool of improved clones from Round 1 of directed evolution and the isolated pro-regions were subjected to DNA shuffling and further mutagenesis to produce a library of $1.5x10^7$ clones. For Round 2 of directed evolution, two screening strategies were performed in parallel (Figure 3.2A). The entire library was first sorted for improvement in TrkB binding and c-*myc* expression levels as was done in Round 1 of directed evolution. Although Round 1 screens that

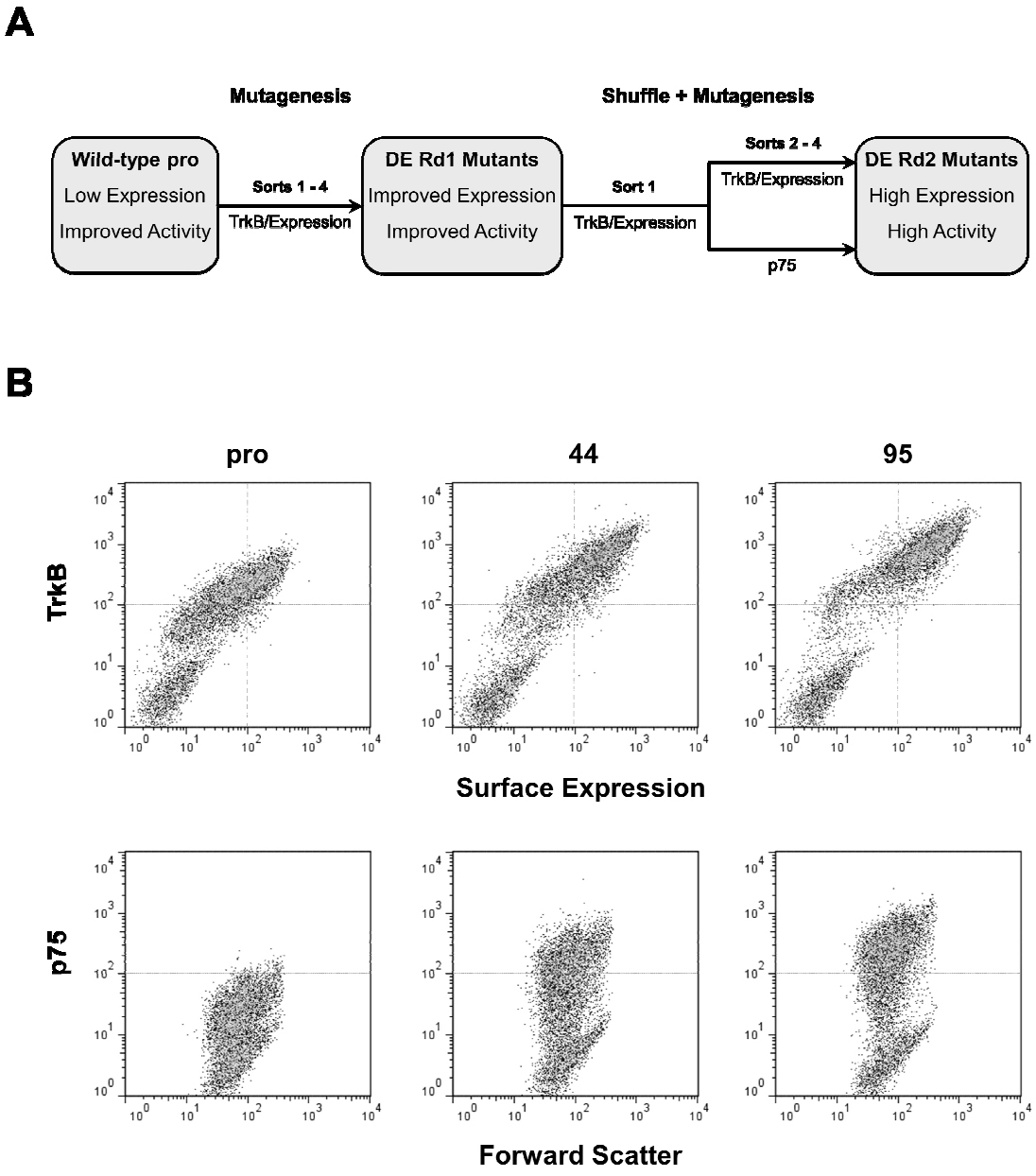

Figure 3.2: Directed evolution of the BDNF pro-region. A) Flow chart of the directed evolution process used to engineer the pro-region including outcomes and screening criteria. B) Flow cytometric data demonstrating outputs of the directed evolution process in terms of BDNF activity (TrkB and p75 binding) and expression (c-*myc*) on the yeast surface. Sample clones 44 from Round 1 and 95 from Round 2, are shown as examples of the Round 1 and Round 2 phenotypes, respectively, and are compared to wild-type pro (pCT4RE-proBDNF). Quantified data for all Round 1 and Round 2 mutants are shown in Table 3.1.

employed TrkB binding also improved the capacity of surface displayed BDNF to bind p75, the binding of p75 remained low. Thus, for sorts 2-4 the library was sorted either for continued improvement of TrkB/c-*myc* or, alternatively, for improved p75 binding (Figure 3.2A). After four sorts, both of the parallel enriched Round 2 pools were nearly identical in all tested characteristics, with additional 1.5-fold increases in expression (c-*myc*) but little effect on specific TrkB binding activity (TrkB/c-*myc*) compared with Round 1 pools (Figure 3.2B, clone 95 example). By contrast, p75 binding activity per molecule (p75/c-*myc*) was improved 2-fold compared with the Round 1 pool, suggesting an additional improvement in the overall fold of the BDNF molecule in the presence of Round 2 mutated pro-regions (Figure 3.2B, clone 95 example).

3.4.3 Effects of evolved pro-regions on properties of surface-displayed BDNF

A total of 35 individual clones were isolated from the sorted Round 1 and Round 2 pools. Six unique pro-region mutants were isolated from the Round 1 pool: 33, 35, 37, 38, 41, and 44. Five unique mutants were isolated from the Round 2 pools: 95 and F2 from the TrkB/c-*myc* pool and 71, 72, and 74 from the p75 pool (Table 3.1). The BDNF mutants isolated from Round 1 each contained a leucine to proline mutation at either position -20 or -23. The importance of these specific mutations are confirmed by mutants 35 and 41, which contained leu(-23)pro and leu(-20)pro, respectively, as their lone alterations. In particular,

mutant 35, exhibits a 1.8-fold improved expression and a 1.7-fold TrkB/c-*myc* improved ligand binding activity (Table 3.1, $p<0.05$) compared to the wild-type pro-region. Examination of mutants 33 and 44 indicated that mutations in addition to leu(-23)pro can further enhance expression up to 2-fold over the wild-type pro-region (Table 3.1, $p<0.05$). While p75 binding per molecule (p75/c-*myc*) was consistently elevated, Round 1 mutants did not display statistically significant improvements (Table 3.1, $p>0.05$). Moving to Round 2 of directed evolution, the leu(-23)pro mutation from Round 1 was conserved in every Round 2 mutant (Table 3.1). Moreover, three of the five mutants isolated in Round 2 also contained the leu(-27)ser mutation from mutant 44 of Round 1. Of interest, four of the five Round 2 mutants contained a new leu(-33)phe mutation. When Round 2 mutant 71 is compared to mutant 44, where the leu(-33)phe mutation is the only additional mutation, improved expression and substantially improved p75 receptor binding was observed (Table 3.1, $p<0.05$). Indeed, every mutant possessing the leu(-33)phe mutation possessed improved p75 receptor binding compared to the wild-type pro-region ($p<0.05$). In contrast, Round 2 did not further improve the TrkB binding activity per molecule (Table 3.1). Taken together, Round 1 led to improvements in expression and specific TrkB binding activity whereas Round 2 led to further improvements in expression and substantial improvements in specific p75 binding activity.

Table 3.1: Mutations and properties of evolved BDNF pro-regions.

pro-region clone	wild-type	pro DE Rd1						pro DE Rd2						
amino acid position	pro	33	35	37	38	41	44	71	72	74	F2	95	95RG	95KR
-107	Lys	-	-	-	-	-	-	-	-	-	*Asp*	-	-	-
-79	Lys	-	-	-	-	-	-	-	-	*Glu*	-	-	-	-
-66	Phe	-	-	-	-	-	-	-	-	*Leu*	-	-	-	-
-65	Glu	-	-	-	-	-	-	-	-	*Gly*	-	-	-	-
-61	Glu	-	-	-	-	-	-	-	-	*Gly*	-	-	-	-
-59	Leu	-	-	-	-	-	-	-	-	*Pro*	-	-	-	-
-58	Leu	-	-	-	-	-	-	-	-	*Ser*	-	-	-	-
-57	Asp	-	-	-	-	-	-	-	-	-	*Ala*	-	-	-
-51	Arg	-	-	-	-	-	-	-	-	*Trp*	-	-	-	-
-50	Pro	-	-	-	-	-	-	-	-	-	-	*Leu*	*Leu*	*Leu*
-33	Leu	-	-	-	-	-	-	*Phe*	*Phe*	-	*Phe*	*Phe*	*Phe*	*Phe*
-30	Gln	-	-	-	-	-	-	-	-	*His*	-	-	-	-
-29	Val	-	-	-	-	-	-	-	-	*Met*	-	-	-	-
-27	Leu	-	-	-	-	-	*Ser*	*Ser*	*Ser*	*Ser*	-	-	-	-
-23	Leu	*Pro*	*Pro*	*Pro*	-	-	*Pro*	*Pro*	*Pro*	*Pro*	*Pro*	*Pro*	*Pro*	*Pro*
-21	Phe	-	-	-	-	-	-	-	-	*Ser*	-	-	-	-
-20	Leu	-	-	-	*Pro*	*Pro*	-	-	-	*Arg*	-	-	-	-
-16	Tyr	*His*	-	-	-	-	-	-	-	-	-	*His*	*His*	*His*
-15	Lys	*Arg*	-	-	-	-	-	-	-	-	-	-	-	-
-14	Asn	-	-	*Asp*	-	-	-	-	-	-	-	-	-	-
-12	Leu	-	-	-	-	-	-	-	-	-	*Pro*	-	-	-
-9	Ala	-	-	-	-	-	-	-	*Val*	-	-	-	-	-
-7	Met	-	-	-	*Thr*	-	-	-	-	-	-	-	-	-
-5	Met	*Val*	-	-	-	-	-	-	-	-	-	-	-	-
-2	Arg	-	-	-	-	-	-	-	-	-	-	-	-	*Lys*
-1	Arg	-	-	-	-	-	-	-	-	-	-	-	*Gly*	-
Relative Display Binding	**pro**	**33**	**35**	**37**	**38**	**41**	**44**	**71**	**72**	**74**	**F2**	**95**	**95RG**	**95KR**
c-*myc*[a]	1.0 ± 0.1	2.1 ± 0.1	1.8 ± 0.2	1.7 ± 0.3	1.5 ± 0.1	1.3 ± 0.3	2.1 ± 0.1	2.9 ± 0.1	2.5 ± 0.1	2.9 ± 0.3	2.8 ± 0.1	2.5 ± 0.1	3.6 ± 0.2	2.7 ± 0.2
TrkB/c-*myc*[b]	1.0 ± 0.1	1.7 ± 0.1	1.7 ± 0.1	1.9 ± 0.2	1.4 ± 0.2	1.4 ± 0.3	1.6 ± 0.1	1.8 ± 0.3	1.2 ± 0.1	1 ± 0.1	1.9 ± 0.4	1.6 ± 0.1	0.7 ± 0.1	1.6 ± 0.2
p75/c-*myc*[c]	1.0 ± 0.2	1.4 ± 0.2	1.2 ± 0.1	1.6 ± 0.4	1.2 ± 0.1	1.2 ± 0.2	1.2 ± 0.4	3.7 ± 0.8	2.2 ± 0.1	2.4 ± 0.4	3.2 ± 1.2	3.0 ± 0.2	1.4 ± 0.1	3.4 ± 0.8

Residues the same as wild type are shown as -. Fold changes represent the means ± S.D. of three independent transformants and are normalized to wild-type pro (pCT4RE-proBDNF). Statistically significant differences were found ($p<0.05$) for expression (c-*myc*) and TrkB binding activity between all mutants and wild-type pro except for 41 and 74. Statistically significant differences were also found ($p<0.05$) for p75 binding activity between wild-type pro and all Round 2 mutants.

a) Expression on the yeast surface as determined by c-*myc* epitope labeling and flow cytometry.

b) Specific binding activity for TrkB as determined by flow cytometry

c) Specific binding activity for p75 as determined by flow cytometry

3.4.4 Effects of evolved pro-regions on properties of secreted BDNF

Based on the results of surface display characterization, yeast secretion constructs were created for all five of the Round 2 pro mutants (Figure 3.1A). Pro mutants 35 and 44 from Round 1 were also included since they possessed the highly conserved leu(-23)pro and leu(-27)ser mutations (Table 3.1). Total secretion titers (pro-form plus mature) increased 1.7 and 2.1 -fold for mutants 35 and 44 compared with wild-type pro-BDNF (Figures 3.3A and 3.3B, $p<0.05$), while Round 2 mutants further increased secretion titers 4.1 to 5.1-fold (Figures 3.3A and 3.3B, $p<0.05$). Yeast supernatants containing the secreted pro-BDNF mutants were also assayed by ELISA to determine the TrkB binding activity per molecule. As generally predicted by the trends of pro-BDNF activity on the yeast surface, TrkB binding activity per molecule for the secreted protein was improved 4.4 to 4.7 -fold after Round 1 (35 and 44) and up to 8.4-fold after Round 2 (mutant 95) when compared to wild-type pro-BDNF (Figure 3.3C, $p<0.05$). As an additional comparison, all pro mutants greatly outperformed a BDNF construct possessing a yeast-derived pro-signal sequence (pRS-BDNF) in terms of expression level (Figure 3.3B, 7.9 to 23-fold, $p<0.05$) and TrkB binding activity per molecule (Figure 3.3C, 7.9 to 17-fold, $p<0.05$). Next, several of the best performing pro-BDNF mutants (35, 71 and 95) were purified (~1 mg/L titer), and as a measure of their biological activity, tested for their capacity to promote intracellular

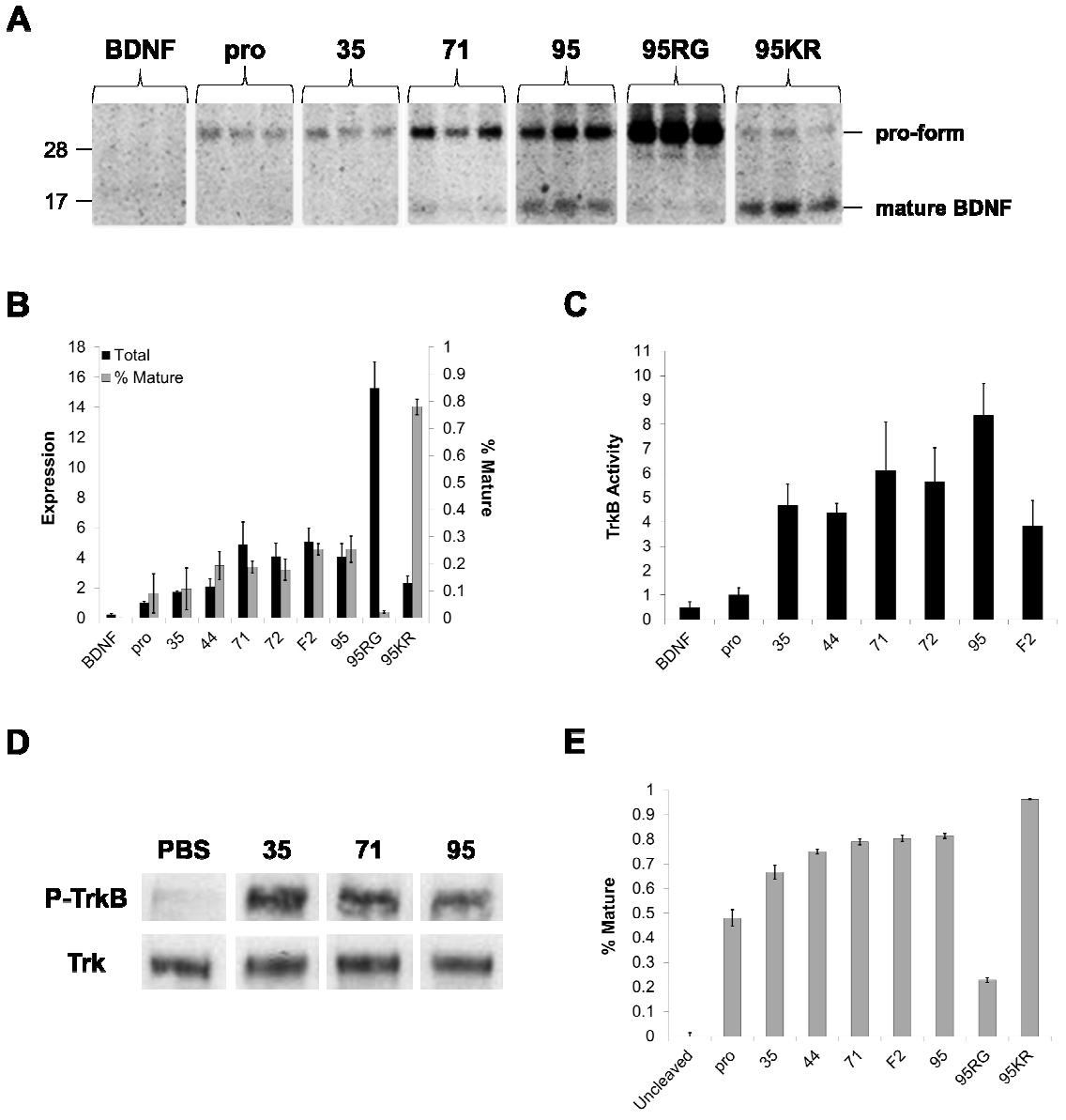

Figure 3.3: Analysis of improved pro-regions on BDNF secretion and processing. A) Sample Western blot data used to quantify secretion and proteolytic cleavage. Triplicate samples are supernatants derived from independent yeast transformants. Molecular mass markers (kDa) are shown on the left and sizes corresponding to pro-form and mature BDNF are indicated on the right. B) Quantification of Western blot data described by panel A) to yield comparative expression levels for secreted proBDNF constructs. Expression level was assessed by summing the total amount of pro-form and mature BDNF.

Percent mature represents the fraction of total secreted protein in the cleaved, mature form. Data are expressed as the means ± S.D. of supernatants from three independent yeast transformants. Expression levels were normalized to total wild-type pro (pRS-proBDNF) C) TrkB activity per molecule of the secreted proBDNF constructs assessed by TrkB capture ELISA. TrkB activity is expressed as means ± S.D. arising from supernatants derived from three independent yeast transformants and normalized to pro-BDNF (pRS-proBDNF) D) TrkB phosphorylation by pro-BDNF mutants 35, 71, and 95. TrkB-transfected PC12 cells were exposed to either the mutants or saline-treated sample (PBS). Western blotting of the pan-Trk-immunoprecipitated product with detection of either the phosphorylated TrkB receptor (P-TrkB) or the total Trk receptor (Trk) was performed. Bands corresponding to the full-length TrkB receptor at ~145 kDa are shown. E) The percentage of surface-displayed BDNF having cleaved pro-region and hence, mature, was assessed by FLAG/c-*myc* ratio using display of BDNF lacking a pro-region (pCT4RE-BDNF) as the “uncleaved” control (see Figure 3.1A). Flow cytometric samples are shown as means ± S.D. for two independent transformants.

phosphorylation of TrkB receptors. TrkB-transfected rat adrenal pheochromocytoma (PC12) neural cells were exposed to purified pro-BDNF mutant protein and TrkB receptor phosphorylation was assessed by immunoprecipitation and Western blotting. All three purified pro-BDNF proteins were capable of driving TrkB receptor phosphorylation (Figure 3.3D). Thus, the engineered pro-regions were capable of increasing both the amount and specific binding activity of secreted BDNF, with the secreted protein also being capable of eliciting TrkB receptor phosphorylation.

3.4.5 Effects of engineered pro-regions on proteolytic pro processing for displayed and secreted BDNF

As described above, the secreted pro-BDNF proteins were incompletely processed by yeast as a secreted product. Thus, we next evaluated how the directed evolution process affected the level of pro-region processing for surface-displayed BDNF by quantitatively measuring the fraction of displayed protein possessing the pro-region. By measuring the presence of the FLAG epitope tag as a fraction of total displayed protein (c-*myc*) and benchmarking to a BDNF display construct lacking pro-region (Figure 3.1A), one can assess the comparative cleavage of the pro-region. Through the two rounds of pro-region evolution, the proteolytic processing of the pro-region improved progressively with a 1.6-fold increase in the percentage of mature protein on the yeast surface

for second round mutants 71, F2, and 95 compared with the wild-type pro-region (Figure 3.3E, $p<0.05$). The increased pro-region processing generally correlated with the increased total surface expression (2.5 to 2.9-fold increases in c-*myc*, Table 3.1).

Since there would be interest in engineering and evaluating properties of BDNF in both its pro-form and mature form, we explored whether or not one could simply mutate the dipeptide recognized by the golgi-resident Kex2p yeast protease to promote display of more homogenous populations of either pro or mature BDNF forms. In its wild-type form, the BDNF pro-region has a basic RR dipeptide naturally recognized by the furin protease in mammalian cells to produce mature BDNF (113), whereas the yeast Kex2p protease functions more efficiently on substrates possessing the KR dipeptide (122). A simple mutation of the mutant 95 pro-region to KR (95KR) was sufficient to remove almost all detectable FLAG epitope signal, indicating nearly quantitative pro-region cleavage and display of mature BDNF (Figure 3.3E). In contrast, changing the dipeptide to RG (95RG) to eliminate Kex2p pro-region cleavage led to display of BDNF in largely pro-form (Figure 3.3E). Overall, surface display levels did not change substantially (<1.2-fold), and the 95KR mutant retained nearly identical activity to mutant 95 in terms of TrkB/c-*myc* and p75/c-*myc* (Table 3.1, $p>0.05$) while the 95RG mutant yielded 2-fold decreases in both TrkB/c-*myc* and p75/c-*myc* binding activity (Table 3.1, $p<0.05$). As secreted products, pro-BDNF variants existed as mixtures of pro-BDNF and mature BDNF forms. Although less

overall cleavage was observed in the secreted products compared with that on the yeast surface, the correlative trend towards increasing percentages of mature BDNF processing over the rounds of directed evolution was maintained (compare Figure 3.3B % Mature to Figure 3.3E). Wild-type pro-BDNF existed almost entirely in its pro form (Figure 3.3B). In contrast, mutant 95 yielded approximately 20% mature BDNF protein. As expected, the 95RG protein yielded almost exclusively pro-linked protein, while also increasing expression levels. Conversely, the 95KR mutant yielded >90% mature BDNF protein with a decrease in total BDNF secretion, but an overall 1.8-fold increase in mature BDNF protein compared with mutant 95 (Figure 3.3B, $p<0.05$). Compared with BDNF having a yeast pro-region, or the construct containing the wild-type BDNF pro-region, the 95KR mutant yielded 8-fold and 20-fold more mature BDNF protein, respectively ($p<0.05$).

3.5 Discussion

In this report we have described the effects of pro-region engineering on yeast display and secretion of BDNF. While use of the wild-type pro-region did yield benefits in terms of BDNF activity, larger gains in both expression level and specific activity both on the yeast surface and as a secreted product were observed using evolved pro-regions. Moreover, the secreted BDNF product employing the evolved pro-regions from either Round 1 (35) or Round 2 (71, 95) was capable of triggering the biologically relevant process of TrkB receptor phosphorylation. The level of pro-region removal during the secretory processing could be regulated by simple point mutation of the dibasic protease recognition site to enable platforms for engineering and production of pro-BDNF or mature BDNF.

In previous studies, various yeast leader sequences were tested for NGF production with the alpha factor pro-region proving optimal (66). In this study, a synthetic pro-region derived from the alpha factor pre-pro was not successful in producing BDNF with substantial specific activity (Figures 3.1C and 3.1D). It is important to note that pro-regions often play important roles in protein folding and production such as in the natural processing of neutrophil alpha-defensins, caspase-3, and subtilisin, among many other proteins (123-125). Thus, the native pro-region of a given protein may be more well-matched to heterologous production than the yeast derived pro-regions. Such an approach was tested for

yeast display of lipase B from *Candida antarctica*, and for this protein, displayed enzyme activity was better in the absence of the native lipase B pro-region (126). By contrast, BDNF surface display expression levels were attenuated by addition of the wild-type pro-region, but its folding was improved as evidenced by the increased receptor binding both on the yeast surface, and as a secreted product. The neurotrophin pro-region has been speculated to act as an intramolecular chaperone for folding neurotrophins into their complex cysteine-knot structures (111, 115), and such an effect could be aiding in the observed baseline increases in BDNF specific activity using the wild-type pro-region.

While use of the wild-type BDNF pro-region offered promise, previous studies have indicated that directed evolution of the yeast alpha factor pre-pro leader sequence could lead to mutants that drive increased expression of antibodies (127). Here we examined a different question as to whether engineering of the native mammalian pro-region, rather than a yeast-derived pro-region, could lead to further improvements in BDNF expression and folding. The first round of directed evolution led to mutated pro-regions that promoted improved expression on the yeast surface and improved TrkB binding per molecule, while the second round served to mainly improve p75 receptor binding per molecule. Since the neurotrophin epitopes involved in Trk and p75 receptor binding are distinct (60, 87, 128), and the TrkB and p75 binding activities did not evolve entirely in concert, these results suggest that pro-region mutations accumulating in Rounds 1 and 2 help correct multiple BDNF folding defects.

In terms of mutation location within the pro-region, it is useful to map the results of BDNF pro-region engineering onto some key findings from the more well-studied pro-NGF system. One important domain was identified in a pro-NGF pro-region deletion study (110). So-called domain I extends from mouse NGF pro positions asn(-53) to arg(-27) and is highly conserved in NGF amongst different species as well as in BDNF and NT-3 (110, 129) (Figure 3.4). When domain I was selectively removed from the NGF pro-region, COS cell secretion of NGF was completely abolished and very little NGF was retained intracellularly (110), indicating an important role in overall NGF processing and secretion within the cell. The homologous counterpart in the human BDNF pro-region comprises lys(-53) to leu(-27), and the most prevalent evolved pro-region mutations, pro(-50)leu, leu(-27)ser, and leu(-33)phe, appear in this domain. In addition, the most conserved mutation at position leu(-23)pro is directly adjacent to BDNF domain I creating a pro-region having three successive proline residues, a sequence naturally observed in the same location of human NT-3 pro-region (129). The Round 2 mutation leu(-33)phe is conserved in human, mouse, and chicken NGF pro-region, while pro(-50)leu and leu(-27)ser are not conserved in other neurotrophin pro-regions. Taken together, each Round 2 mutant included a mutation in the domain I region indicating its importance for yeast processing of properly folded BDNF, similar to the results with the COS cell deletion study with NGF. In addition, previous studies have demonstrated that the NGF pro-region is too flexible to be resolved by x-ray crystallography (130), but hydrogen-deuterium

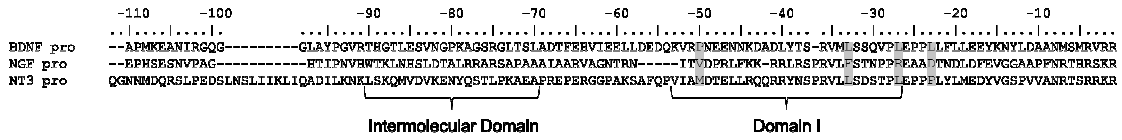

Figure 3.4: ClustalW alignment of human BDNF, NGF, and NT3 pro-regions. Residue numbering is based on BDNF. Based on homology to NGF, the corresponding BDNF Domain I and Intermolecular Domain are underlined and some of the key mutations found during the evolution process are shaded. Sequences are taken from Jones *et al.* (110, 112, 129).

exchange experiments predict that the intramolecular interactions between the NGF pro-region and NGF result from a segment of the NGF pro-region that corresponds to homologous amino acids thr(-90) to leu(-70) of the BDNF pro-region (112). Other than the highly mutated pro-region 74, none of the evolved pro-regions possessed mutations in this region, perhaps indicating that the observed improvements in BDNF processing were not the result of direct intramolecular chaperone-like interactions. However, it is notable that several of the mutations involve changes to proline residues and proline mutations can be beneficial for difficult to process heterologous protein by locking in specific three-dimensional protein configurations (92). While purely speculative, the conserved leu(-23)pro mutation may be playing a similar role in establishing the proper configuration of the pro-region to facilitate its natural intramolecular interaction with BDNF.

Through the two rounds of directed evolution, the pro-region also underwent progressive increases in proteolytic removal although the screening pressure was instead focused on expression level and receptor binding activity. Thus, as the pro-region is evolved to promote more efficient folding, it is also better processed within the secretory pathway. This effect is often observed when secreting proteins from yeast, and retention of the pro-region can occur when the secretory pathway is overloaded with unfolded precursors (36) or under conditions that limit secretion capacity such as elevated temperature (10). Given the differential pro-region processing, we used site-directed mutation to enhance

(95KR) or reduce (95RG) proteolytic cleavage to enable display and secretion of largely homogeneous mature BDNF or pro-BDNF products, while also maintaining much of the beneficial folding and expression effects mediated by the engineered pro-region. Interestingly, enhanced retention of the 95RG pro-region led to a reduced TrkB and p75 specific binding activity, correlating to the aforementioned finding that pro-removal and more efficient folding tracked together during the evolution process. Having the ability to discriminate and engineer selectively the pro- or mature BDNF isoforms could prove important. For instance, mature neurotrophins have preference for their respective Trk receptors and mediate beneficial effects such as cell survival while pro-neurotrophins have preference for the p75 receptor along with co-receptor sortilin and instead promote apoptotic signaling (131-134). Moreover, having a protein engineering platform for pro- and mature BDNF could enable many well developed combinatorial approaches for understanding and modulating BDNF function including affinity maturation (96), stability maturation (72), and epitope mapping (135). Finally, one could envision applying the pro-region engineering tools described here to other members of the neurotrophin family, including NGF, NT-3 and NT-4.

Chapter 4: Improving Heterologous Protein Production in *Saccharomyces cerevisiae* by Tuning the Unfolded Protein Response

(This chapter was produced by Thomas M. Malott and Eric V. Shusta and will be submitted to Biotechnology and Bioengineering for publication)

4.1 Abstract

Although the results in the previous two chapters are exciting, they are very specific to neurotrophins and the yields remain low even when combined (~10 mg/L). There is need for a broad spectrum way of producing many types of proteins, and a new approach is needed. One such approach seeks to optimize cells by regulating hundreds of genes simultaneously through transcription factor engineering. One of the most relevant pathways to protein secretion is the Unfolded Protein Response (UPR). By taking a more holistic approach that is more in line with natural evolution, the UPR was optimized for improved BDNF secretion. Mutants capable of yielding improvements in BDNF expression and folding both as surface displayed and secreted protein resulted from the screening process. It was discovered that these improvements were largely driven by decreased HAC1 expression and the resulting attenuation of UPR activation, rather than by mutations in the hac1p itself. Taken together, these

results demonstrate that tuning of the UPR by regulating HAC1 expression can be used to improve the heterologous production of a difficult to produce protein.

4.2 Introduction

There is longstanding need for improved protein production platforms. The discovery and development of numerous potentially lifesaving protein therapeutics has been hampered by poor production (4, 5). Yeasts because of their relatively inexpensive and rapid growth, are an attractive eukaryotic expression host that could help address protein production issues (11, 136). Although much work has gone into increasing yeast protein production through pro-region engineering (137), fermentation optimization (37), and individual gene overexpression/deletion (6), amongst other strategies, only limited improvement has been achieved (11). One possible limitation in previous approaches is the high interdependence of protein production pathways that often require multiple genes to be altered simultaneously to yield production improvements (15, 138).

One of the most relevant cellular networks for protein secretion is the Unfolded Protein Response (UPR) (22). The UPR is responsible for the homeostasis of the yeast secretory pathway, and as unfolded protein accumulates inside the endoplasmic reticulum (ER), the UPR is activated. UPR activation proceeds through oligomerization of Ire1p via the Ire1p unfolded protein sensing domain and the disassociation of the chaperone, BiP. This leads to Ire1p autophosphorylation and subsequent splicing of *HAC1* mRNA, the central UPR transcription factor (24, 25). Once translated, the hac1p homodimer binds to at least three known UPR response elements (UPREs), and interacts

with other transcription factors and coactivators to directly regulate more than 380 genes (22, 30). These genes affect every part of the secretory pathway including transcription factors central to other pathways such as the heat shock pathway, ER associated degradation (ERAD), phospholipid biosynthesis, amino acid synthesis, and COPII vesicle formation (22, 33, 34, 139, 140). Ultimately, the expression levels of over 1,500 genes, or 25% of yeast genes, are significantly changed by UPR activation during heterologous protein secretion (35). Taken together, the UPR process systematically acts to alleviate cellular stress through a combination of facilitating protein folding and secretion; downregulating gene expression, and increasing protein degradation (25, 35), and thereby, represents an inviting target for protein secretion optimization.

BDNF is a trophic factor that signals the survival of neurons and has been associated with many neurological disorders (40, 41, 44). Its cysteine knot structure has proven difficult to produce in yeast (46, 47, 141), and therefore BDNF was chosen as the candidate target protein for evaluating the effects of UPR modulation on protein display and secretion. To this end, we set out to tune the UPR through directed evolution of the hac1p transcription factor. After two rounds of directed evolution using yeast surface display, positive clones were isolated that improved both the secreted titer and specific binding activity of BDNF. The improvements were demonstrated to largely result from a tuning of UPR strength rather than arising from differential interactions driven by mutated hac1p proteins.

4.3 Materials and Methods

4.3.1 Cells, Media, and Plasmids

Four different strains of *S. cerevisiae* were used in this study. Strains containing chromosomal *HAC1*, referred to as Wild Type, were BJα (MATα ura3-52 trp1 leu2Δ1 his3Δ200 pep4:HIS3 prb1Δ1.6R can1 GAL) and AWY100 (MATa AGA1::GAL1-AGA1::LEU2 ura3-52 trp1 leu2Δ1 his3Δ200 pep4::HIS3 prb1Δ1.6R can1 GAL) and were used for secretion or surface display experiments respectively. Corresponding *HAC1* knockout strains, referred to as *Δhac1*, were created for each of these strains: BJα Δhac1 (MATα ura3-52 trp1 leu2Δ1 his3Δ200 pep4:HIS3 prb1Δ1.6R can1 GAL hac1Δ::G418) for secretion and DHY100 (MATa AGA1::GAL1-AGA1::LEU2 ura3-52 trp1 leu2Δ1 his3Δ200 pep4::HIS3 prb1Δ1.6R can1 GAL hac1Δ::G418) for surfaced display.

Unmutated BDNF without its native pro-region was displayed on the surface of yeast using pCT ESO BDNF(142). This plasmid contains an open reading frame encoding for Aga2-HA-BDNF-c-*myc*. Likewise, pRS316 BDNF contains an open reading frame encoding for BDNF-c-*myc*-His6 and was created for secretion experiments. Spliced *HAC1* was cloned into pRS316(143) under control of the Gal 1-10 promoter to form pRS316 HAC1. This plasmid encoded for cytoplasmic expression of hac1p without any secretion signals or tags. A blank pRS316 plasmid was used for Wild Type controls. The plasmids used to measure UPR activation were obtained as kind gifts from the Jonathan

Weissman Lab, pKT048 (UPRE1)(22), and the Anne Robinson Lab, pRS314-UPRE 1-GFP (144). These reporter plasmids detect hac1p binding to a UPRE adapted from the KAR2/BiP gene using a crippled CYC promoter and four tandem repeats of the UPRE to drive intercellular GFP expression. The Gal inducible synthetic hybrid promoters used to rationally tune *HAC1* were a gift from the Hal Alper Lab(145). *HAC1* was inserted using the XbaI and ClaI1 restriction enzymes sites. The Gal inducible synthetic hybrid promoters used to rationally tune *HAC1* were a gift from the Hal Alper Lab(145). *HAC1* was inserted using the XbaI and ClaI1 restriction enzymes sites.

Plasmids were transformed into yeast using the lithium acetate method and grown in minimal media(146). BJα and BJα Δhac1 strains were grown in SDCAA (20 $^{g}/_{L}$ dextrose, 6.7 $^{g}/_{L}$ yeast nitrogen base, 5.4 $^{g}/_{L}$ Na_2HPO_4, 8.56 $^{g}/_{L}$ $NaH_2PO_4 \cdot H_2O$, 5 $^{g}/_{L}$ casamino acids). AWY100 and DHY100 strains were grown in SDSCAA (20 $^{g}/_{L}$ dextrose, 6.7 $^{g}/_{L}$ yeast nitrogen base, 5.4 $^{g}/_{L}$ Na_2HPO_4, 8.56 $^{g}/_{L}$ $NaH_2PO_4 \cdot H_2O$, 4 $^{g}/_{L}$ SCAA amino acid supplement (adenine sulfate 41.6 $^{mg}/_{L}$, histidine HCl 145.5 $^{mg}/_{L}$, arginine HCl 197.4 $^{mg}/_{L}$, methionine 112.2 $^{mg}/_{L}$, tyrosine 54 $^{mg}/_{L}$, isoleucine 301.3 $^{mg}/_{L}$, lysine HCl 457.1 $^{mg}/_{L}$, phenylalanine 207.8 $^{mg}/_{L}$, glutamic acid 1309.1 $^{mg}/_{L}$, aspartic acid 415.6 $^{mg}/_{L}$, valine 394.8 $^{mg}/_{L}$, threonine 228.6 $^{mg}/_{L}$, and glycine 135.1 $^{mg}/_{L}$)). To induce protein expression, the dextrose was replaced with 20 $^{g}/_{L}$ galactose to produce SGCAA and SGSCAA respectively. Uracil (60 $^{mg}/_{L}$) and tryptophan (80 $^{mg}/_{L}$) were supplemented to the media as needed when working with untransformed strains.

4.3.2 Flow Cytometry

Flow Cytometry was used to assay the amount and quality of BDNF displayed on the yeast surface. Individual colonies were grown overnight in 3 ml SDSCAA at 30°C, reset to 0.3 OD, and then grown to approximately 1 OD_{600nm}. The cultures were then induced by replacing the media with 3 ml SGSCAA and growing for 18 hours at 20°C. $2x10^6$ cells were wash with 500 µl PBS + 1 g/L BSA and labeled with the mouse anti-*c-myc* antibody (9E10) (1:200, Covance), and recombinant human TrkB/Fc chimera (TrkB)(5 µg/ml, R&D Systems) in 100 µl PBS-BSA. After sitting on ice for at least 30 minutes, the cells were washed again and labeled for another 30 minutes on ice with anti-mouse Alexa488 (1:500, Invitrogen) and anti-human phycoerythrin (PE) (1:45, Sigma) in 100 µl PBS-BSA. Cells were washed a final time and analyzed on a Becton Dickinson FACSCalibur bench top flow cytometer. Display levels were determined by the geometric means of the positive populations minus the geometric mean of the nondisplaying populations.

4.3.3 Library Creation and Sorting

The *HAC1* libraries were created using error-prone PCR. Primers were designed such that the entire *HAC1* was subjected to random mutagenesis using the nucleoside analogues 2'-deoxy-p-nucleoside-5'-triphosphate and 8-oxo-2'-

deoxyguanosine-5'-triphosphate (TriLink Biotech)(81). A broad distribution of mutations was created by preforming many reactions with nucleoside analogue concentrations varying between 2 – 200 μM and number of cycles varying between 5 - 20 cycles. All of these mutagenic reactions were amplified, pooled together, gel purified (Zymoclean™ Gel DNA Recovery Kit), and concentrated with pellet paint (Novagen).

The libraries were then created inside the yeast through homologous recombination using electroporation(147). Briefly, 100 ml of cells were grown to 1.6 OD_{600nm} in YPD, washed twice in ice cold water, and once in 1M sorbitol/1M $CaCl_2$. These cells were then incubated in 0.1M LiAc/10mM DTT for 30 minutes at 30°C. The cells were washed twice more with ice cold 1M sorbitol/1M $CaCl_2$, and resuspended to 500 μl in 1M sorbitol/1M $CaCl_2$. 1 μg of linearized pRS316 along with 100 μl of cells were added to a prechilled 2 mm cuvette (Bio-Rad) for a negative control. 40 μg of *HAC1* insert and 4μg of linearized pRS316 were added to the remaining 400 μl of cells, and equally divided between four prechilled 2 mm cuvettes. Cuvettes were electroporated using a Bio-Rad Gene Pulser at 2500V, 25 μF, and 200 Ω. Instantly after electroporation, 2 ml of prewarmed 1M Sorbitol/YPD was added to the cells and they were incubated at 30°C for an hour. Libraries sizes were estimated by plating dilutions, and the libraries were grown overnight in 300 ml of SDSCAA.

The libraries were initially sorted using streptavidin coated magnetic beads (Miltenyi) and the MidiMACS system. After $5x10^9$ cells were grown and induced

for each library as described in the flow cytometry section, they were labeled with biotynlated TrkB and washed in PBSM Buffer, pH 7.4 (NaCl 8 $^{g}/_{L}$, KCl 0.2 $^{g}/_{L}$, Na_2HPO_4 1.44 $^{g}/_{L}$, KH_2PO_4 0.24 $^{g}/_{L}$, BSA 5 $^{g}/_{L}$, EDTA 744 $^{mg}/_{L}$). Next cells were resuspended in 5 ml PBSM with 200 µl streptavidin coated magnetic beads and rotated at 4 °C for 30 minutes. Cell were pelleted and resuspended in 50 ml PBSM and passed over an equilibrated LS column inside a cold room. Then cells were washed with 3 ml PBSM and eluted by removing the column from the magnet assembly and using a plunger.

Next the libraries were sorted five times with increasingly stringent gates for 9E10 and TrkB binding on a Becton Dickinson FACSVantage SE flow cytometric sorter at the UW Carbone Cancer Center Flow Cytometry Laboratory, see Flow Cytometry Section for labeling details. Between each sort, the *HAC1* plasmids were recovered from the yeast using Zymoprep II yeast plasmid miniprep kits (Zymo Research) and amplified using PCR. This was then transformed into yeast using electroporation to create a new library in fresh yeast. This helped to prevent loss of the *HAC1* plasmid and ensure that the phenotype was linked to *HAC1*. After the fifth sort, the final pools were shuffled in a 1:1 ratio with wild-type *HAC1* using SteP (148) and lightly further mutated using nucleoside analogs. The pools were then sorted another four times with flow cytometry for another round of evolution. After the second sort, the mutant *HAC1*s could no longer be PCR recovered from the pools due to smearing and

the last sorts were performed without recovery. This was later found to be a result of Gal promoter truncations and tandem inserts of the *HAC1* gene.

4.3.4 Protein Secretion and Purification

For protein secretion experiments, overnight cultures of single colonies were reset to 0.1 OD in 3 ml of SDCAA and grown for 3 days at 30 °C. Then protein secretion was induced by exchanging the media to 3 ml of SGCAA and growing another 3 days at 20°C. To obtain purified protein, 50 ml of culture was grown up and induced in a similar way. This supernatant was then dialyzed 3 times against 5 L PBS and adjusted to 5 mM imidazole content. The dialyzed supernatant was passed over a Ni-NTA Agarose (Qiagen) column that had been equilibrated with Binding Buffer, pH 8 (0.34 $^{g}/_{L}$ imidazole, 29.2 $^{g}/_{L}$ NaCl, and 3.16 $^{g}/_{L}$ Tris-HCl). The column was then washed with 10 ml Binding Buffer and 10 ml Wash Buffer, pH 8 (6.9 $^{g}/_{L}$ $NaH_2PO_4 \cdot H_2O$, 17.5 $^{g}/_{L}$ NaCl, and 1.36 $^{g}/_{L}$ imidazole) and the protein eluted using Elution Buffer, pH 8 (6.9 $^{g}/_{L}$ $NaH_2PO_4 \cdot H_2O$, 17.5 $^{g}/_{L}$ NaCl, and 17 $^{g}/_{L}$ imidazole).

4.3.5 Western Blotting

Secreted BDNF was quantified using Western Blots. Purified protein or yeast supernatants were boiled for 10 minutes with 4x Lithium Dodecyl Sulfate Sample Buffer (NuPAGE) and 5x Reducing Buffer (100 ^{mg}/ml Sodium Dodecyl

Sulfate and 60 ^{mg}/ml DTT in 400 mM Tris Buffer, pH 6.8) and run on 4-12% Bis-Tris Protein Gels (NuPAGE) at 125V for 90 minutes. After transferring the blot to 0.2 µm nitrocellulose membranes at 30V for 2 hours, the membranes were blocked in 5% milk in TSB, pH 7.6 (2.42 $^{g}/_{L}$ Tris Base, 8 $^{g}/_{L}$ NaCl) for an hour at room temperature. BDNF's *c-myc* tag was labeled with 9E10 (1:1,500, Covance) for an hour followed by anti-ms IR Dye® 800CW (1:15,000, LI-COR) for another hour. All washes and labeling were done using TBST (TBS +1 $^{ml}/_{L}$ Tween 20). Membranes were imagined using the Odyssey® Classic Imaging System (LI-COR) and quantified using Image Studio 4.0. Yeast supernatant samples were normalized to culture density as determined by OD_{600nm} .

4.3.6 ELISA Assay

ELISAs were used to assess the folding of secreted BDNF. 100 $^{µl}/_{well}$ of TrkB in PBS (10 $^{µg}/_{ml}$) was added to a 96-well MaxiSorpTM plate (Nunc) and incubated overnight at 4°C. Wells were blocked with 400 µl PBS-BT (PBS with 1 $^{g}/_{L}$ BSA and 1 $^{ml}/_{L}$ Tween 20) for an hour at 4°C. Serial dilutions of purified protein were added to each well and incubated another hour at 4°C. Unbound protein was washed away with four washes of 400 µl PBS-BT. Bound protein was then labeled for 30 minutes at 4°C with 9E10 (Covance, 1:300) and then with anti-ms HRP (Sigma, 1:2,000) diluted in 100 µl PBS-BT. After each labeling step, wells were washed four times with 400 µl PBS-BT. After 100 µl of 1-Step

Ultra TMB-ELSIA (Pierce) was added and allowed to develop at room temperature, the reaction was stopped by adding 100 µl 2 M H_3PO_4. Absorbance was read at 450 nm and signal was determined by the slope of the linear region of the dilution curves divided by the starting amount of purified protein as determined by western blotting.

4.3.7 qPCR

Yeast cells were lysed with 0.45-0.5 mm glass beads and the mRNA was extracted using Quick-RNA MiniPrep Kits (Zymo Research). After the mRNA was reverse transcribed using the High-Capacity cDNA Reverse Transcription Kit (Life Technologies), multiplex qPCR was performed with the TaqMan® Gene Expression Master Mix (Life Technologies). Custom TaqMan MGB-NFQ probes (Life Technologies) were designed to only amplify spliced *HAC1*, and the TaqMan Gene Expression Assay, SM VIC PL (Life Technologies, Assay Id: Sc04120488_s1) amplified the Actin housekeeping gene. The fold difference was calculated as follows: $Efficiency_{HAC1}$^(*HAC1* $Ct_{wild\text{-}type}$ – *HAC1* Ct_{sample})/($Efficiency_{Actin}$^(Actin $Ct_{wild\text{-}type}$ - Actin Ct_{sample}).

4.4 Results

4.4.1 Effects of wild-type HAC1 on BDNF display and production

Using BDNF as a target therapeutic protein, initial experiments were performed to elicit *HAC1's* effect on heterologous production in *Saccharomyces cerevisiae*. BDNF production was assayed using yeast surface display. Yeast surface display captures BDNF:AGA2 fusion proteins to the yeast cell wall via the AGA1 mating protein (Figure 4.1 A) (75). This preserves the phenotype-genotype linkage and allows for high throughput flow cytometeric screening of large libraries. Full length expression of BDNF was easily assessed by antibody binding to the *c-myc* epitope and proper folding by binding under saturating conditions to BDNF's native receptor, Tropomyosin receptor kinase B (TrkB) (Figure 4.1 A).

Spliced *HAC1* under control of the Gal promoter was overexpressed in the presence of BDNF production in two different strains of *Saccharomyces cerevisiae*: one containing a chromosomal copy of wild-type unspliced *HAC1* (Wild Type) and a corresponding *HAC1* knockout (*Δhac1*). Both *HAC1* deletion and overexpression were detrimental to BDNF production, both on the surface and in secretion. Overexpression of *HAC1* led to increased display of misfolded proteins on the yeast surface and lower secretion into the media in both strains, most likely due to the increased protein misfolding (Figure 4.1 B) (149). Upon knocking out chromosomal *HAC1*, folding remains near wild-type

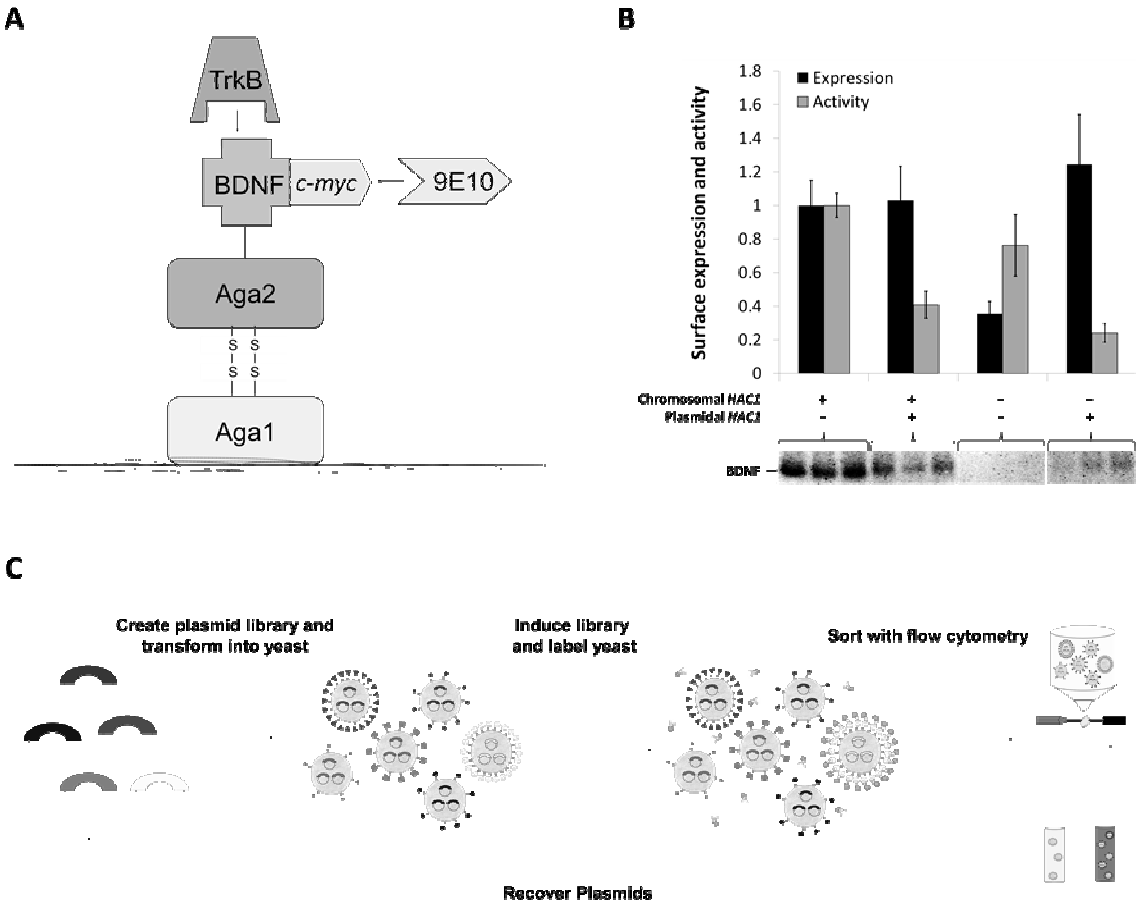

Figure 4.1: BDNF production and screening. A) Schematic of yeast surface display platform. BDNF was secreted as a fusion to Aga2 which was captured to the yeast surface via Aga1. B) BDNF production in yeast either containing chromosomal wild-type *HAC1* or deficient in *HAC1* with and without plasmidal wild-type *HAC1* overexpression. Surface expression was assayed using the c-*myc* epitope tag and activity determined by specific binding to the native TrkB receptor. Data represents means ± S.D. from three independent transformants and is normalized to Wild Type. Under the bar graph is a reducing western showing secreted levels of BDNF in supernatants. C) Screening strategy for directed evolution of BDNF. *HAC1* mutants were recovered from positive pools after every sort to avoid loss of the plasmid.

levels on the surface, but surface expression is attenuated and secretion falls to nearly undetectable levels (Figure 4.1 B). Thus, hac1p activity significantly affects both the amount and quality of BDNF production.

4.4.2 HAC1 Libraries effect on BDNF production

The feasibility of tuning the UPR pathway through directed evolution of hac1p was tested. A *HAC1* library was designed by point mutating the entire spliced form of *HAC1* using nucleoside analogs and cotransforming into Wild Type and *Δhac1* strains in the presence of a UPR sensing plasmid to monitor intracellular hac1p binding and activation (22). Ten random clones from both libraries were chosen. As Figure 4.2 A shows, there was significant variation in the level of UPR activation among the clones, verifying the *HAC1* libraries' ability to influence the UPR and suggesting that the mutation rate was appropriate.

4.4.3 Direct evolution of HAC1

Once confirmed, the *HAC1* DNA library was cotransformed with surface-displayed BDNF to create two yeast libraries: the Wild Type library in the presence of chromosomal *HAC1* and the *Δhac1* library without chromosomal *HAC1*. Both of these libraries were over 10^8 unique clones, 8×10^8 and 1.3×10^8 respectively, with between 1-7 mutations per *HAC1* gene. To further examine

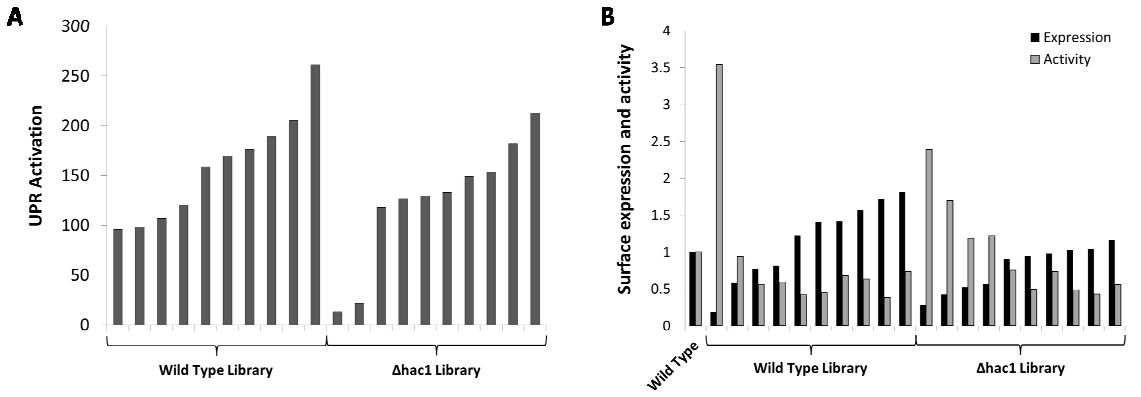

Figure 4.2: Assessing libraries fitness. A) The *HAC1* DNA library was coexpressed with a UPR reporter plasmid in Wild Type and Δhac1 knockout strains. Ten random clones were chosen from each library and their level of UPR activation measured. B) In a similar way, the *HAC1* DNA library was coexpressed with BDNF in Wild Type and Δhac1 knockout strains. Ten random clones were chosen from each library and assessed for expression (c-*myc* tag) and activity (specific binding to TrkB)

the fitness of these libraries, ten random clones were assessed for their ability to produce BDNF and found to have a broad distribution of expression and folding phenotypes, thus confirming hac1p mutants' ability to modulate the UPR and affect the amount and quality of BDNF displayed (Figure 4.2 B). Taken together, these results give confidence to the libraries sequence and functional diversity.

Due to their large size, the libraries were presorted with magnetic beads to enrich for TrkB binders. Afterward, the libraries were screened with flow cytometry for improved expression and binding to the native TrkB receptor. Between sorts the mutant *HAC1*s were recovered from the isolated pools and retransformed into fresh yeast to prevent loss of the *HAC1* or serendipitous mutations arising in the yeast strains (Figure 4.1 C). After five sorts, the mutants in the final pools were shuffled (150) and subjected to a low level of mutagenesis (151). The pools were further sorted four times with flow cytometry for another round of evolution. The Wild Type library did not yield any positive clones that were traceable to the mutant *HAC1*s. Conversely, eight clones with improvements in specific activity to TrkB where isolated from the Δhac1 library.

4.4.4 Deletions in promoter region

Upon sequencing, five of these clones were found to be missing up to 90% of the Gal promoter in addition to mutations in the *HAC1* gene itself (Figure 4.3). When these mutated promoters were isolated from their mutated *HAC1*s

and placed in front of wild-type *HAC1,* the majority of the improvements followed these truncated promoters with up to 6.8-fold improvements in specific TrkB activity ($p<0.05$, Figure 4.4 A). The remaining three clones contained mutations in the *HAC1* nuclear localization or DNA binding domains and improved folding 4.1 to 7.6 fold ($p<0.05$, Figure 4.4 A) (152, 153). These improvements remained when placed under control of a wild-type Gal promoter. Both of these sets of improvements were accompanied by a 40% to 75% drop in expression, signifying a shift to better secretory quality control ($p<0.05$, Figure 4.4 A). Taken together, these findings suggest that the regulation of UPR activation either through *HAC1* transcript levels or hac1p attenuation is important.

Next, these clones' ability to influence BDNF secretion in 50 ml cultures was examined. Given that BDNF secretion in the *Δhac1* strain was severely comprised (Figure 4.1 B), clones were compared to Wild Type yeast containing native chromosomal *HAC1*. The truncated promoters continued to perform well, exceeding Wild Type yeast in both terms of expression, up to 2.3-fold, and specific TrkB binding activity up to 5.5-fold (Figure 4.4 B and C). Conversely, the mutate *HAC1* clones were poorly secreted, suggesting a folding dependence on fusion to Aga2 (Figure 4.5).

To further explore these Gal truncation clones, the clones were coexpressed with a UPR reporter plasmid. As shown in Figure 4.6 A, there is a significant downregulation of UPR activation. This was corroborated with a

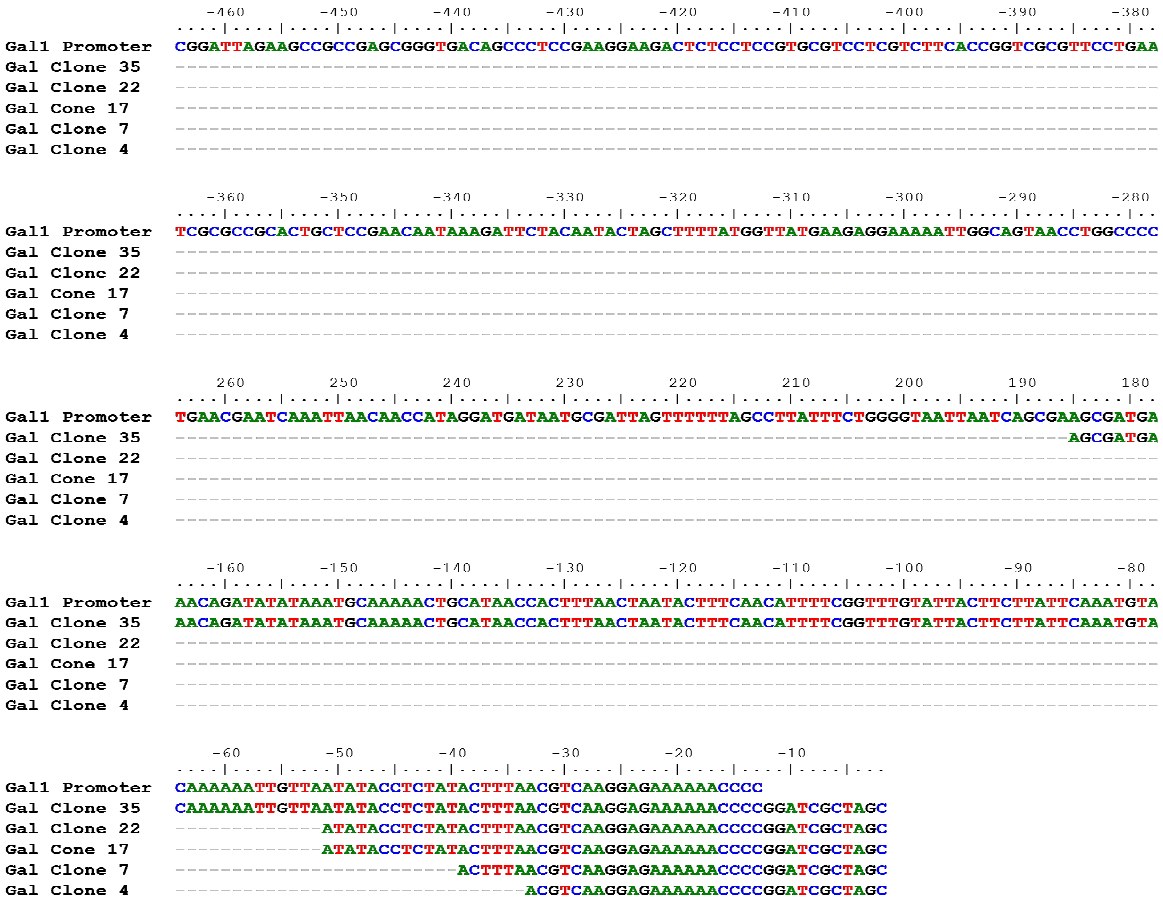

Figure 4.3: Gal promoter deletions. DNA alignment of the promoter region from the five truncation clones compared to wild-type Gal promoter.

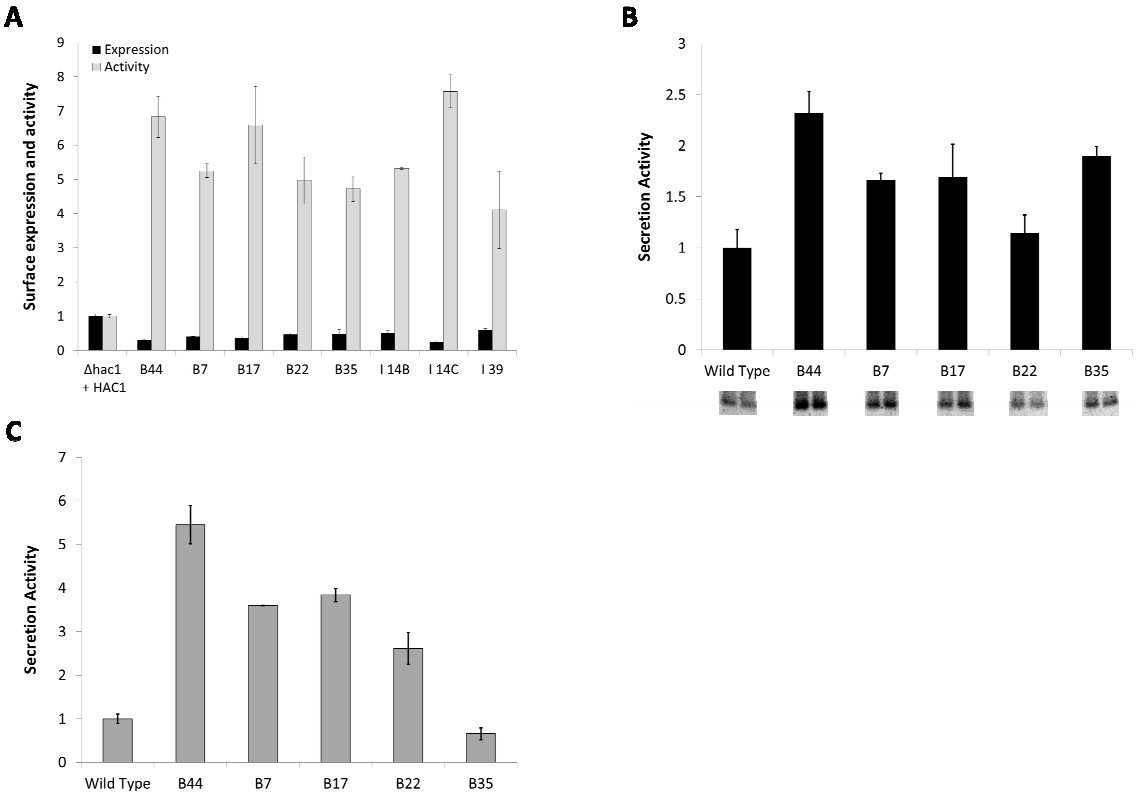

Figure 4.4: Results of Directed Evolution on Hac1p A) Clones isolated from the Δhac1 library were retransformed to confirm the phenotype's linkage to the plasmids. Expression (c-myc) and activity (specific TrkB binding) values were normalized to the background Δhac1 strain. All samples are represented as means ± S.D. of two independent transformants. B) Yeast supernatants from 50 ml cultures were ran on a reducing western. Samples were ran in duplicates ± SD and normalized to yeast containing chromosomal *HAC1* (Wild Type). Western bands used in the quantification are shown below each bar. C) Activity of secreted BDNF as determined by TrkB capture ELISA assays using purified BDNF from the 50 ml cultures above. ELISA signals were divided by protein concentrations and normalized to Wild Type. Means ± S.D. represent three independent transformants.

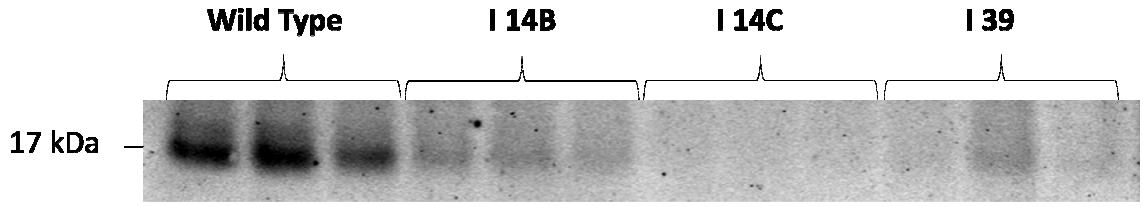

Figure 4.5: Hac1p clone's effect on BDNF secretion. Yeast supernatants from three independent transformations are shown on a reducing western. Wild Type containing a blank plasmid is shown for reference.

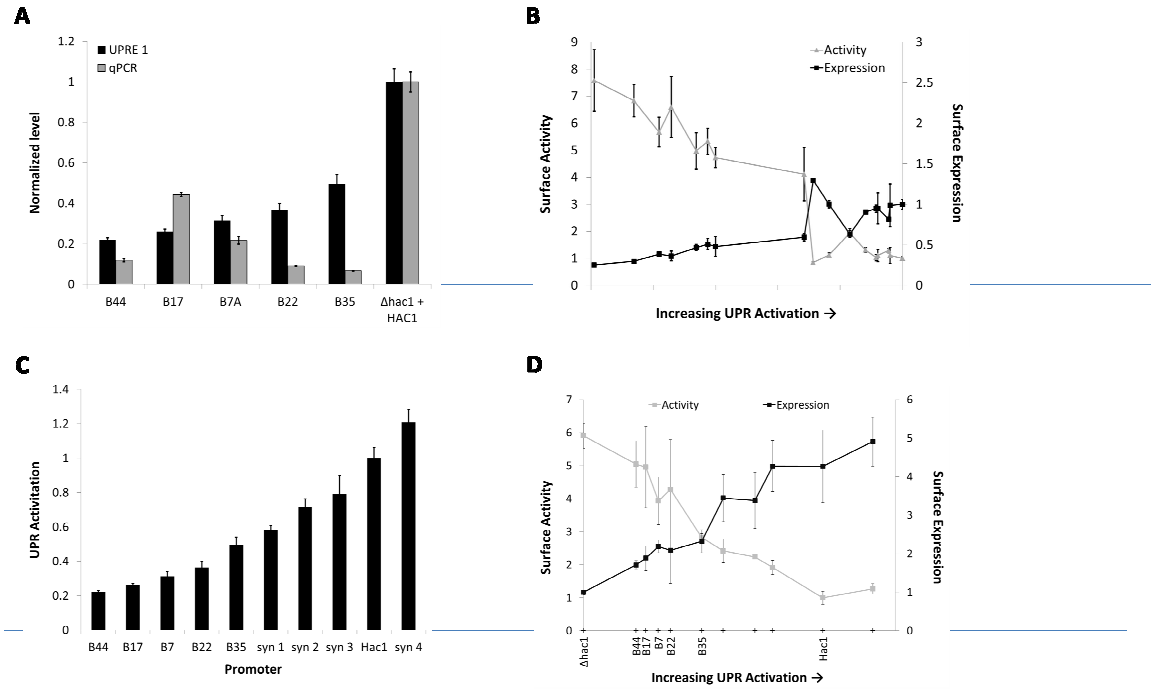

Figure 4.6: Cellular response to promoter mutations. A) Hac1p binding to UPRE was measured in clones using a reporter plasmid. Data were collected from three independent transformants and reported as means ± S.D. All samples are normalized to wild-type *HAC1* expression. Spliced *HAC1* mRNA levels were determined using qPCR and primers specific to the spliced isoform. All samples were run in quadruplicates and the means ± S.D were normalized to wild-type *HAC1* expression. B) All mutant promoters and *HAC1* clones were arranged by UPR activation and assayed for their ability to produce BDNF. BDNF expression was determined using the c-*myc* tag and activity was assessed by specific TrkB binding. All samples were performed in triplicates and normalized to Δhac1. C) UPR activation was tuned by varying *HAC1* expression levels using synthetic promoters of different strength. Gal truncation clones (B*) are shown for reference. UPR activation was assessed using a reporter plasmid. D) Production of yeast surface-displayed BDNF as a function of tuned UPR activation. BDNF expression (c-*myc*) and activity (specific TrkB binding) were normalized to *HAC1* and plotted on separate axes. Means ± S.D. represent triplicate independent transformants.

decrease in intercellular levels of spliced *HAC1* mRNA (Figure 4.6 A). When all of the gathered truncated clones and mutate *HAC1*s from the evolution were arranged according to their UPR activation, an important trend emerged. Surface expression of BDNF inversely correlated with specific TrkB binding activity, with expression increasing up to 4-fold at higher UPR activation and activity increasing up to 7-fold at lower UPR activation ($p<0.05$, Figure 4.6 B). This suggested that the UPR can be optimized for improved BDNF production by tuning *HAC1* expression levels.

4.4.5 Tuning HAC1 expression

To test this hypothesis and eliminate potential compounding effects from the hac1p mutations, a set of synthetic hybrid promoters with a range of defined expression levels were obtained through a kind gift from the Hal Alper Lab (145). Tuning wild-type *HAC1* expression using these hybrid inducible promoters in combination with the truncated promoters allowed for controlled study of a wide range of UPR activation levels up to and surpassing wild-type Gal *HAC1* overexpression (Figure 4.6 C). A similar inverse correlation between expression and folding of surface-displayed BDNF was observed with a folding optimum occurring at low UPR activation (Figure 4.6 D).

4.5 Discussion

In this study we sought to optimize the UPR for improved BDNF production. Heterologous protein production in yeast has much potential, but often production rates are hindered by inaccurate folding. Previous studies in our lab have shown large amounts of protein can become trapped intracellular due to inability to pass quality control checkpoints, and that for BDNF specifically, secretion levels can be markedly increased by improving folding (136). As unfold protein builds up in the ER, it stresses the system and initiates the UPR. This global stress response pathway works to restore proteostasis by upregulating sorting and folding machinery while simultaneously degrading unfolded protein (11, 22). Manipulating this pathway by simply overexpressing or knocking out its central transcription factor, hac1p, was detrimental to both surface-displayed and secreted BDNF. A new approach to cellular engineering is to take a more global focus by engineering transcription factors (14). By adjusting the expression level of hundreds of genes simultaneously, transcription factor engineering better mimics natural evolution, and has been shown to be promising in areas where traditional approaches have only been able to achieved limited gains (15, 16).

After two rounds of directed evolution of the hac1p transcription factor, clones were obtained that increased both the amount and fidelity of secreted BDNF. Surprisingly even with strong selection pressure and a large and diverse starting library, only clones that regulated the strength of the entire pathway were

obtained, either through serendipitous artifacts of the homologous recombination or by mutations in the DNA binding or nuclear localization domains. Given hac1p's independent modes of binding to different DNA elements (39) and its interactions with multiple proteins (30, 31), it was hypothesized that these interactions could have differentially evolved for our advantage.

Upon further inspection, a couple important trends were discovered. Our results suggest that while strong UPR activation increases total protein flux through the secretory pathway, it is detrimental to proper folding. There appears to be a maximum flux of BDNF that the ER can accurately process. Beyond this, the protein processing in the ER collapses and the resulting unfolded BDNF manages to bypass the ER checkpoints and is secreted as unfolded aggregates on the surface. This corroborates with previous studies that suggest that while overexpression of *HAC1* is generally helpful for increasing protein secretion in *S. cerevisiae*, it is only beneficial if process machinery in the ER becomes saturated and limiting (13, 154). Thus, while it may increase total protein flux, *HAC1* overexpression might not be the best strategy for difficult-to-fold/low-yield proteins like BDNF. Previous work in our lab also suggests that for these proteins a lower UPR level is preferred. Haung el al. found that protein secretion can be improved by lowering the induction temperature to 20°C, thereby slowing the onset of the UPR (6, 37). Even though the initial protein secretion rate was slowed by delaying the UPR, the yeast were able to sustain the rate longer before crashing, leading to an overall increase in production.

Taken together, these results allow for simple and quick tuning of yeast strains for heterologous protein production without the need for resource-intensive evolution and screening. While the exact optimum *HAC1* expression level will be protein specific, most proteins are expected to be influenced by the UPR and thus have an optimum level. For many proteins this optimum is different from wild-type strain *HAC1* levels (13, 154). This gives this method a significant advantage over many comparable techniques for improving protein secretion which tend to be protein specific (6, 11, 154). Another distinct advantage of this technology is that it can be easily implemented over existing technologies with little change to existing cell lines and purification processes. Multiple methods exist for rationally tuning gene expression (155-158), allowing for flexibility and accommodation to many hosts. Given that changes in expression levels of XBP1, the mammalian equivalent of *HAC1*, has also been shown to improve the secretion for many proteins, this method is directly transferable to mammalian cells (154).

Bibliography

1. **EvaluatePharma.** 2014. World Preview 2014, Outlook to 2020.

2. **Holmer, A. F.** Pharmaceutical Research and Manufacturers of America.

3. 2015, posting date. Soliris® from Alexion Pharmaceuticals ($536,629 per patient per year)
Naglazyme® from BioMarin Pharmaceuticals ($485,747 per patient per year). [Online.]

4. **Baeshen, N. A., M. N. Baeshen, A. Sheikh, R. S. Bora, M. M. M. Ahmed, H. A. I. Ramadan, K. S. Saini, and E. M. Redwan.** 2014. Cell factories for insulin production. Microbial Cell Factories **13:**141.

5. **Walsh, G.** 2014. Biopharmaceutical benchmarks 2014. Nat Biotech **32:**992-1000.

6. **Wentz, A. E., and E. V. Shusta.** 2007. A Novel High-Throughput Screen Reveals Yeast Genes That Increase Secretion of Heterologous Proteins. Applied and Environmental Microbiology **73:**1189-1198.

7. **Ilmen, M., R. den Haan, E. Brevnova, J. McBride, E. Wiswall, A. Froehlich, A. Koivula, S. Voutilainen, M. Siika-aho, D. la Grange, N. Thorngren, S. Ahlgren, M. Mellon, K. Deleault, V. Rajgarhia, W. van Zyl, and M. Penttila.** 2011. High level secretion of cellobiohydrolases by Saccharomyces cerevisiae. Biotechnology for Biofuels **4:**30.

8. **Shusta, E. V., P. D. Holler, M. C. Kieke, D. M. Kranz, and K. D. Wittrup.** 2000. Directed evolution of a stable scaffold for T-cell receptor engineering. Nature biotechnology **18:**754.

9. **Ghribi, D., N. Zouari, and S. Jaoua.** 2004. Improvement of bioinsecticides production through mutagenesis of Bacillus thuringiensis by uv and nitrous acid affecting metabolic pathways and/or delta-endotoxin synthesis. Journal of Applied Microbiology **97:**338-346.

10. **Hackel, B. J., D. Huang, J. C. Bubolz, X. X. Wang, and E. V. Shusta.** 2006. Production of soluble and active transferrin receptor-targeting single-chain antibody using Saccharomyces cerevisiae. Pharm Res **23:**790-7.

11. **Idiris, A., H. Tohda, H. Kumagai, and K. Takegawa.** 2010. Engineering of protein secretion in yeast: strategies and impact on protein production. Appl Microbiol Biotechnol **86:**403-17.

12. **Butz, J. A., R. T. Niebauer, and A. S. Robinson.** 2003. Co-expression of molecular chaperones does not improve the heterologous expression of mammalian G-protein coupled receptor expression in yeast. Biotechnology and Bioengineering **84:**292-304.

13. **Valkonen, M., M. Penttila, and M. Saloheimo.** 2003. Effects of Inactivation and Constitutive Expression of the Unfolded-Protein Response Pathway on Protein Production in the Yeast Saccharomyces cerevisiae. Applied and Environmental Microbiology **69:**2065-2072.

14. **Tyo, K. E., H. S. Alper, and G. N. Stephanopoulos.** 2007. Expanding the metabolic engineering toolbox: more options to engineer cells. Trends in Biotechnology **25:**132-137.

15. **Alper, H., J. Moxley, E. Nevoigt, G. R. Fink, and G. Stephanopoulos.** 2006. Engineering Yeast Transcription Machinery for Improved Ethanol Tolerance and Production. Science **314:**1565-1568.

16. **Alper, H., and G. Stephanopoulos.** 2007. Global transcription machinery engineering: A new approach for improving cellular phenotype. Metabolic Engineering **9:**258-267.

17. **Santos, C. N., W. Xiao, and G. Stephanopoulos.** 2012. Rational, combinatorial, and genomic approaches for engineering L-tyrosine production in Escherichia coli. Proc Natl Acad Sci U S A **109:**13538-43.

18. **Zhang, H., H. Chong, C. B. Ching, H. Song, and R. Jiang.** 2012. Engineering global transcription factor cyclic AMP receptor protein of Escherichia coli for improved 1-butanol tolerance. Appl Microbiol Biotechnol **94:**1107-17.

19. **Zhang, H., H. Chong, C. B. Ching, and R. Jiang.** 2012. Random mutagenesis of global transcription factor cAMP receptor protein for improved osmotolerance. Biotechnol Bioeng **109:**1165-72.

20. **Asp, L., and T. Nilsson.** 2008. Golgi gets wired up. Nat Cell Biol **10:**885-887.

21. **Romanos, M. A., C. A. Scorer, and J. J. Clare.** 1992. Foreign gene expression in yeast: a review. Yeast **8:**423-488.

22. **Travers, K. J., C. K. Patil, L. Wodicka, D. J. Lockhart, J. S. Weissman, and P. Walter.** 2000. Functional and Genomic Analyses Reveal an Essential Coordination between the Unfolded Protein Response and ER-Associated Degradation. Cell **101:**249-258.

23. **Huang, D., and E. V. Shusta.** Engineer yeast transcription factor Hac1p to increase yeast secretory capacity. Unpublished. For details malott@wisc.edu.

24. **Ruegsegger, U., J. H. Leber, and P. Walter.** 2001. Block of HAC1 mRNA translation by long-range base pairing is released by cytoplasmic splicing upon induction of the unfolded protein response. Cell **107:**103-14.

25. **Korennykh, A., and P. Walter.** 2012. Structural basis of the unfolded protein response. Annu Rev Cell Dev Biol **28:**251-77.

26. **Okamura, K., Y. Kimata, H. Higashio, A. Tsuru, and K. Kohno.** 2000. Dissociation of Kar2p/BiP from an ER Sensory Molecule, Ire1p, Triggers the Unfolded Protein Response in Yeast. Biochemical and Biophysical Research Communications **279:**445-450.

27. **Sidrauski, C., R. Chapman, and P. Walter.** 1998. The unfolded protein response: an intracellular signalling pathway with many surprising features. Trends in Cell Biology **8:**245-249.

28. **Chapman, R., C. Sidrauski, and P. Walter.** 1998. INTRACELLULAR SIGNALING FROM THE ENDOPLASMIC RETICULUM TO THE NUCLEUS. Annual Reviews in Cell and Developmental Biology **14:**459-485.

29. **Cox, J. S., and P. Walter.** 1996. A Novel Mechanism for Regulating Activity of a Transcription Factor That Controls the Unfolded Protein Response. Cell **87:**391-404.

30. **Patil, C. K., H. Li, and P. Walter.** 2004. Gcn4p and Novel Upstream Activating Sequences Regulate Targets of the Unfolded Protein Response. PLOS BIOLOGY **2:**1208-1223.

31. **Welihinda, A. A., W. Tirasophon, S. R. Green, and R. J. Kaufman.** 1997. Gene induction in response to unfolded protein in the endoplasmic reticulum is mediated through Ire1p kinase interaction with a transcriptional coactivator complex containing Ada5p, p. 4289-4294, vol. 94. National Acad Sciences.

32. **Welihinda, A. A., W. Tirasophon, and R. J. Kaufman.** 2000. The Transcriptional Co-activator ADA5 Is Required for HAC1 mRNA Processing in Vivo. Journal of Biological Chemistry **275:**3377-3381.

33. **Friedlander, R., E. Jarosch, J. Urban, C. Volkwein, and T. Sommer.** 2000. A regulatory link between ER-associated protein degradation and the unfolded-protein response. Nature Cell Biology **2:**379-384.

34. **Higashio, H., and K. Kohno.** 2002. A genetic link between the unfolded protein response and vesicle formation from the endoplasmic reticulum. Biochemical and Biophysical Research Communications **296:**568-574.

35. **Tyo, K. E. J., Z. Liu, D. Petranovic, and J. Nielsen.** 2012. Imbalance of heterologous protein folding and disulfide bond formation rates yields runaway oxidative stress. BMC Biology **10:**16-16.

36. **Shusta, E. V., R. T. Raines, A. Plueckthun, and K. D. Wittrup.** 1998. Increasing the secretory capacity of Saccharomyces cerevisiae for production of single-chain antibody fragments. Nature Biotechnology **16:**773-777.

37. **Huang, D., P. R. Gore, and E. V. Shusta.** 2008. Increasing yeast secretion of heterologous proteins by regulating expression rates and post-secretory loss. Biotechnology and Bioengineering **101:**1264-1275.

38. **Pal, B., N. C. Chan, L. Helfenbaum, K. Tan, W. P. Tansey, and M. J. Gething.** 2007. SCFCdc4-mediated Degradation of the Hac1p Transcription Factor Regulates the Unfolded Protein Response in Saccharomyces cerevisiae. Molecular Biology of the Cell **18:**426.

39. **Fordyce, P. M., D. Pincus, P. Kimmig, C. S. Nelson, H. El-Samad, P. Walter, and J. L. DeRisi.** 2012. Basic leucine zipper transcription factor Hac1 binds DNA in two distinct modes as revealed by microfluidic analyses. Proc Natl Acad Sci U S A **109:**E3084-93.

40. **Binder, D. K., and H. E. Scharfman.** 2004. Brain-derived Neurotrophic Factor. Growth factors (Chur, Switzerland) **22:**123-131.

41. **Autry, A. E., and L. M. Monteggia.** 2012. Brain-Derived Neurotrophic Factor and Neuropsychiatric Disorders. Pharmacological Reviews **64:**238-258.

42. **Chao, M. V., R. Rajagopal, and F. S. Lee.** 2006. Neurotrophin signalling in health and disease. Clin Sci (Lond) **110:**167-73.

43. **Monteggia, L. M.** 2011. Toward neurotrophin-based therapeutics. Am J Psychiatry **168:**114-6.

44. **Zhang, Y., and W. M. Pardridge.** 2006. Blood–brain barrier targeting of BDNF improves motor function in rats with middle cerebral artery occlusion. Brain Research **1111:**227-229.

45. **Hoshino, K., A. Eda, Y. Kurokawa, and N. Shimizu.** 2002. Production of brain-derived neurotrophic factor in Escherichia coli by coexpression of Dsb proteins. Bioscience, biotechnology, and biochemistry **66:**344-350.

46. **Vitt, U. A., S. Y. Hsu, and A. J. Hsueh.** 2001. Evolution and classification of cystine knot-containing hormones and related extracellular signaling molecules. Mol Endocrinol **15:**681-94.

47. **Burns, M. L., T. M. Malott, K. J. Metcalf, B. J. Hackel, J. R. Chan, and E. V. Shusta.** 2014. Directed evolution of brain-derived neurotrophic factor for improved folding and expression in Saccharomyces cerevisiae. Appl Environ Microbiol **80:**5732-42.

48. **Boder, E. T., and K. D. Wittrup.** 1997. Yeast surface display for screening combinatorial polypeptide libraries. Nat Biotechnol **15:**553-7.

49. **Boder, E. T., and K. D. Wittrup.** 2000. Yeast surface display for directed evolution of protein expression, affinity, and stability. Methods Enzymol **328:**430-44.

50. **Kieke, M. C., E. V. Shusta, E. T. Boder, L. Teyton, K. D. Wittrup, and D. M. Kranz.** 1999. Selection of functional T cell receptor mutants from a yeast surface-display library. Proc Natl Acad Sci U S A **96:**5651-6.

51. **Kim, Y. S., R. Bhandari, J. R. Cochran, J. Kuriyan, and K. D. Wittrup.** 2006. Directed evolution of the epidermal growth factor receptor extracellular domain for expression in yeast. PROTEINS: Structure, Function, and Bioinformatics **62**.

52. **Pezet, S., and M. Malcangio.** 2004. Brain-derived neurotrophic factor as a drug target for CNS disorders. Expert Opin.Ther.Targets **8:**391-399.

53. **Tapia-Arancibia, L., F. Rage, L. Givalois, and S. Arancibia.** 2004. Physiology of BDNF: focus on hypothalamic function. Frontiers in neuroendocrinology **25:**77-107.

54. **Nagahara, A. H., D. A. Merrill, G. Coppola, S. Tsukada, B. E. Schroeder, G. M. Shaked, L. Wang, A. Blesch, A. Kim, J. M. Conner, E. Rockenstein, M. V. Chao, E. H. Koo, D. Geschwind, E. Masliah, A. A. Chiba, and M. H. Tuszynski.** 2009. Neuroprotective effects of brain-derived neurotrophic factor in rodent and primate models of Alzheimer's disease. Nat Med **15:**331-337.

55. **Tsukahara, T., M. Takeda, S. Shimohama, O. Ohara, and N. Hashimoto.** 1995. Effects of Brain-derived Neurotrophic Factor on 1-Methyl-4-phenyl-1,2,3,6-tetrahydropyridine-induced Parkinsonism in Monkeys. Neurosurgery **37:**733-741.

56. **Canals, J. M., J. R. Pineda, J. F. Torres-Peraza, M. Bosch, R. Martín-Ibañez, M. T. Muñoz, G. Mengod, P. Ernfors, and J. Alberch.** 2004. Brain-Derived Neurotrophic Factor Regulates the Onset and Severity of Motor Dysfunction Associated with Enkephalinergic Neuronal Degeneration in Huntington's Disease. The Journal of Neuroscience **24:**7727-7739.

57. **Jeong, H. H., S. Piao, J. N. Ha, I. G. Kim, S. H. Oh, J. H. Lee, H. J. Cho, S. H. Hong, S. W. Kim, and J. Y. Lee.** 2013. Combined Therapeutic Effect of Udenafil and Adipose-derived Stem Cell (ADSC)/Brain-derived Neurotrophic Factor (BDNF)–Membrane System in a Rat Model of Cavernous Nerve Injury. Urology **81:**1108.e7-1108.e14.

58. **Barbacid, M.** 1994. The Trk family of neurotrophin receptors. Journal of neurobiology **25:**1386-1403.

59. **Heumann, R.** 1994. Neurotrophin signalling. Current opinion in neurobiology **4:**668-679.

60. **Banfield, M. J., R. L. Naylor, A. G. Robertson, S. J. Allen, D. Dawbarn, and R. L. Brady.** 2001. Specificity in Trk receptor:neurotrophin interactions: the crystal structure of TrkB-d5 in complex with neurotrophin-4/5. Structure (London, England) **9:**1191-1199.

61. **Butte, M. J., P. K. Hwang, W. C. Mobley, and R. J. Fletterick.** 1998. Crystal structure of neurotrophin-3 homodimer shows distinct regions are used to bind its receptors. Biochemistry (John Wiley & Sons) **37:**16846-16852.

62. **Wiesmann, C., M. H. Ultsch, S. H. Bass, and A. M. de Vos.** 1999. Crystal structure of nerve growth factor in complex with the ligand-binding domain of the TrkA receptor. Nature **401:**184-188.

63. **Colangelo, A. M., N. Finotti, M. Ceriani, L. Alberghina, E. Martegani, L. Aloe, L. Lenzi, and R. Levi-Montalcini.** 2005. Recombinant human nerve growth factor with a marked activity in vitro and in vivo. Proceedings of the National Academy of Sciences of the United States of America **102:**18658-18663.

64. **Philo, J. S., R. Rosenfeld, T. Arakawa, J. Wen, and L. O. Narhi.** 1993. Refolding of brain-derived neurotrophic factor from guanidine hydrochloride: kinetic trapping in a collapsed form which is incompetent for dimerization. Biochemistry **32:**10812-8.

65. **Fandl, J. P., N. J. Tobkes, N. Q. McDonald, W. A. Hendrickson, T. E. Ryan, S. Nigam, A. Acheson, H. Cudny, and N. Panayotatos.** 1994. Characterization and crystallization of recombinant human neurotrophin-4. J. Biol. Chem. **269:**755-759.

66. **Nishizawa, M., F. Ozawa, T. Higashizaki, K. Hirai, and F. Hishinuma.** 1993. Biologically active human and mouse nerve growth factors secreted by the yeast Saccharomyces cerevisiae. Applied Microbiology and Biotechnology **38:**624-630.

67. **Fukuzono, S., K. Fujimori, and N. Shimizu.** 1995. Production of biologically active mature brain-derived neurotrophic factor in Escherichia coli. Bioscience, biotechnology, and biochemistry **59:**1727-1731.

68. **Shusta, E. V., P. D. Holler, M. C. Kieke, D. M. Kranz, and K. D. Wittrup.** 2000. Directed evolution of a stable scaffold for T-cell receptor engineering. Nature biotechnology **18:**754-759.

69. **Traxlmayr, M. W., M. Faissner, G. Stadlmayr, C. Hasenhindl, B. Antes, F. Rüker, and C. Obinger.** 2012. Directed evolution of stabilized IgG1-Fc scaffolds by application of strong heat shock to libraries displayed on yeast. Biochimica et Biophysica Acta (BBA) - Proteins and Proteomics **1824:**542-549.

70. **Kim, Y. S., R. Bhandari, J. R. Cochran, J. Kuriyan, and K. D. Wittrup.** 2006. Directed evolution of the epidermal growth factor receptor extracellular domain for expression in yeast. Proteins **62:**1026-1035.

71. **Pepper, L. R., Y. K. Cho, E. T. Boder, and E. V. Shusta.** 2008. A decade of yeast surface display technology: where are we now? Comb Chem High Throughput Screen **11:**127-34.

72. **Pavoor, T. V., Y. K. Cho, and E. V. Shusta.** 2009. Development of GFP-based biosensors possessing the binding properties of antibodies. Proc Natl Acad Sci U S A **106:**11895-900.

73. **Huang, D., and E. V. Shusta.** 2005. Secretion and Surface Display of Green Fluorescent Protein Using the Yeast Saccharomyces cerevisiae. Biotechnology Progress **21:**349-357.

74. **Wentz, A. E., and E. V. Shusta.** 2006. A Novel High Throughput Screen Reveals Yeast Genes that Increase Heterologous Protein Secretion. Applied and Environmental Microbiology.

75. **Boder, E. T., and K. D. Wittrup.** 1997. Yeast surface display for screening combinatorial polypeptide libraries. Nature biotechnology **15:**553-557.

76. **Gietz, R. D., and R. A. Woods.** 2006. Yeast transformation by the LiAc/SS Carrier DNA/PEG method. Methods in molecular biology (Clifton, N.J.) **313:**107-120.

77. **Watson, J. V.** 1992. Flow cytometry data analysis: basic concepts and statistics. Cambridge University Press, Cambridge ; New York, NY, USA.

78. **Tillotson, B. J., Y. K. Cho, and E. V. Shusta.** 2013. Cells and cell lysates: A direct approach for engineering antibodies against membrane proteins using yeast surface display. Methods **60:**27-37.

79. **Colby, D. W., B. A. Kellogg, C. P. Graff, Y. A. Yeung, J. S. Swers, and K. D. Wittrup.** 2004. Engineering antibody affinity by yeast surface display. Methods in enzymology **388:**348-358.

80. **Swers, J. S., B. A. Kellogg, and K. D. Wittrup.** 2004. Shuffled antibody libraries created by in vivo homologous recombination and yeast surface display. Nucleic acids research **32:**e36.

81. **Zaccolo, M., D. M. Williams, D. M. Brown, and E. Gherardi.** 1996. An approach to random mutagenesis of DNA using mixtures of triphosphate derivatives of nucleoside analogues. Journal of Molecular Biology **255:**589-603.

82. **Stemmer, W. P.** 1994. DNA shuffling by random fragmentation and reassembly: in vitro recombination for molecular evolution. Proceedings of the National Academy of Sciences of the United States of America **91:**10747-10751.

83. **Huang, D., and E. V. Shusta.** 2005. Secretion and Surface Display of Green Fluorescent Protein Using the Yeast Saccharomyces cerevisiae. Biotechnol. Prog. **21:**349-357.

84. **Jaboin, J., C. J. Kim, D. R. Kaplan, and C. J. Thiele.** 2002. Brain-derived Neurotrophic Factor Activation of TrkB Protects Neuroblastoma Cells from Chemotherapy-induced Apoptosis via Phosphatidylinositol 3'-Kinase Pathway. Cancer Research **62:**6756-6763.

85. **Kaplan, D. R., B. L. Hempstead, D. Martin-Zanca, M. V. Chao, and L. F. Parada.** 1991. The trk proto-oncogene product: a signal transducing receptor for nerve growth factor. Science **252:**554-558.

86. **Vesa, J., A. Kruttgen, and E. M. Shooter.** 2000. p75 reduces TrkB tyrosine autophosphorylation in response to brain-derived neurotrophic factor and neurotrophin 4/5. The Journal of biological chemistry **275:**24414-24420.

87. **He, X. L., and K. C. Garcia.** 2004. Structure of nerve growth factor complexed with the shared neurotrophin receptor p75. Science **304:**870-875.

88. **Pattarawarapan, M., and K. Burgess.** 2003. Molecular basis of neurotrophin-receptor interactions. Journal of medicinal chemistry **46:**5277-5291.

89. **Kaplan, D. R., B. L. Hempstead, D. Martin-Zanca, M. V. Chao, and L. F. Parada.** 1991. The trk proto-oncogene product: a signal transducing receptor for nerve growth factor. Science **252:**554-8.

90. **Ellgaard, L., and A. Helenius.** 2003. Quality control in the endoplasmic reticulum. Nat Rev Mol Cell Biol **4:**181-191.

91. **Acklin, C., K. Stoney, R. A. Rosenfeld, J. A. Miller, M. F. Rohde, and M. Haniu.** 1993. Recombinant human brain-derived neurotrophic factor (rHuBDNF). Disulfide structure and characterization of BDNF expressed in CHO cells. Int J Pept Protein Res **41:**548-52.

92. **Schweickhardt, R. L., X. Jiang, L. M. Garone, and W. H. Brondyk.** 2003. Structure-expression relationship of tumor necrosis factor receptor mutants that increase expression. Journal of Biological Chemistry **278:**28961-28967.

93. **Robinson, R. C., C. Radziejewski, G. Spraggon, J. Greenwald, M. R. Kostura, L. D. Burtnick, D. I. Stuart, S. Choe, and E. Y. Jones.** 1999. The structures of the neurotrophin 4 homodimer and the brain-derived neurotrophic factor/neurotrophin 4 heterodimer reveal a common Trk-binding site. Protein science : a publication of the Protein Society **8:**2589-2597.

94. **Naylor, R. L., A. G. Robertson, S. J. Allen, R. B. Sessions, A. R. Clarke, G. G. Mason, J. J. Burston, S. J. Tyler, G. K. Wilcock, and D. Dawbarn.** 2002. A discrete domain of the human TrkB receptor defines the binding sites for BDNF and NT-4. Biochem Biophys Res Commun **291:**501-7.

95. **Dechant, G., S. Biffo, H. Okazawa, R. Kolbeck, J. Pottgiesser, and Y. A. Barde.** 1993. Expression and binding characteristics of the BDNF receptor chick trkB. Development **119:**545-58.

96. **Boder, E. T., K. S. Midelfort, and K. D. Wittrup.** 2000. Directed evolution of antibody fragments with monovalent femtomolar antigen-binding affinity. Proceedings of the National Academy of Sciences of the United States of America **97:**10701-10705.

97. **Ibanez, C. F., L. L. Ilag, J. Murray-Rust, and H. Persson.** 1993. An extended surface of binding to Trk tyrosine kinase receptors in NGF and BDNF allows the engineering of a multifunctional pan-neurotrophin. The EMBO journal **12:**2281-2293.

98. **Ibanez, C. F., T. Ebendal, and H. Persson.** 1991. Chimeric molecules with multiple neurotrophic activities reveal structural elements determining the specificities of NGF and BDNF. The EMBO journal **10:**2105-2110.

99. **Nieba, L., A. Honegger, C. Krebber, and A. Pluckthun.** 1997. Disrupting the hydrophobic patches at the antibody variable/constant domain interface: improved in vivo folding and physical characterization of an engineered scFv fragment. Protein Eng **10:**435-44.

100. **Robinson, R. C., C. Radziejewski, D. I. Stuart, and E. Y. Jones.** 1995. Structure of the brain-derived neurotrophic factor/neurotrophin 3 heterodimer. Biochemistry (John Wiley & Sons) **34:**4139-4146.

101. **Bibel, M., and Y. A. Barde.** 2000. Neurotrophins: key regulators of cell fate and cell shape in the vertebrate nervous system. Genes Dev **14:**2919-37.

102. **Castren, E., H. Thoenen, and D. Lindholm.** 1995. Brain-derived neurotrophic factor messenger RNA is expressed in the septum, hypothalamus and in adrenergic brain stem nuclei of adult rat brain and is increased by osmotic stimulation in the paraventricular nucleus. Neuroscience **64:**71-80.

103. **Ernfors, P., C. Wetmore, L. Olson, and H. Persson.** 1990. Identification of cells in rat brain and peripheral tissues expressing mRNA for members of the nerve growth factor family. Neuron **5:**511-26.

104. **Katoh-Semba, R., I. K. Takeuchi, R. Semba, and K. Kato.** 1997. Distribution of brain-derived neurotrophic factor in rats and its changes with development in the brain. Journal of neurochemistry **69:**34-42.

105. **Kawamoto, Y., S. Nakamura, S. Nakano, N. Oka, I. Akiguchi, and J. Kimura.** 1996. Immunohistochemical localization of brain-derived neurotrophic factor in adult rat brain. Neuroscience **74:**1209-1226.

106. **Schulte-Herbruggen, O., A. Braun, S. Rochlitzer, M. C. Jockers-Scherubl, and R. Hellweg.** 2007. Neurotrophic factors--a tool for therapeutic strategies in neurological, neuropsychiatric and neuroimmunological diseases? Curr Med Chem **14:**2318-29.

107. **Philo, J. S., R. Rosenfeld, T. Arakawa, J. Wen, and L. O. Narhi.** 1993. Refolding of brain-derived neurotrophic factor from guanidine hydrochloride: kinetic trapping in a collapsed form which is incompetent for dimerization. Biochemistry (John Wiley & Sons) **32:**10812-10818.

108. **Ilag, L. L., R. Curtis, D. Glass, H. Funakoshi, N. J. Tobkes, T. E. Ryan, A. Acheson, R. M. Lindsay, H. Persson, and G. D. Yancopoulos.** 1995. Pan-neurotrophin 1: a genetically engineered neurotrophic factor displaying multiple specificities in peripheral neurons in vitro and in vivo. Proceedings of the National Academy of Sciences of the United States of America **92:**607-611.

109. **Negro, A., V. Corsa, C. Moretto, S. D. Skaper, and L. Callegaro.** 1992. Synthesis and purification of biologically active rat brain-derived neurotrophic factor from Escherichia coli. Biochemical and biophysical research communications **186:**1553-1559.

110. **Suter, U., J. V. Heymach, Jr., and E. M. Shooter.** 1991. Two conserved domains in the NGF propeptide are necessary and sufficient for the biosynthesis of correctly processed and biologically active NGF. EMBO J **10:**2395-400.

111. **Rattenholl, A., M. Ruoppolo, A. Flagiello, M. Monti, F. Vinci, G. Marino, H. Lilie, E. Schwarz, and R. Rudolph.** 2001. Pro-sequence assisted folding and disulfide bond formation of human nerve growth factor. Journal of Molecular Biology **305:**523-533.

112. **Kliemannel, M., R. Golbik, R. Rudolph, E. Schwarz, and H. Lilie.** 2007. The pro-peptide of proNGF: structure formation and intramolecular association with NGF. Protein Sci **16:**411-9.

113. **Seidah, N. G., S. Benjannet, S. Pareek, M. Chretien, and R. A. Murphy.** 1996. Cellular processing of the neurotrophin precursors of NT3 and BDNF by the mammalian proprotein convertases. FEBS Lett **379:**247-50.

114. **Hauburger, A., M. Kliemannel, P. Madsen, R. Rudolph, and E. Schwarz.** 2007. Oxidative folding of nerve growth factor can be mediated by the pro-peptide of neurotrophin-3. FEBS Lett **581:**4159-64.

115. **Rattenholl, A., H. Lilie, A. Grossmann, A. Stern, E. Schwarz, and R. Rudolph.** 2001. The pro-sequence facilitates folding of human nerve growth factor from Escherichia coli inclusion bodies. European journal of biochemistry / FEBS **268:**3296-3303.

116. **Kliemannel, M., A. Rattenholl, R. Golbik, J. Balbach, H. Lilie, R. Rudolph, and E. Schwarz.** 2004. The mature part of proNGF induces the structure of its pro-peptide. FEBS Lett **566:**207-12.

117. **Marshall, C. J., N. Agarwal, J. Kalia, V. A. Grosskopf, N. A. McGrath, N. L. Abbott, R. T. Raines, and E. V. Shusta.** Facile Chemical Functionalization of Proteins through Intein-Linked Yeast Display. Bioconjugate Chemistry **24:**1634-1644.

118. **Gietz, R. D., and R. A. Woods.** 2006. Yeast transformation by the LiAc/SS Carrier DNA/PEG method. Methods Mol Biol **313:**107-20.

119. **Raymond, C. K., T. A. Pownder, and S. L. Sexson.** 1999. General method for plasmid construction using homologous recombination. Biotechniques **26:**134-8, 140-1.

120. **Huang, D., and E. V. Shusta.** 2006. A yeast platform for the production of single-chain antibody-green fluorescent protein fusions. Appl Environ Microbiol **72:**7748-59.

121. **Fayard, B., S. Loeffler, J. Weis, E. Vögelin, and A. Krüttgen.** 2005. The secreted brain-derived neurotrophic factor precursor pro-BDNF binds to

TrkB and p75NTR but not to TrkA or TrkC. Journal of neuroscience research **80:**18-28.

122. **Brenner, C., and R. S. Fuller.** 1992. Structural and enzymatic characterization of a purified prohormone-processing enzyme: secreted, soluble Kex2 protease. Proceedings of the National Academy of Sciences **89:**922-926.

123. **Feeney, B., and A. C. Clark.** 2005. Reassembly of active caspase-3 is facilitated by the propeptide. J Biol Chem **280:**39772-85.

124. **Inouye, M.** 1991. Intramolecular chaperone: the role of the pro-peptide in protein folding. Enzyme **45:**314-21.

125. **Wu, Z., X. Li, B. Ericksen, E. de Leeuw, G. Zou, P. Zeng, C. Xie, C. Li, J. Lubkowski, W. Y. Lu, and W. Lu.** 2007. Impact of pro segments on the folding and function of human neutrophil alpha-defensins. J Mol Biol **368:**537-49.

126. **Tanino, T., T. Ohno, T. Aoki, H. Fukuda, and A. Kondo.** 2007. Development of yeast cells displaying Candida antarctica lipase B and their application to ester synthesis reaction. Applied Microbiology and Biotechnology **75:**1319-1325.

127. **Rakestraw, J. A., L. S. Stephen, P. Andrea, A. Eugene, and K. D. Wittrup.** 2009. Directed evolution of a secretory leader for the improved expression of heterologous proteins and full-length antibodies in <I>Saccharomyces cerevisiae</I>. Biotechnology and Bioengineering **103:**1192-1201.

128. **Gong, Y., P. Cao, H.-j. Yu, and T. Jiang.** 2008. Crystal structure of the neurotrophin-3 and p75NTR symmetrical complex. Nature **454:**789-793.

129. **Jones, K. R., and L. F. Reichardt.** 1990. Molecular cloning of a human gene that is a member of the nerve growth factor family. Proc Natl Acad Sci U S A **87:**8060-4.

130. **Feng, D., T. Kim, E. Özkan, M. Light, R. Torkin, K. K. Teng, B. L. Hempstead, and K. C. Garcia.** 2010. Molecular and Structural Insight into proNGF Engagement of p75NTR and Sortilin. Journal of Molecular Biology **396:**967-984.

131. **Boutilier, J., C. Ceni, P. C. Pagdala, A. Forgie, K. E. Neet, and P. A. Barker.** 2008. Proneurotrophins require endocytosis and intracellular proteolysis to induce TrkA activation. J Biol Chem **283:**12709-16.

132. **Lee, R., P. Kermani, K. K. Teng, and B. L. Hempstead.** 2001. Regulation of cell survival by secreted proneurotrophins. Science **294:**1945-8.

133. **Lu, B., P. T. Pang, and N. H. Woo.** 2005. The yin and yang of neurotrophin action. Nat Rev Neurosci **6:**603-14.

134. **Schweigreiter, R.** 2006. The dual nature of neurotrophins. Bioessays **28:**583-94.

135. **Cochran, J. R., Y. S. Kim, S. M. Lippow, B. Rao, and K. D. Wittrup.** 2006. Improved mutants from directed evolution are biased to orthologous substitutions. Protein Eng Des Sel **19:**245-53.

136. **Huang, D., and E. V. Shusta.** 2006. A Yeast Platform for the Production of Single-Chain Antibody-Green Fluorescent Protein Fusions? Applied and Environmental Microbiology **72:**7748-7759.

137. **Rakestraw, J. A., S. L. Sazinsky, A. Piatesi, E. Antipov, and K. D. Wittrup.** 2009. Directed evolution of a secretory leader for the improved expression of heterologous proteins and full-length antibodies in Saccharomyces cerevisiae. Biotechnology and Bioengineering **103:**1192-1201.

138. **Jonikas, M. C., S. R. Collins, V. Denic, E. Oh, E. M. Quan, V. Schmid, J. Weibezahn, B. Schwappach, P. Walter, J. S. Weissman, and M. Schuldiner.** 2009. Comprehensive characterization of genes required for protein folding in the endoplasmic reticulum. Science **323:**1693-7.

139. **Weindling, E., and S. Bar-Nun.** 2015. Sir2 links the unfolded protein response and the heat shock response in a stress response network. Biochemical and Biophysical Research Communications **457:**473-478.

140. **Herzog, B., B. Popova, A. Jakobshagen, H. Shahpasandzadeh, and G. H. Braus.** 2013. Mutual Cross Talk between the Regulators Hac1 of the Unfolded Protein Response and Gcn4 of the General Amino Acid Control of Saccharomyces cerevisiae. Eukaryotic Cell **12:**1142-1154.

141. **Pattarawarapan, M., and K. Burgess.** 2003. Molecular Basis of Neurotrophin-Receptor Interactions. J Med Chem **46:**5277-5291.

142. **Piatesi, A., S. W. Howland, J. A. Rakestraw, C. Renner, N. Robson, J. Cebon, E. Maraskovsky, G. Ritter, L. Old, and K. D. Wittrup.** 2006. Directed evolution for improved secretion of cancer–testis antigen NY-ESO-1 from yeast. Protein Expression and Purification **48:**232-242.

143. **Sikorski, R. S., and P. Hieter.** 1989. A System of Shuttle Vectors and Yeast Host Strains Designed for Efficient Manipulation of DNA in Saccharomyces ceratisiae. **122:**19-27.

144. **Xu, P.** 2008. Sensing and analyzing unfolded protein response during heterologous protein production.

145. **Blazeck, J., R. Garg, B. Reed, and H. S. Alper.** 2012. Controlling promoter strength and regulation in Saccharomyces cerevisiae using synthetic hybrid promoters. Biotechnol Bioeng **109:**2884-95.

146. **Gietz, R. D., and R. H. Schiestl.** 2007. High-efficiency yeast transformation using the LiAc/SS carrier DNA/PEG method.

147. **Swers, J. S., B. A. Kellogg, and K. D. Wittrup.** 2004. Shuffled antibody libraries created by in vivo homologous recombination and yeast surface display. Nucleic Acids Research **32:**e36-e36.

148. **Zhao, H., and W. Zha.** 2006. In vitro 'sexual' evolution through the PCR-based staggered extension process (StEP). Nat Protoc **1:**1865-71.

149. **Xu, P., and A. S. Robinson.** 2009. Decreased secretion and unfolded protein response up-regulation are correlated with intracellular retention for single-chain antibody variants produced in yeast. Biotechnology and Bioengineering **104:**20-29.

150. **Zhao, H., L. Giver, Z. Shao, J. A. Affholter, and F. H. Arnold.** 1998. Molecular evolution by staggered extension process (StEP) in vitro recombination. Nat Biotechnol **16:**258-61.

151. **Hackel, B. J., A. Kapila, and K. D. Wittrup.** 2008. Picomolar affinity fibronectin domains engineered utilizing loop length diversity, recursive mutagenesis, and loop shuffling. J Mol Biol **381:**1238-52.

152. **Pal, B., N. C. Chan, L. Helfenbaum, K. Tan, W. P. Tansey, and M.-J. Gething.** 2007. SCF(Cdc4)-mediated Degradation of the Hac1p Transcription Factor Regulates the Unfolded Protein Response in Saccharomyces cerevisiae. Molecular Biology of the Cell **18:**426-440.

153. **Fujii, Y., T. Shimizu, T. Toda, M. Yanagida, and T. Hakoshima.** 2000. Structural basis for the diversity of DNA recognition by bZIP transcription factors. Nat Struct Biol **7:**889-93.

154. **Thomas, D. R., and A. M. Walmsley.** 2014. The effect of the unfolded protein response on the production of recombinant proteins in plants. Plant Cell Rep **34:**179-87.

155. **Nevozhay, D., R. M. Adams, K. F. Murphy, K. i. JosiÄ‡, and G. b. BalÃ¡zsi.** 2009. Negative autoregulation linearizes the dose-response and suppresses the heterogeneity of gene expression. Proceedings of the National Academy of Sciences.

156. **Babiskin, A. H., and C. D. Smolke.** 2011. Synthetic RNA modules for fine-tuning gene expression levels in yeast by modulating RNase III activity. Nucleic Acids Res **39:**8651-64.

157. **Ferreira, J. P., K. W. Overton, and C. L. Wang.** 2013. Tuning gene expression with synthetic upstream open reading frames. Proceedings of the National Academy of Sciences **110:**11284-11289.

158. **Rajkumar, A. S., N. Denervaud, and S. J. Maerkl.** 2013. Mapping the fine structure of a eukaryotic promoter input-output function. Nat Genet **45:**1207-1215.